Gas hydrate in sediments on the Southern Chile continental slope

Dissertation zur Erlangung des Doktorgrades
Dr. rer. nat.

der Mathematisch-Naturwissenschaftlichen Fakultät der
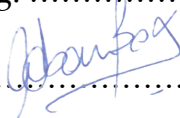Christian-Albrechts-Universität zu Kiel

vorgelegt von

Lucía Villar-Muñoz

Kiel, 2019

Erster Gutachter: …….….………………………… Prof. Dr. Jan H. Behrmann (Betreuer)

Zweiter Gutachter: ………………………….….. Prof. Dr. Sebastian Krastel-Gudegast

Tag der mündlichen Prüfung: …… 11 November …. 2019
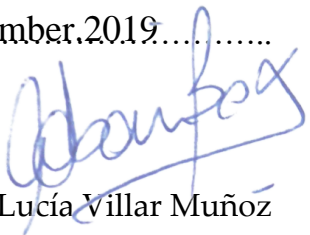
Zum Druck genehmigt: ……………………………..

…………………………….

Der Dekan

ERKLÄRUNG

Hiermit erkläre ich, dass ich die vorliegende Doktorarbeit selbständig und ohne Zuhilfenahme unerlaubter Hilfsmittel erstellt habe. Weder diese noch eine ähnliche Arbeit wurde an einer anderen Abteilung oder Hochschule im Rahmen eines Prüfungsverfahrens vorgelegt, veröffentlicht oder zur Veröffentlichung vorgelegt. Ferner versichere ich, dass die Arbeit unter Einhaltung der Regeln guter wissenschaftlicher Praxis der Deutschen Forschungsgemeinschaft entstanden ist.

Kiel, den ..11..November.2019.....

Lucía Villar Muñoz

To my husband and my sweet Josefina

PREFACE

This thesis includes three independent articles already published in international journals. As a consequence, these articles were peer-reviewed during the process of publication. Each article was lead-authored by the presenter of this thesis, and is a stand-alone article with its own abstract, introduction, methodology, results, discussion, conclusion and reference list.

The first article published was "Heat flow in the southern Chile forearc controlled by large-scale tectonic processes". Lucía Villar-Muñoz, Jan H. Behrmann, Juan Diaz-Naveas, Dirk Klaeschen, Jens Karstens. 2013. Geo-Marine Letters. Here I presented the results of the regional mapping of the bottom-simulating reflector (BSR) and a resulting analysis of heat flow along the Chilean margin, between Valparaíso and the Taitao Peninsula.

The second paper is entitled "A first estimation of gas hydrates offshore Patagonia (Chile)". Lucía Villar-Muñoz, Joaquim P. Bento, Dirk Klaeschen, Umberta Tinivella, Iván de la Cruz Vargas-Cordero, Jan H. Behrmann. 2018. Marine and Petroleum Geology. Special attention had this article in my country, Chile, which promoted once again gas hydrates projects and studies in the Patagonian region.

The third article has the title "Gas Hydrate Estimate in an Area of Deformation and High Heat Flow at the Chile Triple Junction". Lucía Villar-Muñoz, Iván Vargas-Cordero, Joaquim P. Bento, Umberta Tinivella, Francisco Fernandoy, Michela Giustiniani, Jan H. Behrmann, Sergio Calderon-Diaz. 2019. Geosciences. Here I estimated the hydrate content and analyzed this anomalous area (in terms of heat

flow values) where the hydrate is highly susceptible to be released into the ocean system.

During the preparation of these articles, I had used the following methods and procedures:

1. For BSR-derived heat flow: Over 100 seismic reflection profiles were analyzed using the Kingdom Suite software to define the BSR. Then, the heat flow was calculated using MATLAB. Morphostructural features were interpreted in the seismic profiles related to fluids escape structures and tectonic faults.

2. For gas hydrate estimates: On specific seismic lines, advanced seismic processing was performed, including velocity models and gas phases (gas hydrates and free gas) concentration models. These parameters were used to calculate regional estimates of hydrate and free gas concentrations.

A very valuable part of my work was the data acquisition, data processing as well as data presentation, as oral presentations or posters at conferences and, moreover, the preparation of the three scientific articles mentioned above.

ABSTRACT

From a geological point of view, Chile lies in an incomparable area of the globe, which include four lithospheric plates moving relative to each other (Nazca, Antarctic, South American and Scotia plates), geometrically constraining two triple junctions (the Chile and Fuegian triple junctions). The convergent plate margins in this system are the scene of numerous mega-earthquakes and associated tsunamis.

On the South American Plate overriding the downgoing Nazca and Antarctic Plates there are more than 500 active volcanoes, the Andes Orogen, and vast mineral resources associated with active or fossil hydrothermal systems. One of the natural resources that came into the focus of the Chilean government and institutions is gas hydrate in the offshore area of the Pacific Ocean margin, which is a solid ice-like form of water that contains gas molecules highly-concentrated in methane.

Since Chile imports most of its gas budget, the discovery of this new resource opens a new window for the national economy. It is also relevant for geoscientific research, due to methane that escapes from sediments and enter to the ocean or even reaches the atmosphere could pose a great environmental threat. To identify the presence of hydrates, in this thesis it was used the bottom-simulating reflector BSR, which has the half amplitude and opposite polarity relative to the seafloor.

Moreover, fluids play a key role in the nucleation and rupture propagation of earthquakes in convergent margins, since are a major agent of advective heat transfer from depth to the Earth's surface. If we provide enough information for the regional heat flow we will improve our knowledge of the tectono-thermal signature of the convergent margins. For this purpose, it is crucial to know the BSR-depth,

which serves to calculate the steady-state heat flow q (mW m^{-2}) by using a simple formula, and therefore, the heat flow can be envisaged in a regional overview.

This thesis aims to investigate the tectonic processes of the Chilean forearc through the calculation of the regional BSR-derived heat flow, identification of fluid escape sites, description of the distribution of gas hydrates and estimation of the gas hydrate and free gas reservoirs.

One of the major results of this work is the regional overview of the thermal regime and BSR-based gas hydrate distribution along the Chilean forearc. Here, the BSR was identified in the marine sediments mainly along the accretionary prism between 33°-57°S, at around 2000 m water depth, and between 90-600 meters below seafloor (mbsf).

The heat flow estimated through the forearc on the upper and middle continental slope, from Valparaiso to Chiloe (33°-43°S), shows common values of heat flow for the continental basement and overlying slope sediments. However, on the lower slope of the actively deforming accretionary wedge, some places show unexpected heat flow values, indicating that advecting pore fluids from deeper sources may transport a considerable part of the heat there.

Further to the south, a second approach was made over a large area of anomalous, very high heat flow that is associated with a major tectonic feature: the Chile Triple Junction. Here, the Nazca, Antarctic and South American plates converge in a Ridge-Trench-Trench triple junction, constraining subduction of an active spreading centre (the Chile Rise) beneath the South America continental plate. Here, gas hydrates are located in very shallow sediments and the extreme values of

heat flow estimated (< 280 mW m^{-2}) indicate that the overriding South American Plate is effectively heated by subjacent zero-age oceanic plate material. In order to improve the understanding of the geological risk, in case the methane is released to the ocean/atmosphere system, it was tried to estimate the concentration of gas hydrate in this particular region.

Finally, at the southernmost tip of the continent (offshore Patagonia), the heat flow estimated shows a range of values typical for subduction zones of oceanic crust older than 10 Ma. Here, a high concentration of methane hydrate is present beneath the active margin. The average thickness of the gas hydrate layer modelled is almost 300 m and the volume of methane estimated is more than 3×10^{13} m^3 at standard pressure-temperature conditions, allowing the conclusion that the active forearc of the Chilean Patagonia is an important reservoir of methane hydrates.

RESUMEN

Desde un punto de vista geológico, Chile yace en una área del globo incomparable, la cual incluye cuatro placas tectónicas moviéndose entre sí (placas de Nazca, Antártica, Sudamericana y de Escocia), limitados geométricamente por dos triple uniones de placa (triple puntos de Chile y Fueguino). Los márgenes convergentes de estas placas son escenario de numerosos mega-terremotos y tsunamis asociados.

Sobre la placa Sudamericana, suprayacente a las placas de Nazca y Antártica, hay más de 500 volcanes activos, la cordillera de los Andes, y una vasta cantidad de recursos minerales asociados con sistemas hidrotermales activos y fósiles. Uno de los recursos naturales donde el gobierno de Chile e instituciones académicas se han enfocado los últimos años es en los hidratos de gas, localizados en la costa afuera del margen del Océano Pacífico, los cuales son una forma de sólida de agua similar al hielo que contiene moléculas de gas altamente concentradas en metano.

Debido a que Chile importa la mayoría de su presupuesto de gas, el descubrimiento de este nuevo recurso abre una nueva ventana para la economía nacional. Esto también es relevante para las investigaciones geocientíficas, debido a que el metano que escapa desde los sedimentos y entra al océano, o inclusive que sale a la atmósfera, podrían actuar como una amenaza medioambiental. Para identificar la presencia de hidratos, en esta tesis se usó el reflector sísmico que simula el fondo marino (BSR por sus siglas en inglés), el cual tiene la mitad de amplitud y polaridad opuesta relativa al fondo marino.

Además, los fluidos juegan un rol clave en la nucleación y propagación de ruptura de terremotos en márgenes convergentes, ya que son el mayor agente de transferencia de calor advectivo desde las profundidades hasta la superficie de la Tierra. Si proveemos suficiente información para el flujo de calor regional, mejoraremos nuestro conocimiento de la señal tectono-térmica de los márgenes continentales. Para este propósito, es crucial conocer la profundidad del BSR, el cual sirve para calcular el flujo de calor estacionario q (mW m^{-2}) usando una simple fórmula, y por lo tanto, el flujo de calor puede ser visualizado de una manera regional.

El propósito de esta tesis es investigar los procesos tectónicos del antearco chileno a través del cálculo del flujo de calor regional derivado del BSR, identificación de sitios de escape de fluidos, descripción de la distribución de los hidratos de gas y la estimación de las reservas de hidratos y gas libre.

Uno de los resultados más destacados de este trabajo, es la visión regional del régimen térmico y la distribución de hidratos basada en el BSR a lo largo del margen chileno. Aquí, el BSR fue identificado dentro de los sedimentos marinos principalmente de lo largo del prisma de acreción entre los 33°-57°S, alrededor de los 2000 m de profundidad de agua de mar, y entre 90-600 m bajo el fondo marino (mbsf).

El flujo de calor estimado a través del antearco sobre el talud continental superior y medio, desde Valparaíso hasta Chiloé (33°- 43°S), muestra valores normales para el basamento continental y sedimentos que yacen sobre el talud. Sin embargo, en el pie del talud asociado a la deformación activa del prisma de acreción, algunos sectores muestran valores inesperados de flujo de calor, indicando que

fluidos advectivos desde las profundidades pueden transportar una parte considerable del calor hacia estos lugares.

Más al sur, un segundo enfoque fue hecho sobre una gran área de flujo de calor extremadamente anómalo que es asociado con una característica tectónica: el Triple Punto de Chile (CTJ, por sus siglas en inglés). En este lugar, las placas de Nazca, Antártica y Sudamericana convergen en una triple unión Dorsal-Fosa-Fosa; restringiendo la subducción de un centro de expansión (la dorsal de Chile) bajo la placa continental Sudamericana. Aquí, los hidratos de gas están localizados a poca profundidad del fondo marino y los valores de flujo de calor estimados (< 280 mW m^{-2}) indican que la placa Sudamericana suprayacente es efectivamente calentada por el material de edad-cero de la placa subyacente. Además, con el fin de mejorar la comprensión del riesgo geológico, en el caso que el metano sea liberado al sistema océano/atmósfera, fue estimada la concentración de los hidratos de gas en esta región particular.

Finalmente, en el punto más austral del continente (costa afuera de la Patagonia), el flujo de calor estimado muestra un rango de valores típicos para zonas de subducción de corteza oceánica mayores de 10 Ma. Aquí, una alta concentración de hidratos de metano (MHCZ, por sus siglas en inglés) está presente bajo el margen activo. El espesor promedio de la capa de hidrato modelada es de casi 300 m, con concentraciones hasta el 10% y por lo tanto el volumen de metano estimado es superior a 3×10^{13} m^3 en condiciones de presión y temperatura estándar, concluyendo que el antearco activo de la Patagonia es un reservorio importante de hidratos de metano.

KURZFASSUNG

In geologischer Hinsicht liegt Chile in einem einzigartigen Teil der Erde, in dem sich vier Lithosphärenplatten relativ zueinander bewegen (Nazca_Platte, Antarktische Platte, Südamerikanische Platte und Scotia Platte) und damit geometrisch zwei Tripelpunkte definieren (der Chile-Tripelpunkt und der Feuerland-Tripelpunkt). Die konvergenten Plattenränder dieses Systems sind die Ursprünge vieler Erdbeben und der damit zusammenhängenden Tsunamis.

Auf der die Nazca Platte und die Antarktische Platte überfahrenden Südamerikanischen Platte befinden sich mehr als 500 aktive Vulkane, das Orogen der Anden, sowie große Metallvorkommen, die durch aktive oder fossile Hydrothermalsysteme gebildet wurden. Einer der natürlichen Rohstoffe, die in den Mittelpunkt des Interesses der chilenischen Regierung und anderer Institutionen ist, sind die Gashydrate, die sich in den Sedimenten unter dem Meeresboden des Pazifischen Kontinentalrandes befinden. Gashydrate sind feste, eisartige Mischungen aus Wasser und Kohlenwasserstoffen, vorherrschend Methan.

Da Chile den größten Teil des benötigten Erdgases importieren muss, eröffnet die Entdeckung dieser neuen Ressource neue Möglichkeiten für die nationale Wirtschaft. Die Gashydrate sind ebenfalls von wissenschaftlichem Interesse, denn Methan aus der Dissoziation von Gashydrat kann durch das Sediment wandern, den Meeresboden – oder durch das Ozeanwasser hindurch – sogar die Atmosphäre erreichen und somit eine große Bedrohung für die Umwelt darstellen. In dieser Arbeit wird zum Nachweis von Gashydrat der seismische "Bottom Simulating Reflector" (BSR) genutzt, der die halbe Amplitude und umgekehrte Polarität des Meeresbodenreflektors besitzt.

Darüber hinaus spielen Fluide eine Schlüsselrolle bei der Nukleation und Propagation von seismischen Rupturen an konvergenten Plattenrändern, auch weil sie einer der wichtigsten Träger advektiven Wärmetransports aus dem tiefen Untergrund an die Erdoberfläche darstellen. Wenn wir genug Information über die Wärmestromdichte erzeugen ist es möglich, die tektono-thermische Signatur von konvergenten Plattenrändern besser zu verstehen. Zu diesem Zweck ist eine zuverlässige Bestimmung der Tiefenlage des BSR entscheidend, um daraus die stetige Wärmestromdichte q (mW m^{-2}) abzuleiten. Mittels einfacher Gleichungen ist es somit möglich, die regionale Verteilung der Wärmestromdichte abzubilden.

Ziel dieser Dissertation ist, die tektonischen Prozesse im chilenischen forearc durch die Berechnung der regionalen Verteilung der Wärmestromdichte aus der Analyse von BSR, durch die Identifikation von Fluidaustritten, durch die Verteilung von Gashydraten und durch eine Abschätzung der Mengen von Gashydrat und freiem Gas im Sediment zu erhellen.

Eines der wichtigsten Ergebnisse ist die Gewinnung eines regionalen Überblicks all dieser parameter im forearc von Chile. Der BSR ist in marinen Sedimenten, vor allem in denen des Akkretionskeils, zwischen 33°S und 57°S nachweisbar. Am häufigsten kommt er in etwa 2000 m Wassertiefe vor, und dort in Tiefen zwischen 90 m und 600 m unter dem Meeresboden.

Die geschätzte Wärmestromdichte auf dem oberen und mittleren Kontinentalabhang zwischen Valparaiso und Chiloe (33°S bis 43°S) zeigt Werte, wie sie für kontinentales Grundgebirge und überlagernde Hangsedimente typisch sind. Auf dem unteren Kontinentalabhang im Bereich des Akkretionskeils gibt es jedoch

einige Bereiche mit anomal hoher Wärmestromdichte. Dies legt nahe, dass es dort Bereiche advektiven Wärmetransports durch Fluide tiefen Ursprungs gibt, die einen erheblichen Teil des Wärmetransports übernehmen.

Weiter südlich wurde eine zweite Studie in einem großen Gebiet anomal hoher Wärmestromdichte im Bereich des Chile-Tripelpunkts durchgeführt. Hier kommt es zur Subduktion eines aktiven Spreizungsrückens (Chile-Rücken) unter die Südamerikanische Kontinentalplatte. Hier kommen Gashydrate in sehr oberflächennahen Sedimenten vor. Die extrem hohen Wärmestromdichten von bis zu 280 mW m^{-2} zeigen, dass die überfahrende Südamerikanische Platte effektiv durch die rezent entstandene ozeanische Kruste und Lithosphäre aufgeheizt wird.

Um die geologischen Gefahren durch mögliche, plötzliche Dissoziation der Gashydrate und Freisetzung großer Mengen von Methan besser zu verstehen, wurde eine quantitative Abschätzung der Mengen von Gashydraten in dieser Region unternommen.

Schließlich wurde das pazifische Seegebiet vor Patagonien an der Südspitze des Kontinents durch die Analyse der vorhandenen BSR in reflexionsseismischen Profilen untersucht. Die Wärmestromdichten dort sind typisch für die etwa 10 Ma alte ozeanische Kruste, die dort subduziert wird. Die Gashydratkonzentrationen im Sediment landwärts der aktiven Plattengrenze sind hoch. Die mittlere Dicke der Gashydratschicht ist etwa 300 m. Das geschätzte Volumen von Methan in dieser Region ist wohl größer als 3×10^{13} m^3 unter Standardbedingungen für Druck und Temperatur. Dies erlaubt den Schluss, dass der active forearc des chilenischen Teils von Patagonien ein wichtiges Reservoir für Methanhydrat darstellt

CONTENTS

   Villar-Muñoz, L.; Behrmann, J.H.; Diaz-Naveas, J.; Klaeschen, D.; Karstens, J. 2014. *Heat flow in the southern Chile forearc controlled by large-scale tectonic processes*. Geo-Marine Letters. 34: 185. doi: 10.1007/s00367-013-0353-z.

   Villar-Muñoz, L.; Bento, J.P.; Klaeschen, D.; Tinivella, U.; Vargas-Cordero, I.; Behrmann, J.H. 2018. A first estimation of gas hydrates offshore Patagonia (Chile). Marine and Petroleum Geology. 96: 232-239. doi: 10.1016/j.marpetgeo.2018.06.002.

1. INTRODUCTION

1.1. GAS HYDRATES

Natural gas hydrates are crystalline ice-like solids formed by water molecules that enclose mainly methane (Kvenvolden, 1988, 1993, 2003; Fig.1,2). Methane hydrates are located over almost all the continental margins and permafrost if sufficient methane is present (Fig. 3). In those places, the molecules stay stable over a range of mid-pressure (>0.6 MPa) and low temperature (<25 °C) conditions (P-T conditions) (Sloan, 2003). The zone where gas hydrates are stables in the marine sediments is called the Gas Hydrate Stability Zone (GHSZ), and its thickness and position vary from one place to another.
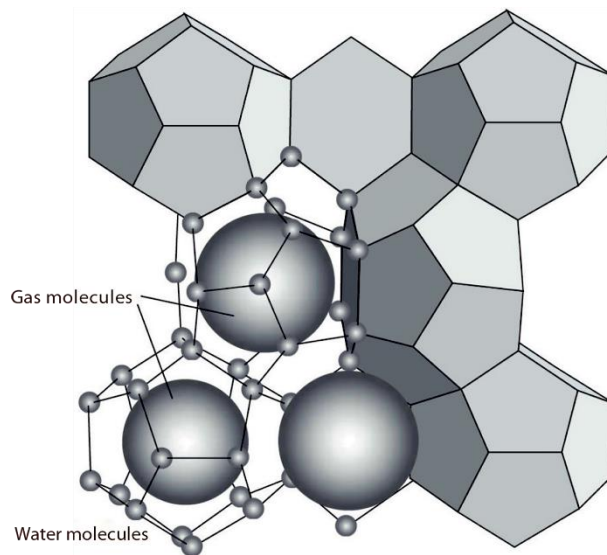

Figure 1: Typical molecular structure of gas hydrate, water molecules (small ball) linked together to form a cage enclosing a gas molecule (large ball). This kind of molecular arrange is called clathrate (Maslin et al, 2010).

Figure 2: Sample of methane hydrate taken offshore Concepcion, Chile (840 meters below sea level), drilled by the research vessel Vidal Gormaz (Cruise VG04). Credit: FONDEF Project D04I1111.
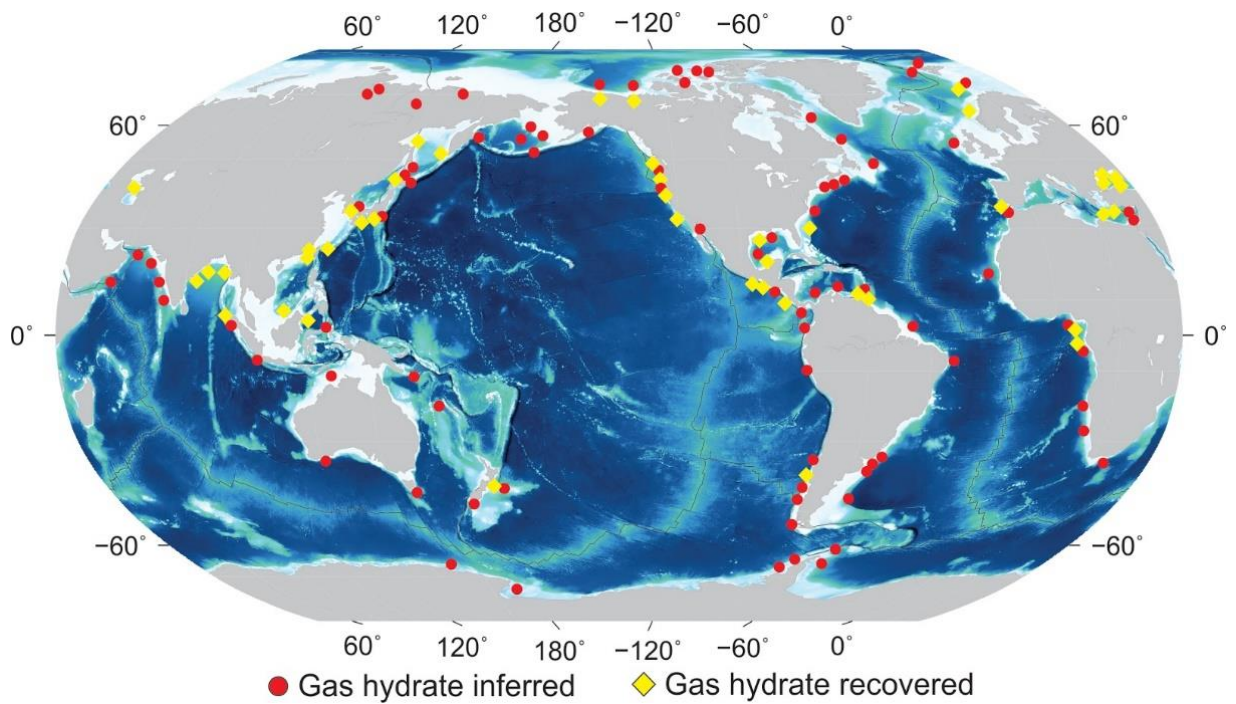

Figure 3: Map showing worldwide locations of inferred gas hydrate deposits (red circles) and locations where gas hydrate has been recovered (yellow diamonds). Modified after Collett, 2009.

The global abundance of gas hydrates in marine sediments remains poorly constrained. Estimates range from 1×10^2 to 5.6×10^4 GtC and a consensus value has not emerged over the past decades (Piñero et al., 2013). Moreover, it is considered that approximately 99% of methane (CH_4) hydrates are found in the marine environment (Max et al., 2013; Ruppel, 2014).

The methane gas can develop in the seafloor sediments in three different ways (Fig. 4):

a) *Microbial methane*: It is formed in the seafloor by the microbial decompose of the remains of marine life (dead planktonic organisms). This process is known as methanogenesis (Whiticar et al, 1986).

b) *Thermogenic methane*: It is formed chemically (without the activity of microorganisms) in deeper sedimentary strata and occurs due to the breakup of organic matter, forced by elevated temperatures (>150 °C) and pressures (Stolper et al., 2014).

c) *Abiotic methane*: It is formed in ultraslow-spreading ocean basins, occurring during the high-temperature (>200 °C) serpentinization of ultramafic rocks (Johnson et al., 2015).

Through either method of methane formation (microbially at shallow depth, thermogenic from a deeper source, or as result of serpentinization in spreading centers) the gases are thought to migrate through advective transport along pathways as fracture networks, faults or shear zones (e.g. Schmidt et al, 2005) and, upon contact with cold seawater, to crystallize into hydrate (Fig.4).
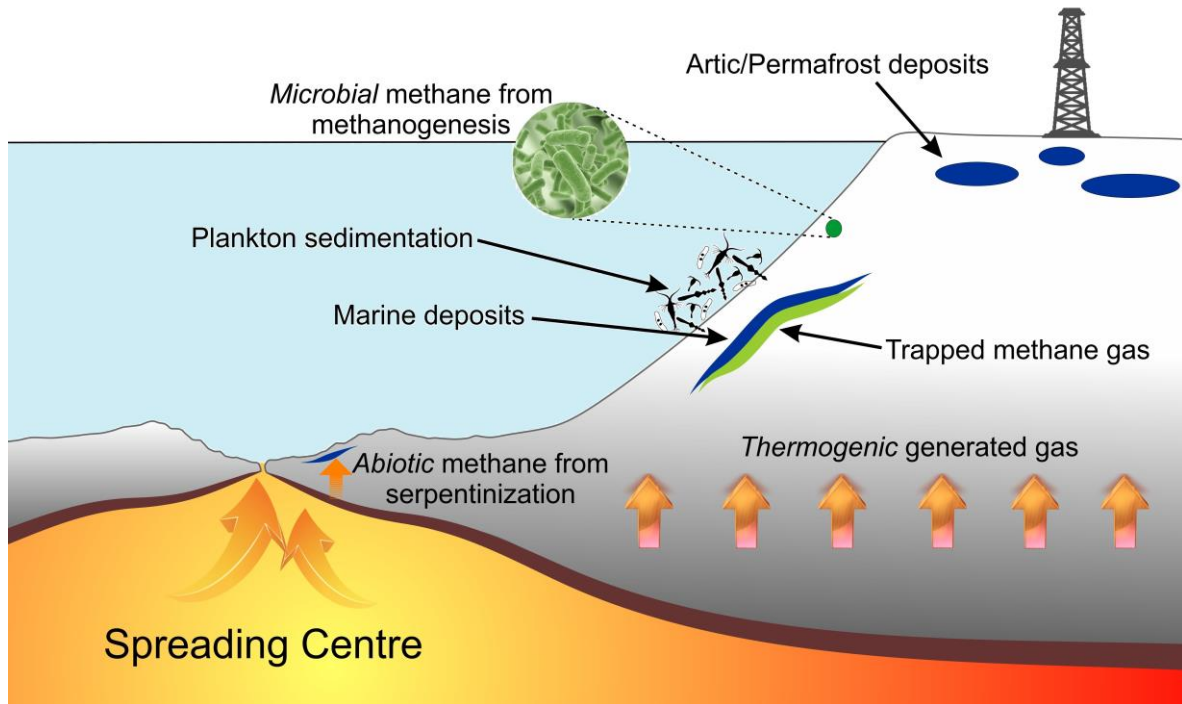
Figure 4: Types of methane hydrate deposits (abiotic, biogenic and thermogenic methane origin) present in the marine sediments (diagram not scaled).

It is important to note that 1 m³ of hydrate will yield 0.8 m³ of water and 164 m³ of methane at standard pressure and temperature (STP: 0°C, 0.101325 Mpa) conditions (Sloan, 1998; Fig. 5). A significant amount of hydrate may be both: an unconventional-potential energy resource (Collet, 2002) and an important player in the global climate change, geo-hazards and potential drilling hazards (e.g. Dickens, 2001; Kvenvolden, 2002; Crutchley et al., 2016; Hovland et al., 2001; Kretschmer et al., 2015; Mountjoy et al., 2014; Ruppel et al., 2017).
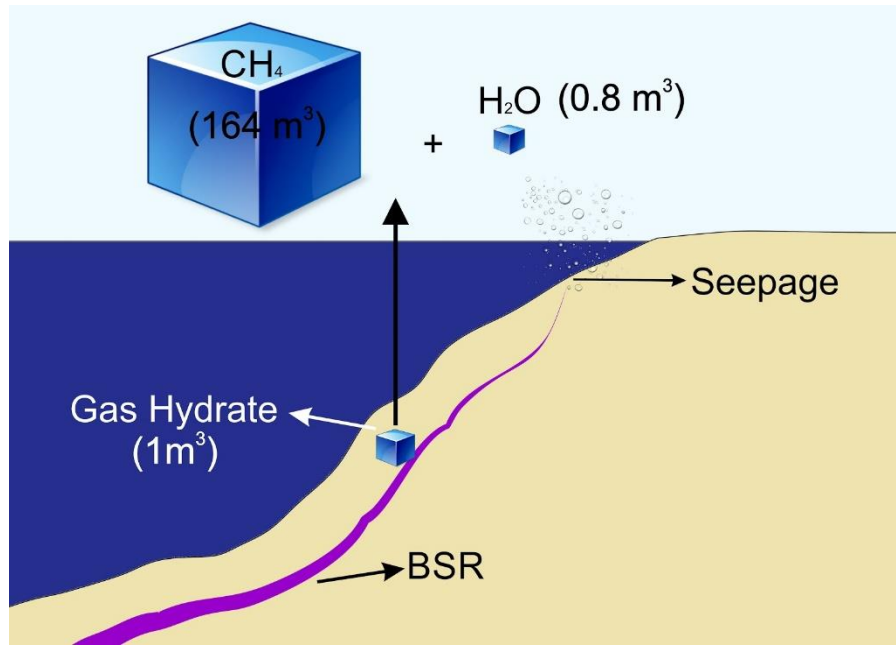
Figure 5: *One cubic meter of gas hydrate yields 164 m³ of gas and 0.8 m³ of water at standard temperature and pressure (diagram not scaled).*

The methane is stored as gas hydrates and can be easily identified in seismic profiles as a prominent reflector so-called bottom-simulating reflector (BSR) (e.g. Hyndman and Spence, 1992). BSRs are probably the most widely used indicators for the presence of natural gas hydrates and mark the base of the gas stability zone. The reflection is caused by the acoustic impedance contrast between sediments containing gas hydrate above and free gas below the gas hydrate stability zone, respectively (e.g. Berndt et al. 2004). Sometimes, the base of the gas reflector (BGR) is also identified in seismic profiles, which helps to calculate the thickness of the sediment layer that contains free gas (Fig. 6).
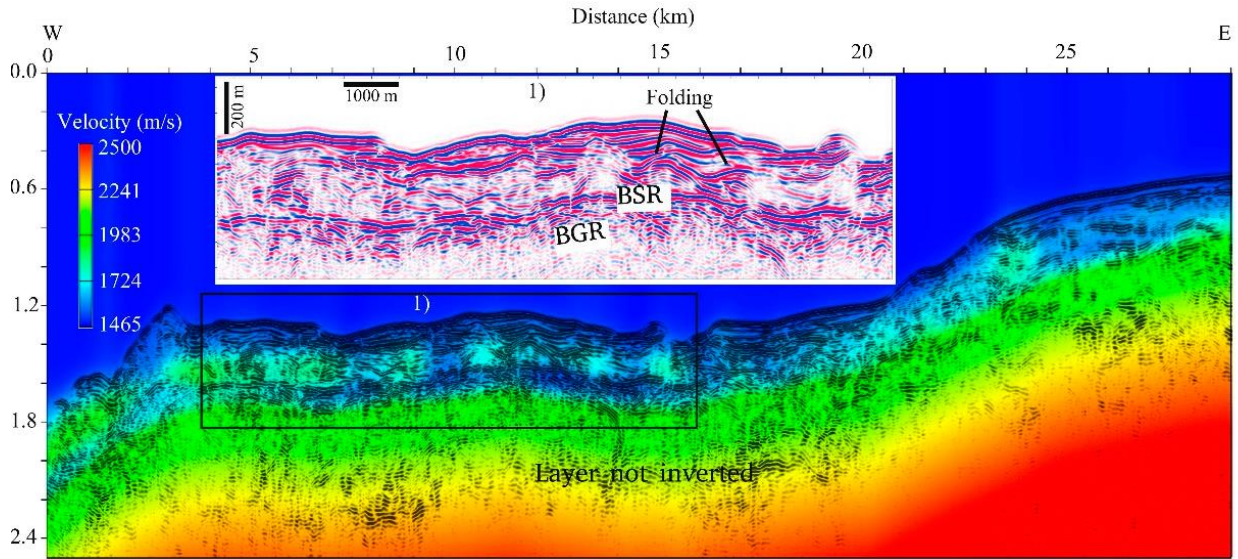
Figure 6: *RC2901–731 seismic section. Pre-stack depth sections with superimposed velocity models. Black boxes indicated with numbers show the blow-ups. Modified from Vargas-Cordero et al., 2018.*

1.2. BSR-DERIVED HEAT FLOW

The stability of gas hydrates is controlled by temperature and pressure conditions (e.g. Grevemeyer et al. 2003), therefore it is used the gas hydrate BSRs to calculate the steady-state heat flow q (mW m^{-2}) using the following formula:

$$q = \frac{T_z - T_0}{\int_0^z \frac{\mathrm{d}z'}{k(z')}}$$

where T_z and T_0 are the temperatures at the BSR and the seafloor respectively (Villinger et al. 2010), k is the thermal conductivity and z denotes the BSR depth. The BSR and seafloor depths can be obtained from seismic profiles; seafloor temperatures are usually taken from CTD measurements (e.g. World Ocean Data Base - http://www.nodc.noaa.gov/); and the thermal conductivity is based on drillcore data (i.e. ODP, IODP, DSDP Legs).

6

The temperature at the depth of the BSR, T_z, is calculated by using the dissociation temperature-pressure function (Dickens and Quinby-Hunt 1994):

$$1/T = 3.79 \times 10^{-3} - 2.83 \times (\log p)$$

where p is the hydrostatic pressure (MPa) and T the temperature (Kelvin). Gas in the system is usually assumed to be pure methane, with a pore water salinity of 35 g l^{-1}. Hydrostatic and lithostatic pressures and depth can be calculated by converting the measured TWT (two way travel time) at the BSR using a velocity-depth function derived from the seismic data (Kaul et al. 2000) or, where available, data from ODP, IODP, DSDP drillholes. To convert water column TWT into depth, a seawater compressional wave velocity of 1,500 m s^{-1} is usually used.

Because of a few uncertain factors, the accuracy of the estimated values is not very high, but the values are consistent with those measured by conventional means (Yamano et al., 1982) and it can be obtained relevant information on the regional distribution of the heat flow.

1.3. **GEOLOGICAL SETTING OF THE CHILEAN CONVERGENT MARGIN**

Along the Chilean margin, it is possible to find two oceanic plates (Nazca and Antarctic plates) subducting below two continental plates (South American and Scotia plates; Fig. 7), and many tectonic features as following from north to south:

a) Between 32° - 46° S the margin is mostly shaped by the subduction of the oceanic Nazca Plate beneath the South American Plate. The present-day rate of convergence is about 6,6 km/Ma, slightly dextrally oblique with an 80° azimuth (Angermann et al. 1999). The age of the subducting Nazca Plate increases northwards of the Chile Triple Junction (e.g. Behrmann et al. 1992,

1994) to about 35 Ma at 32°S, where the Juan Fernandez Ridge merges with the marine forearc (e.g. Tebbens et al.,1997). The shallow Juan Fernandez Ridge (Fig. 7 and 8) comprises a series of seamounts extending for about 900 km in an ENE–WSW direction (von Huene et al. 1997). Where it approaches the Chile trench the ridge forms an efficient barrier for trench-parallel sediment transport from the south, resulting in a trench between 32°S-47°S that is filled with about 1.5-2 km of sediment (Völker et al. 2006) of terrigenous to hemipelagic composition (e.g. Behrmann et al. 1992; Mix et al. 2003; Heberer et al. 2010).

Today, a substantial fraction of the incoming trench sediment along the margin is frontally accreted (e.g. Diaz-Naveas 1999; Geersen et al. 2011), building an active accretionary prism on the lower continental slope. Some of the sediment, however, is also being subducted and brought to greater depths along with the subducting Nazca Plate (Behrmann et al., 2001).
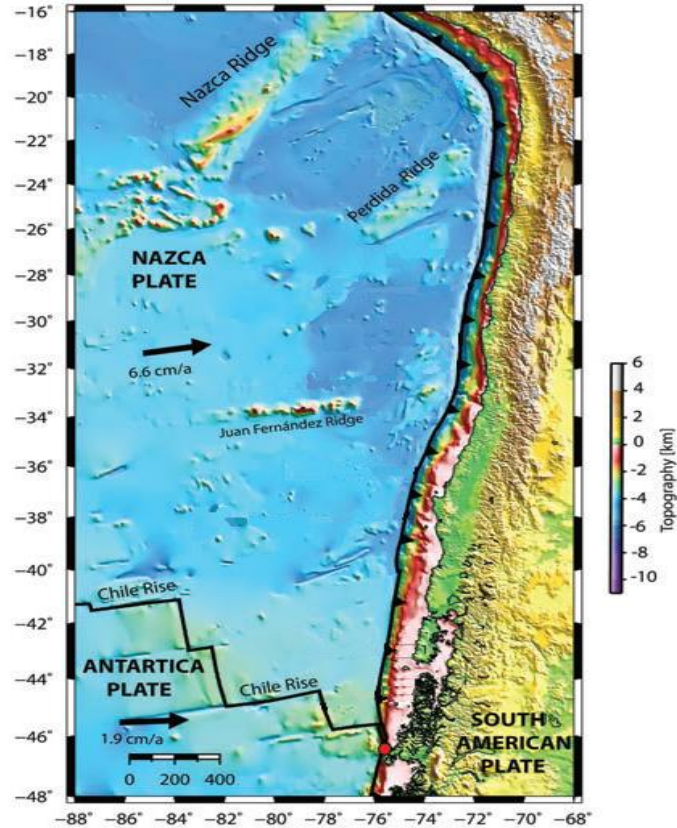
Figure 7: *Geodynamic setting of Nazca, Antarctic and South American plates. The red dot indicates the Chile Triple Junction. The oceanic Nazca Plate is segmented by several fracture zones, resulting in strong variability of the age of the subducting plate. Modified from Contreras et al., 2010.*

Sediment accretion in this area has likely been active since the late Miocene or early Pliocene, following a period of non-accretion or subduction erosion (e.g. Kukowski and Oncken 2006). The switch from subduction erosion to sediment accretion may have been triggered by the glaciation of the Patagonian Andes that became significant about 6 Ma ago, resulting in an increased sediment flux to the trench (e.g. Bangs et al., 1997). Seven major submarine canyons are deeply incised in the forearc and operate as major pathways for sediment transport to the trench (Fig. 8). They are directly connected to river systems that drain the Andes and the coastal Cordillera,

9

and form a link to submarine fans in the trench with silt-sand dominated patterns of sedimentation (e.g. Heberer et al. 2010).
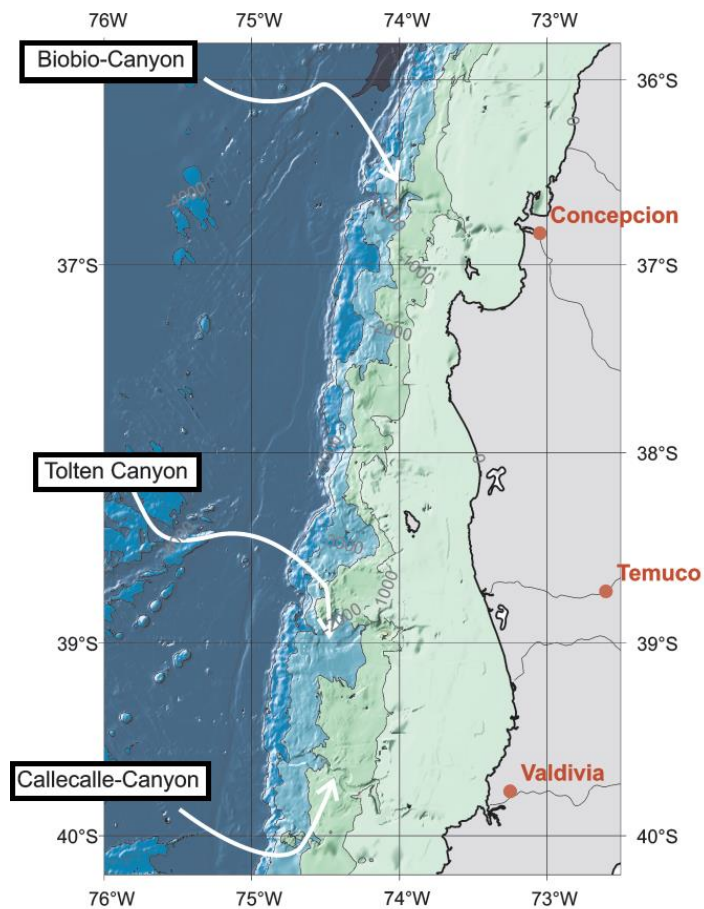

Figure 8: *Example of the three major submarine canyon systems of the 36° S to 41° S sector of the Chilean continental margin. Modified from Völker et al., 2006.*

The active accretionary prism extends upslope from the deformation front to a water depth of about 2,500 m. It is characterized by a sequence of landward-dipping thrust faults that separate individual thrust sheets (Bangs et al., 1997; Geersen et al. 2011a). Deformation results in rough seafloor topography. Further upslope, the Mesozoic palaeo-accretionary prism has a much smoother bathymetric expression, mainly due to a cover of 0.5-2 km of slope and shelf sediments. Active faulting there is restricted to relatively few out-

10

of-sequence thrusts or normal faults (Behrmann et al. 1994; Geersen et al. 2011a). Near the Chilean coastline, there is a transition in the subsurface from the palaeo-accretionary prism to the continental metamorphic basement. In addition to the segmentation across the slope, there is a pronounced structural and seismotectonic north-south segmentation along strike of the plate boundary. For the forearc, this has been interpreted in terms of earthquake rupture (Lomnitz 1970; Comte et al. 1986; Campos et al. 2002; Ruegg et al. 2009), seismicity (Bohm et al. 2002; Haberland et al. 2006), the gravity field (Hackney et al. 2006; Tasárová 2007), the distribution and intensity of submarine mass wasting (Geersen et al. 2011b, 2013; Völker et al. 2012), subduction channel thickness and accretionary prism width (Bangs et al., 1997; Contreras-Reyes et al. 2010; Geersen et al. 2011a), and topography (Rehak et al. 2008).

b) At 46° S the Chile Triple Junction (CTJ) is the site of the intersection of three tectonic plates: Nazca, Antarctic and South America (Behrmann et al., 1994; Cande et al., 1986; Cande et al., 1987). Here, the Chile Rise (CR), an active spreading ridge center, is being subducted beneath the South American continental margin (Fig. 9). Ridge subduction began near Tierra del Fuego 14 million years ago (Ma) and, then, migrated northwards to its current position north of the Taitao Peninsula (e.g. Brown et al., 1996). The Nazca plate subducts beneath South America in an ENE direction at a rate of about 80-90 mm/a north of the CTJ, and the Antarctic plate subducts in an ESE direction at about 20 mm/a south of the CTJ (e.g. Cande et al., 1986). The CR spreading rate has been estimated about 70 km/Ma over the past 5 Ma, but within the last 1 Ma it has slowed down to about 60 km/Ma (e.g. Herron et al., 1981).
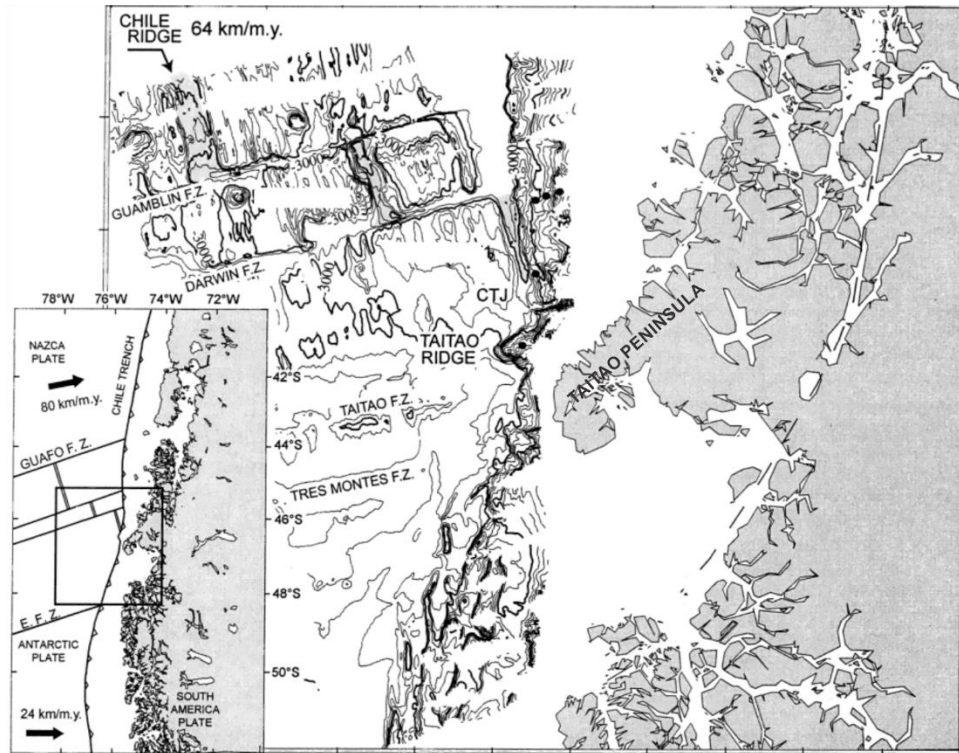
Figure 9: *Bathymetric map of the region around the Chile Triple Junction (CTJ). Modified from*
Bourgois et al., 2000.

In this complex region, we find both active margin tectonic regimes: subduction erosion and subduction accretion occurring in close proximity (e.g., Behrmann et al., 2001). Bourgois et al. (1996) assume that the tectonic evolution of the Chile margin in the area reflects the evolution of the tectonic regime at depth: subduction erosion from 5-5.3 to 1.5-1.6 Ma followed by subduction accretion since 1.5-1.6 Ma. Bangs et al. (1997) suspect that subduction accretion occurring today along the pre-subduction segment is linked to a dramatic post-glacial increase in trench sediment supply. From evidence found by drilling at Ocean Drilling Program (ODP) Site 863 at the CTJ proper, it was concluded that accretion ceased in late Pliocene, and presently the small frontal accretionary prism is undergoing tectonic erosion (Behrmann et al., 1992; Behrmann et al., 1994).

c) The Patagonian area is located in the southernmost tip of South America and is a tectonically complex area (Pelayo and Wiens, 1989), where not only the Antarctic and South American plates are involved, but also the Scotia plate plays an important role in the tectonic (Fig. 10).
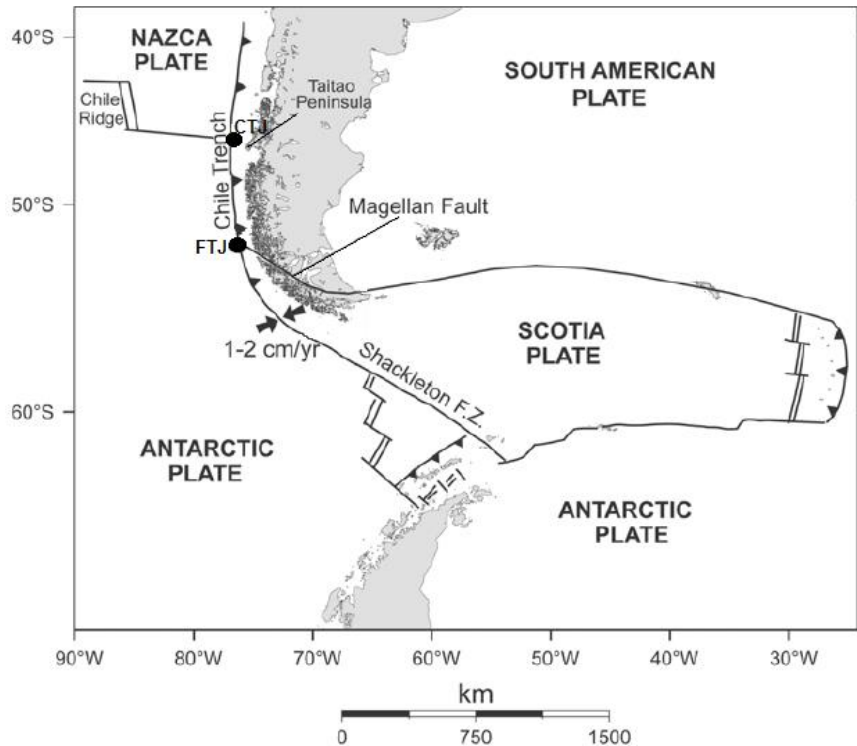
Figure 10: *Regional structural map of the Patagonian region. Black dots indicate the triple junctions (CTJ: Chile Triple Junction, FTJ: Fuegian Triple Junction). Modified from Polonia et al., 2007.*

In the north area, the Antarctic plate is being subducted beneath the South American plate at a rate of 1.9 cmyr^{-1} (Cisterna and Vera, 2008) and the Chilean trench represents the limits of these plates. In the middle area, close to the Evangelistas lighthouse, the Magallanes-Fagnano fault system intersects the Chile trench defining a triple point between the Antarctic, South American and Scotia plates, named as the Fuegian Triple Junction (FTJ)

(Polonia et al., 2001), and it is interpreted to be an unstable and diffused area of deformation (Forsyth, 1975; Cunningham, 1993). Finally, south of FTJ, the Antarctic plate is subducting below the Scotia plate at a rate of 1.3 cmyr^{-1} (Fig. 10) and in turn, the Scotian plate is subducting beneath the South American plate at a rate of 0.7 cmyr^{-1} (Cisterna and Vera, 2008). The convergence direction of the Antarctic plate is almost margin-perpendicular around 52° S and becomes progressively more oblique toward the south (over 60° at ~ 57° S), due to the counter-clockwise rotation of the Patagonian orocline (Cunningham, 1993). Despite that, the seismicity is smaller and less frequent than in the north of Chile, it has been recorded two major earthquakes in the region (Martinic, 1988, 2006; Cisterna and Vera, 2008): in 1879 (~7.5 M) and, seventy years later, in 1949 (7.5 M). During the last episode, were observed landslides, big waves and anomalous currents.

A large volume of incoming sediments marks plate convergence in southern Chile, and von Huene and Scholl (1991) classified this region as a typical accretionary margin. The present-day accretionary prism is interpreted to be post late Miocene in age (Polonia et al., 1999). A well-defined and locally broad late Miocene accretionary prism is growing at the toe of the continental basement (Cande and Leslie, 1986). In the northern part of the study area, between 50° and 53° S, the prism is very narrow and characterized by intense deformation of prism sediments (Loreto, 2005), the décollement level is very shallow, the wedge taper is generally larger than 15°, and frontal thrusts, if present, are seaward vergent. In the southern part, between 53° and 57° S, the deformation style is notably different. Here, the prism is locally very large, its sediment shows clear deformational structures (folds and faults), the taper is 7°-19°, the décollement is deep and sub-horizontal, sediments are locally proto-deformed at the trench along seaward and landward vergent thrusts,

and a large and undeformed forearc basin is present (Polonia et al., 1999, 2001; Loreto, 2005).

1.4. STATE OF THE ART AND HYPOTHESIS

With increasing knowledge of the gas hydrate reservoirs on Earth came a decrease in the estimations how much gas-hydrate bound carbon is stored in the global subsurface. Initially, Kvenvolden (1988) estimated 10,000 Gt of carbon stored in the hydrate and showed its global distribution, present in permafrost (onshore in continental sediments and offshore in sediments of the continental shelves) and in marine sediments of the continental slope. In the oceans, vast areas with hydrates were inferred mainly from marine seismic records via the distribution of the BSR. This first educative estimation was the beginning of gas hydrate exploration worldwide, despite the fact that this later turned out to be an overestimation.

Milkov et al. (2004) published new values of the inventory, ranging from 500 to 2500 Gt of carbon, demonstrating through ODP drillings that the previous values of the concentration in the pore space (around 10%) were overestimations, and suggesting that the role of gas hydrate in global change may also be overestimated.

One of the newest global inventories of the total carbon stored in hydrate reservoirs showed values <500 Gt (Wallmann, 2012), which is two orders of magnitude less than initial values. The latter study was based on improved and better constrained estimates of the global pore volume within the modern GHSZ, the particulate organic carbon accumulation rate, the global rate of microbial methane production in the deep biosphere and the inventory of methane hydrates in marine sediments.

Despite the lower modern estimates, gas hydrates still play an important role in the characterization of the global carbon cycle and climate evolution (Dickens et al., 1995; Maslin et al., 2004; Ruppel et al., 2017), because methane is 25 times more effective than CO2 in defining the warming potential in the atmosphere over a century (IPCC, 2013). Besides, methane hydrate acidifies the seawater and it works as a sink of atmospheric methane, but also could be a source if the trapped methane is released. Since a significant amount of methane is suggested to be trapped in the marine sediments as indicated in the Intergovernmental Panel on Climate Change (IPCC, 2014) and because gas hydrates can dissociate under ocean warming or relative sea-level lowering, the >2,000 km of the Chilean margin between 33°S and 57°S can be considered as one of the most suitable study cases for the quantity and dynamics of gas hydrate reservoirs.

By the end of the Eighties of the past century, many authors had reported gas hydrate occurrences in the accretionary prism along the Chilean margin (Fig. 11), mainly from Valparaíso to the Patagonia region (Bangs et al., 1993; Brown et al., 1996; Diaz-Naveas, 1999; Grevemeyer et al., 2006; Loreto et al, 2007; Morales, 2003; Polonia et al., 1999-2007; Vargas-Cordero 2010-2018). This was by analyzing the BSR in available seismic profiles, as well as by direct identification of cold seeps releasing methane gas at the seafloor during the last years (Coffin et al., 2007; Geersen et al., 2016; German et al., 2010; Jessen et al., 2011; Oliver et al., 2005; Sellanes et al., 2004-2008; Scholz et al., 2013; Völker et al., 2014). The latter evidence brought new insights about the heat transfer through the accretionary prism, especially in the geothermally anomalous Chile Triple Junction area.

In the year 2000, the Chilean government together with national and international Universities started a survey along the continental margin between Valparaiso and

Taitao Peninsula (33-46°S), with the objective to identify the distribution of the hydrate layer and made heat flow measurements for future prospections of the energy potential (Coffin et al., 2006, 2007). Other authors started to explore how to estimate the methane content in this area from gas-phase concentrations by fitting modelled velocity with theoretical velocity in the absence of gas (e.g. Tinivella et al., 2001). These estimates yielded averages ~20% and 1% of the total volume of gas hydrate and free gas concentrations, respectively (e.g. Vargas-Cordero 2010-2018).

Other authors focused on heat flow measurements by heat probes (Grevemeyer et al., 2005, 2006) as well as BSR-derived heat flow (Brown et al., 1995; Grevemeyer et al., 2003). However, those studies were made in restricted areas of the Chilean margin, without an evaluation of the forearc heat flow on a regional scale (>1,000 km strike length).

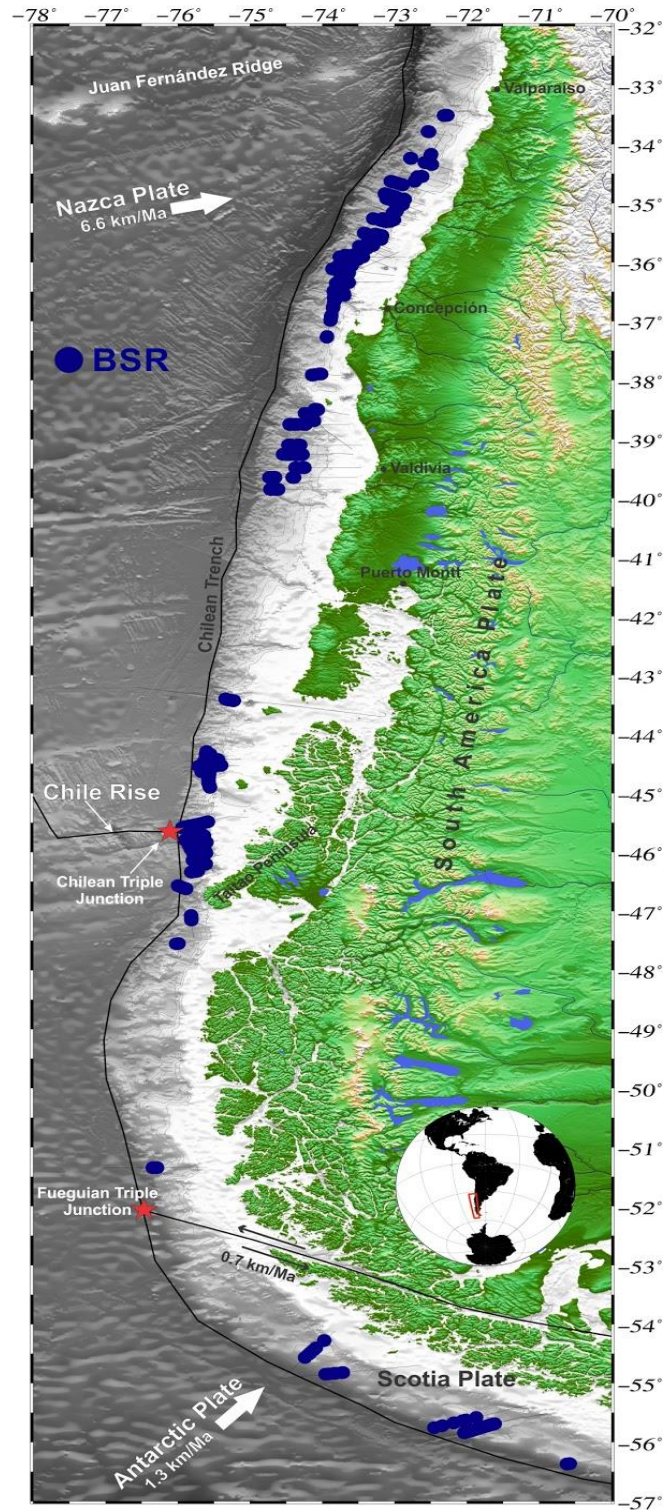***Figure 11****: Overview map of the distribution of the BSR along the Chilean margin (data from GEBCO_08 Grid; version 20091120, http://www.gebco.net). Blue circles indicate BSRs identified on seismic profiles over the accretionary prism and red stars indicate the triple junctions.*

Finally, BSR's were identified in the Patagonia region (Polonia et al., 1999, 2007; Rubio et al., 2000; Loreto et al., 2007), despite the fact that only a few seismic profiles are currently available to the south of Taitao Peninsula (see Fig. 11). In the same way to the northern area, however, so far there has been no evaluation with respect to regional heat flow, nor a semi-quantitative estimation of the gas volume at standard conditions in this interesting area. This is because the accreted sedimentary section there is thick, forearc deformation is strong, and documentation of BSR in seismic sections is widespread.
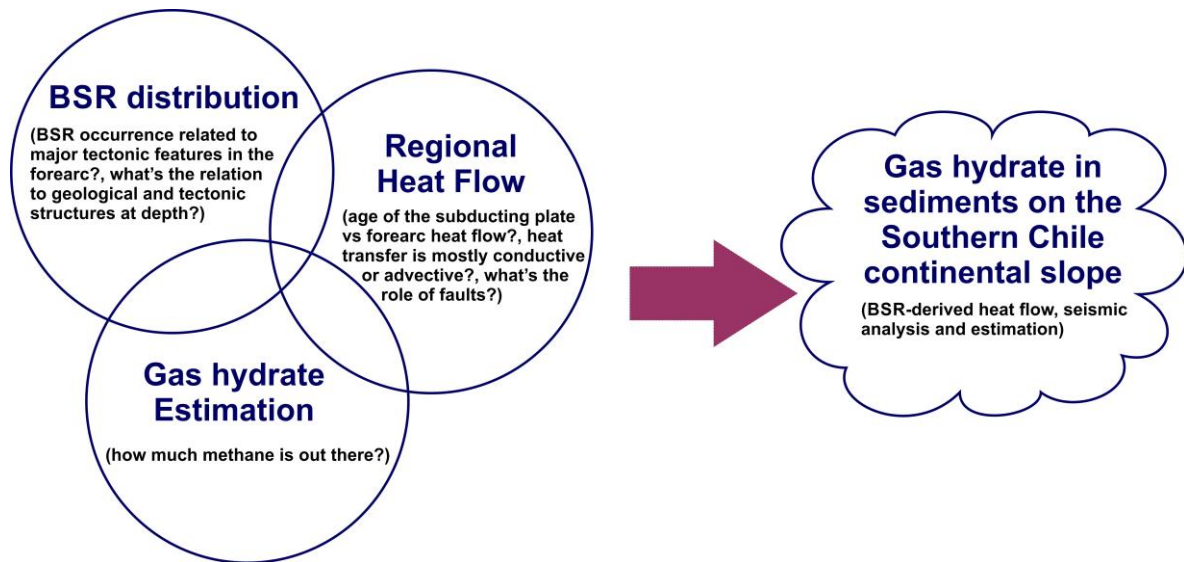
Figure 12: Diagram of the main questions and topics involved in this thesis generation.

From the things said above, I derive some key scientific questions and hypotheses to guide the work reported in this thesis. These are:

- Gas hydrate occurrence along the Chilean convergent plate margin is primarily a reflection of source rock capacity, i.e. the presence of thick terrigenous and hemipelagic sediment sequences that become accreted to the South American continental plate during subduction of the oceanic lower plates.

- Crustal heat flow along the margin is strongly influenced by the age of the subducted slab. These differences constrain the activity of geofluid systems, and the rates at which methane in the sediment can be generated, and migrated into gas hydrate reservoirs.

- Deformation processes in the sediments at the toe of the overriding plate and in the middle and upper forearc influence the formation, continuity, and localization of gas hydrates.

1.5. THESIS OUTLINE

The next chapters (4, 5 and 6) represent stand-alone articles published in scientific journals. They focus on individual aspects related to the distribution of hydrates, the thermal regime, and the estimate of the gas reservoir over the continental margin of Chile. Chapter 7 summarizes the results of the three stand-alone articles and evaluates the main results in the context of the heat flow estimations and gas hydrate researches.

In **Chapter 4**, numerous reflection seismic data are used to identify the BSR distribution and therefore calculate the heat flow variations of the Central-South Chilean Forearc (33°S - 47°S). The novel approach here is the use of BSR-depth data to estimate the thermal regime (heat flow) over a vast region. The results of this study let to visualize and validate the fact of the Nazca plate is heated as it approaches its source: the Chile Triple Junction.

In **Chapter 5**, few reflection seismic data are used to estimate the BSR-derived heat flow in the marine sediments of the western Patagonia region (50°S - 57°S). Additionally, a seismic profile is analyzed and the velocity model is converted into a gas-phase concentration model. The results of this investigation had a huge impact

in Chile, due to the huge amount of methane in the Patagonian reservoir, estimated for the first time, could feed the country's energy matrix for hundreds of years.

Finally, **Chapter 6** concentrates on the analysis of the Chile Triple Junction investigated in the study described in chapter 4. Here, gas hydrates are identified over an extremely anomalous heat flow area that enables vigorous fluid advection. The results describe the conditions that could set the stage for potential massive releases of methane to the ocean.

1.6. ADDITIONAL CONTRIBUTIONS TO PEER-REVIEWED ARTICLES

In addition to the three major manuscripts that form the main body of this thesis, I contributed to new data, observations and interpretations as a co-author to four more articles containing information and knowledge concerning my thesis project. They are entitled:

i. Gas hydrate and free gas estimation from seismic analysis offshore Chiloé island (Chile). **2016**. Iván de la Cruz Vargas-Cordero, Umberta Tinivella, **Lucía Villar-Muñoz** and Michela Giustiniani. Andean Geology. DOI:10.5027/andgeoV43n3-a02.

ii. Gas Hydrate and Free Gas Concentrations in Two Sites inside the Chilean Margin (Itata and Valdivia Offshores). **2017**. Iván Vargas-Cordero, Umberta Tinivella and **Lucía Villar-Muñoz**. Energies. DOI:10.3390/en10122154.

iii. High gas hydrate and free gas concentrations: an explanation for seeps offshore south Mocha Island. **2018**. Iván de la Cruz Vargas-Cordero, Umberta Tinivella, **Lucía Villar-Muñoz** and Joaquim P. Bento. Energies. 11(11), 3062, DOI:10.3390/en11113062.

iv. Pore-water in marine sediments associated to gas hydrate dissociation offshore Lebu, Chile. **2019**. Carolina Cárcamo, Iván Vargas-Cordero, Francisco Fernandoy, Umberta Tinivella, Diego López-Acevedo, Joaquim P. Bento, **Lucía Villar-Muñoz**, Nicole Foucher, Marion San Juan and Alessandra Rivero. Marine and Petroleum Geology. *For Peer Review*.

1.7. REFERENCES FROM INTRODUCTION

Angermann, D.; Klotz, J.; Reigber, C. 1999. Space-geodetic estimation of the Nazca-South America Euler vector. Earth Planet Sci Lett 171: 329–334. doi:10.1016/S0012-821X(99)00173-9.

Bangs, N.L.; Sawyer, D.S.; Golovchenko, X. 1993. Free gas at the base of the gas hydrate zone in the vicinity of the Chile triple Junction. Geology. 21: 905–908.

Bangs, N.L.; Cande, S.C. 1997. Episodic development of a convergent margin inferred from structures and processes along the southern Chile margin. Tectonics. 16: 489–503.

Behrmann, J.H.; Lewis, S.D.; Musgrave, R.; Bangs, N.; Bodén, P.; Brown, K.; Collombat, H.; Didenko, A.N.; Didyk, B.M.; Froelich, P.N.; et al. 1992. Chile Triple Junction. In Proc. ODP. Init. Repts. (Pt. A). 141: 1–708.

Behrmann, J.H.; Lewis, S.D.; Cande, S.C. 1994. Tectonics and geology of spreading ridge subduction at the Chile Triple Junction: A synthesis of results from Leg 141 of the Ocean Drilling Program. Geol. Rundsch. 83: 832–852.

Behrmann, J.H.; Kopf, A. 2001. Balance of tectonically accreted and subducted sediment at the Chile Triple Junction. Int. J. Earth Sci. 90: 753–768.

Berndt, C.; Bünz, S.; Clayton, T.; Mienert, J.; Saunders, M. 2004. Seismic character of bottom simulating reflectors: examples from the mid- Norwegian margin. Mar. Petrol. Geol. 21:723–733.

Bohm, M.; Luth, S.; Echtler, H.; Asch, G.; Bataille, K.; Bruhn, C.; Rietbrock, A.; Wigger, P. 2002. The Southern Andes between 36 degrees and 40 degrees S latitude: seismicity and average seismic velocities. Tectonophysics. 356: 275–289.

Bourgois, J.; Martin, H.; Lagabrielle, Y.; Le Moigne, J.; Frutos Jara, J. 1996 . (Chile margin triple junction area) Subduction erosion related to spreading-ridge subduction: Taitao peninsula. Geology. 24: 723–726.

Bourgois, J.; Guivel, C.; Lagabrielle, Y.; Calmus, T.; Boulègue, J.; Daux, V. 2000. Glacial-interglacial trench supply variation, spreading-ridge subduction, and feedback controls on the Andean margin development at the Chile triple junction area (45–48°S), J. Geophys. Res. 105(B4): 8355–8386. doi:10.1029/1999JB900400.

Brown, K.M.; Bangs, N.L.; Froelich, P.N.; Kvenvolden, K.A. 1996. The nature, distribution, and origin of gas hydrate in the Chile Triple Junction region. Earth Planet. Sci. Lett. 139: 471–483.

Campos, J.; Hatzfeld, D.; Madariaga, R.; Lopez, G.; Kausel, E.; Zollo, A.; Iannacone, G.; Fromm, R.; Barrientos, S.; Lyon-Caen, H. 2002. A seismological study of the 1835

seismic gap in south-central Chile. Phys. Earth Planet Interiors. 132: 177–195. doi:10.1016/S0031-9201(02)00051-1.

Cande, S.C.; Leslie, R.B. 1986. Late Cenozoic tectonics of the southern Chile trench. J. Geophys. Res. 91, 471–496.

Cande, S.C.; Leslie, R.B.; Parra, J.C.; Hodbart, M. 1987. Interaction between the Chile ridge and Chile trench: Geophysical and geothermal evidences. J. Geophys. Res. 92, 495–520.

Cisterna, A.; Vera, E. 2008. Sismos históricos y recientes en Magallanes. Magallania. 36(1): 43-51.

Coffin, R.; Sellanes, J. 2007. Gas Hydrate Exploration, Mid Chilean Coast; Geochemical-Geophysical Survey.

Coffin, R.; Pohlman, J.; Gardner, J.; Downer, R.; Wood, W.; Hamdan, L.; Walker, S.; Plummerg, R.; Gettrus, J.; Diaz, J. 2007. Methane hydrate exploration on the mid Chilean coast: A geochemical and geophysical survey. J. Pet. Sci. Eng. 56: 32–41.

Collett, T. S. 2002. Energy resource potential of natural gas hydrates: AAPG Bulletin. 86(11): 1971-1992.

Collett, T. S.; Johnson A. H.; Knapp C. C.; Boswell R. 2009. Natural Gas Hydrates: A Review, in T. Collett, A. Johnson, C. Knapp, and R. Boswell, eds., Natural gas hydrates - Energy resource potential and associated geologic hazards: AAPG Memoir. 89: 146-219.

Comte, D.; Eisenberg, A.; Lorca, E.; Pardo, M.; Ponce, L.; Saragoni, R.; Singh, S.K.; Suarez, G. 1986. The 1985 central Chile earthquake: a repeat of previous great earthquakes in the region? Science 233:449–453. doi: 10.1126/science.233.4762.449.

Contreras-Reyes, E.; Osses, A. 2010. Lithospheric flexure modelling seaward of the Chile trench: implications for oceanic plate weakening in the Trench Outer Rise region. Geophysical Journal International, 182: 97-112. doi:10.1111/j.1365-246X.2010.04629.x

Crutchley, G.J.; Mountjoy, J.J.; Pecher, I.A.; Gorman, A.R.; Henrys, S.A. 2016. Submarine Slope Instabilities Coincident with Shallow Gas Hydrate Systems: Insights from New Zealand Examples. In Submarine Mass Movements and their Consequences; Advances in Natural and Technological Hazards Research; Lamarche, G., Mountjoy, J., Bull, S., Hubble, T., Krastel, S., Lane, E., Micallef, A., Moscardelli, L., Mueller, C., Pecher, I., Eds.; Springer: Cham, Switzerland. 41p.

Cunningham, W.D. 1993. Strike-slip faults in the southernmost Andes and the development of the Patagonian orocline. Tectonics. 12: 169-186.

Diaz-Naveas, J. 1999. Sediment subduction and accretion at the Chilean convergent margin between 35° and 40°S. PhD Dissertation, University of Kiel, Kiel.

Dickens, G.R.; Quinby-Hunt, M.S. 1994. Methane hydrate stability in seawater. Geophys. Res. Lett. 21:2115–2118.

Dickens, G. R.; O´Neil, J. R.; Rea, D. K.; Owen, R. M. 1995. Dissociation of oceanic methane hydrate as a cause of the carbon isotope excursion at the end of the Paleocene. Paleoceanography. 10: 965-971.

Dickens, G.R. 2001. On the fate of past gas: what happens to methane released from a bacterially mediated gas hydrate capacitor? Geochem. Geophys. Geosystems. 2, 131.

Forsyth, D.W. 1975. Fault plane solutions and tectonics of the South Atlantic and Scotia Sea. Journal of Geophysical. 80: 1429-1443.

Geersen, J.; Behrmann, J.H.; Völker, D.; Krastel, S.; Ranero C.R.; Diaz-Naveas, J.; Weinrebe, W. 2011a. Active tectonics of the South Chilean marine forearc (35°S-40°S). Tectonics 30, TC3006. doi:10.1029/2010TC002777.

Geersen, J.; Voelker, D.; Behrmann, J.H.; Reichert, C.; Krastel, S. 2011b. Pleistocene giant slope failures offshore Arauco Peninsula, Southern Chile. J. Geol. Soc. 168: 1237–1248.

Geersen, J.; Völker, D.; Behrmann, J.H.; Kläschen, D.; Weinrebe, W.; Krastel, S.; Reichert, C. 2013. Seismic rupture during the 1960 Great Chile and the 2010 Maule earthquakes limited by a giant Pleistocene submarine slope failure. Terra Nova. 25: 472–477.

Geersen, J.; Scholz, F.; Linke, P.; Schmidt, M.; Lange, D.; Behrmann, J.H.; Volker, D.; Hensen, C. 2016. Fault zone controlled seafloor methane seepage in the rupture area

of the 2010 Maule earthquake, Central Chile. Geochem. Geophys. Geosyst. 17: 4802–4813.

German, C.R.; Shank, T.M.; Lilley, M.D.; Lupton, J.E.; Blackman, D.K.; Brown, K.M.; Baumberger, T.; FrühGreen, G.; Greene, R.; Saito, M.A.; et al. 2010. Hydrothermal Exploration at the Chile Triple Junction-ABE's Last Adventure. In AGU Fall Meeting Abstracts; American Geophysical Union: Washington, DC, USA.

Grevemeyer, I.; Diaz-Naveaz, J.L.; Ranero, C.R.: Villinger, H.W. 2003. Heat flow over the descending Nazca plate in Central Chile, 32°S to 41°S: observations from ODP Leg 202 and the occurrence of natural gas hydrates. Earth Planet. Sci. Lett. 213:285–298.

Grevemeyer, I.; Kaul, N.; Díaz-Naveas, J.L. 2006. Geothermal evidence for fluid flow through the gas hydrate stability field off Central Chile-transient flow related to large subduction zone earthquakes? Geophys. J. Int. 166: 461–468.

Hackney, R.I.; Echtler, H.P.; Franz, G.; Götze, H-J.; Lucassen, F.; Marchenko, D.; Melnick, D.; Meyer, U.; Schmidt, S.; Tasárová, Z.; Tassara, A.; Wiedecke, S. 2006. The segmented overriding plate and coupling at the South-Central Chilean margin (36–42°S). In: Oncken O, Chong G, Franz G, Giese P, Götze H-J, Ramos VA, Strecker MR, Wigger P (eds) The Andes - active subduction orogeny. Springer, Berlin, pp 355–374.

Heberer, B.; Roeser, G.; Behrmann, J.H.; Rahn, M.; Kopf, A. 2010. Holocene sediments from the Southern Chile Trench: a record of active margin magmatism, tectonics, and paleo seismicity. J. Geol. Soc. 167: 539–553. doi:10.1144/0016-76492009-015.

Herron, E.M.; Cande, S.C.; Hall, B.R. 1981. An active spreading center collides with a subduction zone: A geophysical survey of the Chile margin triple Junction. Mem. Geol. Soc. Am. 154, 683–701.

Hovland, M.; Orange, D.; Bjorkum, P.A.; Gudmestad, O.T. 2001. Gas hydrate and seeps-effects on slope stability: The "hydraulic model". In Proceedings of the Eleventh International Offshore and Polar Engineering Conference, Stavanger, Norway, 17–22. 1: 471–476.

Hyndman, R.D.; Spence, G.D. 1992. A seismic study of methane hydrate marine bottom-simulating-reflectors. J. Geophys. Res. 97: 6683–6698.

Intergovernmental Panel on Climate Change (IPCC). 2013. Climate Change 2013: The Physical Science Basis. Contribution of Working Group I to the Fifth Assessment Report of the Intergovernmental Panel on Climate Change, Cambridge Univ. Press, Cambridge, U.K., and New York.

Intergovernmental Panel on Climate Change (IPCC). 2014. Climate Change 2014: Synthesis Report. Contribution of Working Groups I, II and III to the Fifth Assessment Report of the Intergovernmental Panel on Climate Change. Core Writing Team, R.K. Pachauri and L.A. Meyer, Geneva 151 pp.

Jessen, G.L.; Pantoja, S.; Gutierrez, M.A.; Quinones, R.A.; Gonzalez, R.R.; Sellanes, J.; Kellermann, M.Y.; Hinrichs, K.U. 2011. Methane in shallow cold seeps at Mocha Island off central Chile. Cont. Shelf Res. 31: 574–581.

Johnson, J.E.; Mienert, J.; Plaza-Faverola, A.; Vadakkepuliyambatta, S.; Knies, J.; Bünz, S.; Andreassen, K.; Ferré, B. 2015. Abiotic methane from ultraslow-spreading ridges can charge Arctic gas hydrates. Geology. 43, 371–374.

Kaul, N.; Rosenberger, A.; Villinger, H. 2000. Comparison of measured and BSR-derived heat flow values, Makran accretionary prism, Pakistan. Mar. Geol. 164: 37–51.

Kretschmer, K.; Biastoch, A.; Rüpke, L.; Burwicz, E. Modeling the fate of methane hydrates under global warming. 2015. Glob. Biogeochem. Cycles. 29: 610–625.

Kukowski, N.; Oncken, O. 2006. Subduction erosion – the "normal" mode of fore-arc material transfer along the Chilean Margin? In: Oncken O, Chong G, Franz G, Giese P, Götze H-J, Ramos VA, Strecker MR, Wigger P (eds) The Andes – active subduction orogeny. Springer, Berlin, pp 217–236.

Kvenvolden, K.A. 1988. Methane hydrate-a major reservoir of carbon in the shallow geosphere? Chem. Geol. 71: 41-51.

Kvenvolden, K.A; Ginsburg, G.D.; Soloviev, V.A.1993. Worldwide distribution of subaquatic gas hydrates. Geo-Marine Lett. 13: 32-40.

Kvenvolden, K.A. 2002. Methane hydrate in the global organic carbon cycle. Terra Nova 14 (5), 302-306.

Kvenvolden, K. A. and Lorenson, T. D. 2013. The Global Occurrence of Natural Gas Hydrate. In Natural Gas Hydrates: Occurrence, Distribution, and Detection (eds C. K. Paull and W. P. Dillon). doi:10.1029/GM124p0003.

Lomnitz, C. 1970. Major earthquakes and tsunamis in Chile during the period 1535 to 1955. Geol Rdsch 59: 938–960. doi:10.1007/BF02042278.

Loreto, M.F. 2005. Analisi dei processi di subduzione della Placca Antartica al largo della Terra del Fuoco (Cile Meridionale). PhD thesis, University of Parma, Dip. of Earth Science.

Loreto, M.F.; Tinivella, U.; Ranero, C. 2007. Evidence for fluid circulation, overpressure and tectonic style along the Southern Chilean margin. Tectonophysics. 429: 183–200.

Martinic, M. 1988. El gran temblor de tierra de 1879 en la Patagonia Austral. Revista Patagónica. 30-31.

Martinic, M. 2006. Documentos inéditos para la historia de Magallanes. El fallido intento colonizador en Muñoz Gomero 1969-1971. Magallania. 34(2): 119-124.

Maslin, M.; Owen, M.; Day, S.; Long, D. 2004. Linking continental-slope failure and climate change: testing the clathrate gun hypothesis. Geology. 32: 53-56.

Maslin, M.; Owen, M.; Betts, R.; Day, S.; Dunkley Jones, T.; Ridgwell, A. 2010. Gas hydrates: past and future geohazard?. Philosophical Transactions of the Royal Society A: Mathematical, Physical and Engineering Sciences. 368: 2369-2393.

Max, M.D.; Johnson, A.H.; Dillon, W.P. 2013. Natural Gas Hydrate e Arctic Ocean Deepwater Resource Potential. Springer Cham, Heidelberg New York Dordrecht London, doi:10.1007/978-3-319-02508-7.

Mix, A.C.; Tiedemann, R.; Blum, P.; et al. 2003. Proc Ocean Drilling Program Initial Reports, vol 202. Ocean Drilling Program, College Station, TX.

Morales, E. 2003. Methane hydrates in the Chilean continental margin. Electron J. Biotechnol 6(2). http://ejb.ucv.cl/content/vol6/issue2/issues/1/

Mountjoy, J.J.; Pecher, I.; Henrys, S.; Crutchley, G.; Barnes, P.M.; Plaza-Faverola, A. 2014. Shallow methane hydrate system controls ongoing, downslope sediment transport in a low-velocity active submarine landslide complex, Hikurangi Margin, New Zealand. Geochem. Geophys. Geosyst. 15: 4137–4156.

Piñero, E.; Marquardt, M.; Hensen, C.; Haeckel, M.; Wallmann, K. 2012. Estimation of the global inventory of methane hydrates in marine sediments using transfer functions. Biogeosciences. 10: 959–975. doi:10.5194/bg-10-959-2013.

Oliver, P.G.; Sellanes, J. 2005. New species of Thyasiridae from a methane seepage area off Concepción, Chile. Zootaxa. 1092: 1–20.

Pelayo, A.M.; Wiens, D.A. 1989. Seismotectonics and relative plate motion in the Scotia Sea region. Journal of Geophysical Research. 94: 7293-7320.

Polonia, A.; Brancolini, G.; Torelli, L.; Vera, E. 1999. Structural variability at the active continental margin off southernmost Chile. J. Geodyn. 27, 289–307.

Polonia, A.; Brancolini, G.; Torelli, L. 2001. The accretionary complex of southernmost Chile from the strait of Magellan to the Drake passage. Terra Antarct. 8: 87–98.

Polonia, A.; Torelli, L.; Brancolini, G.; Loreto, M.F. 2007. Tectonic accretion versus erosion along the southern Chile trench: Oblique subduction and margin segmentation. Tectonics. 26, TC3005.

Rehak, K.; Strecker, M.R.; Echtler, H.P. 2008. Morphotectonic segmentation of an active forearc, 37°–41°S, Chile. Geomorphology 94: 98–116.

Rubio, E.; Torné, M.; Vera, E.; Díaz, A. 2000. Crustal structure of the southernmost Chilean margin from seismic and gravity data. Tectonophysics. 323: 39-60.

Ruegg, J.C.; Rudloff, A.; Vigny, C.; Madariaga, R.; de Chabalier, J.B.; Campos, J.; Kausel, E.; Barrientos, S.; Dimitrov, D. 2009. Interseismic strain accumulation measured by GPS in the seismic gap between Constitución and Concepción in Chile. Phys. Earth Planet Interiors. 175: 78–85. doi:10.1016/j.pepi.2008.02.015

Ruppel, C. 2014. Permafrost-Associated Gas Hydrate: Is It Really Approximately 1 % of the Global System? Journal of Chemical & Engineering Data. 60(2):429-436, doi: 10.1021/je500770m.

Ruppel, C.D.; Kessler, J.D. 2017. The interaction of climate change and methane hydrates. Rev. Geophys. 55: 126-168.

Sellanes, J.; Quiroga, E.; Gallardo, V. 2004. First direct evidence of methane seepage and associated chemosynthetic communities in the bathyal zone off Chile. J. Mar. Biol. Assoc. UK. 84: 1065–1066.

Sellanes, J.; Krylova, E. 2005. A new species of Calyptogena (Bivalvia, Vesicomyidae) from a recently discovered methane seepage area off Concepción Bay, Chile (36S). J. Mar. Biol. Assoc. UK. 85: 969–976.

Sellanes, J.; Quiroga, E.; Neira, C. 2008. Megafaunal community structure and trophic relationships of the recently discovered Concepción Methane Seep Area (Chile, 36S). ICES J. Mar. Sci. 65: 1102–1111.

Schmidt, M.; Hensen, C.; Morz, T.; Müller, C.; Grevemeyer, I.; Wallmann, K.; Mau, S.; Kaul, N. 2005. Methane hydrate accumulation in Mound 11 mud volcano, Costa Rica forearc. Mar. Geol. 216, 77–94.

Scholz, F.; Hensen, C.; Schmidt, M.; Geersen, J. 2013. Submarine weathering of silicate minerals and the extent of pore water freshening at active continental margins. Geochim. Cosmochim. Acta. 100: 200–216.

Sloan, E.D. Clathrate Hydrates of Natural Gases, 2nd ed. 1998. CRC Press: Boca Raton, FL, USA. 705p.

Sloan, E.D. Fundamental principles and applications of natural gas hydrates. 2003. Nature. 426: 353-363.

Stolper, D.A.; Lawson, M.; Davis, C.L.; Ferreira, A.A.; Santos Neto, E.V.; Ellis, G.S.; Lewan, M.D.; Martini, A.M.; Tang, Y.; Schoell, M.; Sessions, A.L.; Eiler, J.M. 2014. Gas formation. Formation temperatures of thermogenic and biogenic methane. Science. 344(6191):1500-3. doi: 10.1126/science.1254509.

Tasárová, Z. 2007. Towards understanding the lithospheric structure of the southern Chilean subduction zone (36°S–42°S) and its role in the gravity field. Geophys. J. Int. 170: 995–1014.

Tebbens, S.F.; Cande, S.C. 1997. Southeast Pacific tectonic evolution from early Oligocene to Present. J. Geophys. Res. Solid Earth. 102: 12061–12084. doi:10.1029/96JB02582.

Tinivella, U.; Carcione, J.M. 2001. Estimation of gas-hydrate concentration and free-gas saturation from log and seismic data. Lead Edge. 20: 200-203.

Vargas-Cordero, I.; Tinivella, U.; Accaino, F.; Loreto, M.F.; Fanucci, F. 2010. Thermal state and concentration of gas hydrate and free gas of Coyhaique, Chilean Margin (44° 30′ S). Mar. Pet. Geol. 27: 1148–1156.

Vargas-Cordero, I.; Tinivella, U.; Accaino, F.; Fanucci, F.; Loreto, M.F.; Lascano, M.E.; Reichert, C. 2011. Basal and Frontal Accretion Processes versus BSR Characteristics along the Chilean Margin. J. Geol. Res. 2011: 1–10.

Vargas-Cordero, I.; Tinivella, U.; Villar-Muñoz, L.; Giustiniani, M. 2016. Gas hydrate and free gas estimation from seismic analysis offshore Chiloé island (Chile). Andean Geol. 43: 263–274.

Vargas-Cordero, I.; Tinivella, U.; Villar-Muñoz, L. 2017. Gas Hydrate and Free Gas Concentrations in Two Sites inside the Chilean Margin (Itata and Valdivia Offshores). Energies. 10, 2154.

Vargas-Cordero, I.; Tinivella, U.; Villar-Muñoz, L.; Bento, J.P. 2018. High Gas Hydrate and Free Gas Concentrations: An Explanation for Seeps Offshore South Mocha Island. Energies. 11, 3062.

Villinger, H.; Tréhu, A.M.; Grevemeyer, I. 2010. Seafloor marine heat flux measurements and estimation of heat flux from seismic observations of bottom simulating reflectors. In: Riedel M, Willoughby EC, Chopra S (eds) Geophysical characterization of gas hydrates. Society of Exploration Geophysicists, Tulsa, OK, 279–300.

Völker, D.; Wiedicke, M.; Ladage, S.; Gaedicke, C.; Reichert, C.; Rauch, K.; Kramer, W.; Heubeck, C. 2006. Latitudinal variation in sedimentary processes in the Peru-Chile Trench off Central Chile. In: Oncken O, Chong G, Franz G, Giese P, Götze H-J, Ramos VA, Strecker MR, Wigger P (eds) The Andes – active subduction orogeny. Springer, Berlin. 193–216.

Völker, D.; Geersen, J.; Behrmann, J.H.; Weinrebe, W.R. 2012. Submarine mass wasting off southern central Chile: distribution and possible mechanisms of slope failure at an active continental margin. In: Yamada Y, Kawamura K, Ikehara K, Ogawa Y, Urgeles R, Mosher D, Chaytor J, Strasser M (eds) Submarine mass movements and their consequences. Springer, Heidelberg, pp 379–389. doi:10.1007/978-94-007-2162-3_34.

Völker, D.; Geersen, J.; Contreras-Reyes, E.; Sellanes, J.; Pantoja, S.; Rabbel, W.; Thorwart, M.; Reichert, C.; Block, M.; Weinrebe, W.R. 2014. Morphology and geology of the continental shelf and upper slope of southern Central Chile (33S–43S). Int. J. Earth Sci. (Geol. Rundsch.). 103, 1765.

von Huene, R.; Scholl, D.V. 1991. Observations at convergent margins concerning sediment subduction, subduction erosion, and the growth of continental crust. Reviews of Geophysics. 29(3): 279-316. doi:10.1029/91RG00969.

von Huene, R.; Corválan, J.; Flueh, E.R.; Hinz, K.; Korstgard, J.; Ranero, C.R.; Weinrebe, W.; Scientists CONDOR. 1997. Tectonic control of the subducting Juan Fernández Ridge on the Andean margin near Valparaiso, Chile. Tectonics. 16: 474-488.

Wallmann, K.; Pinero, E.; Burwicz, E.; Haeckel, M.; Hensen, C.; Dale, A.; Ruepke, L. 2012. The Global Inventory of Methane Hydrate in Marine Sediments: A Theoretical Approach. Energies. 5: 2449-2498.

Whiticar, M.J.; Faber, E. 1986. Methane oxidation in sediment and water column environments. Isotope evidence, Organic Geochemistry. 10(4–6): 759-768, doi:10.1016/S0146-6380(86)80013-4.

Yamano, M.; Uyeda, R.M.; Aoki, Y.; Shipley, T.H. 1982. Estimates of heat flow derived from gas hydrates. Geology 10: 339–343.

2. MANUSCRIPT #1

Villar-Muñoz, L.; Behrmann, J.H.; Diaz-Naveas, J.; Klaeschen, D.; Karstens, J. 2014. *Heat flow in the southern Chile forearc controlled by large-scale tectonic processes*. Geo-Marine Letters. 34: 185. doi: 10.1007/s00367-013-0353-z.

ORIGINAL

Heat flow in the southern Chile forearc controlled by large-scale tectonic processes

Lucia Villar-Muñoz · Jan H. Behrmann ·
Juan Diaz-Naveas · Dirk Klaeschen · Jens Karstens

Abstract Between 33°S and 47°S, the southern Chile forearc is affected by the subduction of the aseismic Juan Fernandez Ridge, several major oceanic fracture zones on the subducting Nazca Plate, the active Chile Ridge spreading centre, and the underthrusting Antarctic Plate. The heat flow through the forearc was estimated using the depth of the bottom simulating reflector obtained from a comprehensive database of reflection seismic profiles. On the upper and middle continental slope along the whole forearc, heat flow is about 30–60 mW m^{-2}, a range of values common for the continental basement and overlying slope sediments. The actively deforming accretionary wedge on the lower slope, however, in places shows heat flow reaching about 90 mW m^{-2}. This indicates that advecting pore fluids from deeper in the subduction zone may transport a substantial part of the heat there. The large size of the anomalies suggests that fluid advection and outflow at the seafloor is overall diffuse, rather than being restricted to individual fault structures or mud volcanoes and mud mounds. One large area with very high heat flow is associated with a major tectonic feature. Thus, above the subducting Chile Ridge at 46°S, values of up to 280 mW m^{-2} indicate that the overriding South American Plate is effectively heated by subjacent zero-age oceanic plate material.

L. Villar-Muñoz (✉) · J. H. Behrmann · D. Klaeschen · J. Karstens
GEOMAR Helmholtz Centre for Ocean Research,
Wischhofstr 1-3, 24148 Kiel, Germany
e-mail: lvillar@geomar.de

J. Diaz-Naveas
Escuela de Ciencias del Mar, Pontificia Universidad Católica de
Valparaíso, Av. Altamirano, 1480 Valparaíso, Chile

Introduction

Subduction zones are the global sinks for lithospheric rocks and fluids, and the sedimentary rocks covering the oceanic crust on the incoming plate are highly porous and fluid-filled. They also contain variable amounts of organic carbon beneath the overriding plate, which is converted to methane and, to a lesser extent, higher hydrocarbons by biogenic or thermogenic processes. In subduction zones, fluids play a key role in the nucleation and rupture propagation of earthquakes, and are a major agent of advective heat transfer from depth to the Earth's surface. Measurements in drillholes by means of near-surface heat flow probes are a first-order data source but often do not provide enough information for the regional analysis of crustal heat flow. On the other hand, gas hydrates occur in vast areas worldwide in sediments beneath continental slopes (e.g. Kvenvolden 1998; Milkov 2004), and their stability relations can serve to estimate geothermal gradients and, thus, heat flow and its regional variations (e.g. Ganguly et al. 2000). Thus, a prominent feature on reflection seismic profiles is the bottom-simulating reflector (BSR) marking the base of the gas hydrate stability zone (e.g. Hyndman and Spence 1992; Berndt et al. 2004); its depth is a constraint for pressure and temperature in the subsurface.

In this paper the results of an analysis of regional crustal heat flow on the southern and central Chilean continental margin between approx. 33° and 47° southern latitude are presented. For this purpose the BSR distribution was used, and the results were calibrated with the help of available independent heat flow data from near-surface probes and drillholes. Here, gas hydrate occurrence is widespread and has been documented in numerous studies dealing with smaller segments of the margin (e.g. Bangs et al. 1993; Bangs and Brown 1995; Froelich et al. 1995; Brown et al. 1996; Grevemeyer and Villinger 2001; Morales 2003; Grevemeyer et al. 2003, 2006; Vargas Cordero 2009;

Vargas Cordero et al. 2010a, 2010b, 2011). However, to date there has not been a coherent evaluation of forearc heat flow on the scale of a large (>1,000 km strike length) segment of the Chile convergent plate boundary. By such an analysis, the following questions can be addressed:

1. What is the relationship between the age of the subducting plate and forearc heat flow?
2. Is heat transfer through the forearc primarily conductive, or is there evidence for focused advective heat transfer through areas of distributed deformation, like fold-fault packages in accretionary wedges, or individual major fault structures?
3. Does BSR occurrence relate to major tectonic features in the forearc and, if so, what is the relation to geological and tectonic structures at depth?

Geological and tectonic setting

The Chilean margin between 32°S–47°S is mostly shaped by the subduction of the oceanic Nazca Plate beneath the South American Plate (Fig. 1a). The present-day rate of convergence is about 66 mm per year, slightly dextrally oblique with an 80° azimuth (Angermann et al. 1999). The age of the subducting Nazca Plate increases northwards of the Chile Triple Junction (e.g. Behrmann et al. 1992, 1994) to about 35 Ma at 32°S, where the Juan Fernandez Ridge merges with the marine forearc (e.g. Tebbens and Cande 1997). The shallow Juan Fernandez Ridge (Fig. 1) comprises a series of seamounts extending for about 900 km in an ENE–WSW direction (von Huene et al. 1997). Where it approaches the Chile trench the ridge forms an efficient barrier for trench-parallel sediment transport from the south, resulting in a trench between 32°S–47°S that is filled with about 1.5–2 km of sediment (Völker et al. 2006) of terrigenous to hemipelagic composition (e.g. Behrmann et al. 1992; Mix et al. 2003; Heberer et al. 2010).

Today, a substantial fraction of the incoming trench sediment along the margin is frontally accreted (e.g. Diaz-Naveas 1999; Geersen et al. 2011a), building an active accretionary prism on the lower continental slope. Some of the sediment, however, is also being subducted and brought to greater depths along with the subducting Nazca Plate (Behrmann and Kopf 2001). Sediment accretion in the study area has likely been active since the late Miocene or early Pliocene, following a period of non-accretion or subduction erosion (e.g. Kukowski and Oncken 2006). The switch from subduction erosion to sediment accretion may have been triggered by the glaciation of the Patagonian Andes that became significant about 6 Ma ago, resulting in an increased sediment flux to the trench (e.g. Bangs and Cande 1997). Seven major submarine canyons are deeply incised in the forearc, and operate as major pathways for sediment transport to the trench. They are directly connected to river systems that drain the Andes and the coastal Cordillera,

and form a link to submarine fans in the trench with silt–sand dominated patterns of sedimentation (e.g. Heberer et al. 2010).

In contrast to the tectonic processes generating the very uniform morphology of the oceanic Nazca Plate, those constraining the more complex morphology and structure of the overriding South American Plate vary strongly from north to south, and also show distinct across-slope segmentation (see, for example, Geersen et al. 2011a for detailed description). Here the most important features are briefly reviewed. Viewed in an upslope direction, the south–central Chilean margin is composed of a young (Pliocene) active accretionary prism, an older (Mesozoic) palaeo-accretionary prism that takes the role of a tectonic backstop of the active accretionary wedge, and continental metamorphic basement (e.g. Bangs and Cande 1997; Contreras-Reyes et al. 2010; Geersen et al. 2011a). The active accretionary prism extends upslope from the deformation front to a water depth of about 2,500 m. It is characterized by a sequence of landward-dipping thrust faults that separate individual thrust sheets (Bangs and Cande 1997; Geersen et al. 2011a). Deformation results in a rough seafloor topography. Further upslope, the Mesozoic palaeo-accretionary prism has a much smoother bathymetric expression, mainly due to a cover of 0.5–2 km of slope and shelf sediments. Active faulting there is restricted to relatively few out-of-sequence thrusts or normal faults (Behrmann et al. 1994; Geersen et al. 2011a). Near the Chilean coastline there is a transition in the subsurface from the palaeo-accretionary prism to the continental metamorphic basement.

In addition to the segmentation across the slope, there is a pronounced structural and seismotectonic north–south segmentation along strike of the plate boundary. For the forearc, this has been interpreted in terms of earthquake rupture (Lomnitz 1970; Comte et al. 1986; Campos et al. 2002; Ruegg et al. 2009), seismicity (Bohm et al. 2002; Haberland et al. 2006), the gravity field (Hackney et al. 2006; Tasárová 2007), the distribution and intensity of submarine mass wasting (Geersen et al. 2011b, 2013; Völker et al. 2012), subduction channel thickness and accretionary prism width (Bangs and Cande 1997; Contreras-Reyes et al. 2010; Geersen et al. 2011a), and topography (Rehak et al. 2008). At the southern termination of the study area near the Chile Triple Junction, most of the forearc has been destroyed by erosion due to the subducting Chile Ridge, to be rebuilt further south by sediment offscraping and accretion from the Antarctic Plate (Behrmann et al. 1994; Behrmann and Kopf 2001; Maksymowicz 2013).

Materials and methods

Database

This study is based on multi-channel seismic reflection data collected along numerous profiles during five geophysical
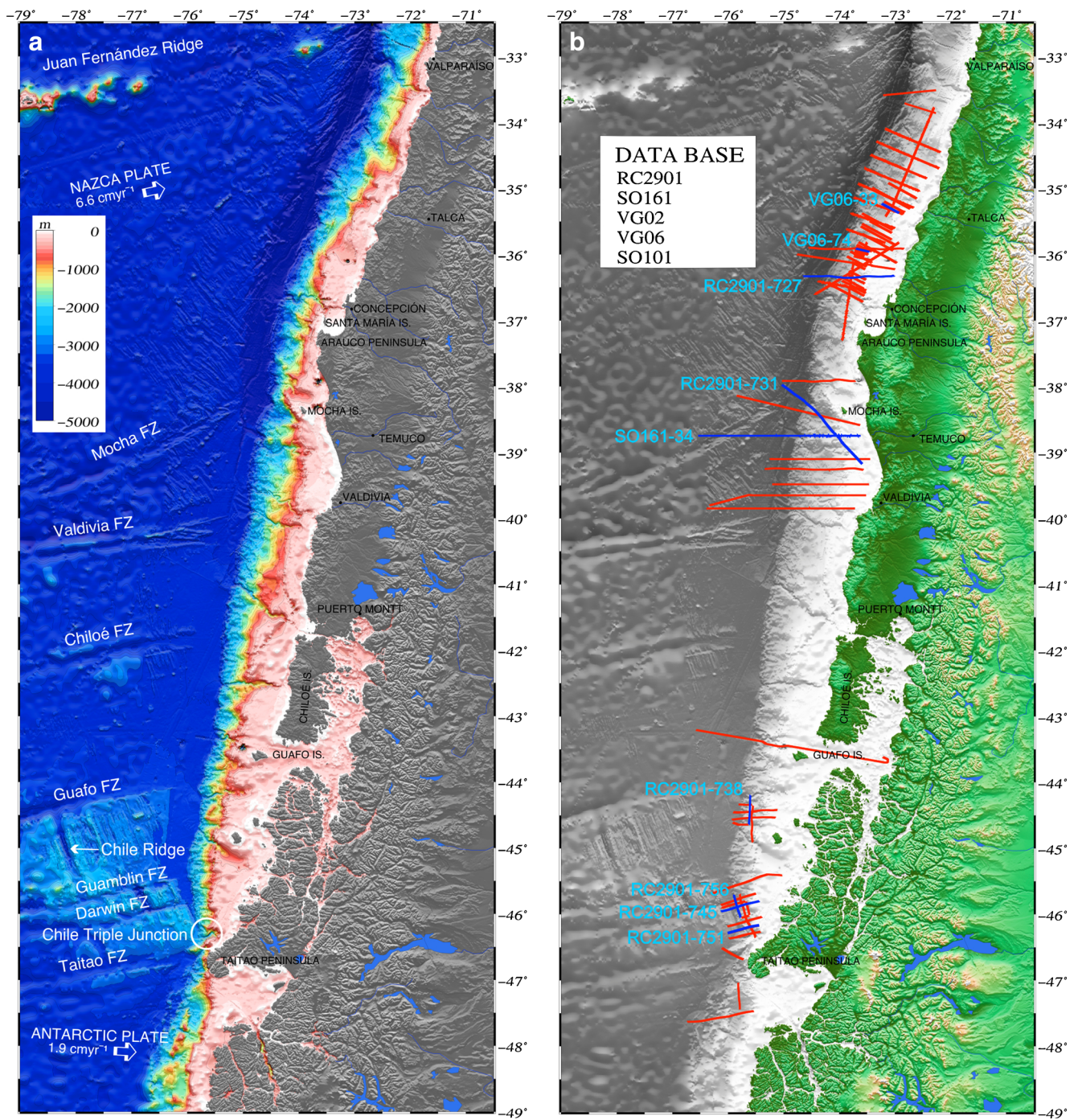
Fig. 1 Location map of the study area offshore Chile, the bathymetry being based on GEBCO_08 Grid (version 20091120, http://www.gebco.net). **a** Tectonic setting of the Nazca, Antarctic and South American plates. Note the aseismic Juan Fernandez Ridge, the fracture zones (FZ) responsible for the age variations of the subducted Nazca and Antarctic plates, and the Chile Ridge today being subducted at 46.4°S. **b** Locations of seismic profiles and ODP legs forming the database used in this study. *Blue lines* Sections presented in other figures

cruises off central–south Chile (32°S–48°S). The locations of all seismic profiles are given in Fig. 1b. Those profiles illustrated in other figures and discussed in more detail are shown in blue, the others in red.

The seismic profiles of research cruise RC2901 aboard R/V Conrad (January–February 1988) were obtained during the

"Mid-Ocean Spreading Ridge (Chile Ridge)" project for the Chilean national oil company Empresa Nacional del Petroleo (ENAP), prior to the geophysical survey of the southern Chile margin conducted in preparation for ODP Leg 141 drilling (Bangs and Cande 1997). Most profiles are oriented approx. east–west, perpendicular to the direction of maximum slope

angle (Geersen et al. 2011a); some are oriented parallel to the coast, mainly in the vicinity of the Chile Triple Junction. RC2901 sections were acquired by means of a 3,000-m-long digital streamer, with 240 channels and an intertrace of 12.5 m. A 10-airgun tuned array provided the seismic source, with a total volume of 61.34 l and a shot spacing of 50 m.

R/V Sonne Cruise SO161 of January–February 2001 was carried out within the framework of the "Subduction Processes off Chile (SPOC)" project along the Chile continental margin between 28°S and 44°S, with the general aim of defining the processes and constraints that control the formation of the Chilean continental margin (Reichert et al. 2002). Seismic profiles were acquired using a 3,000-m-long digital streamer with 132 channels. The seismic source was a tuned array of 20 airguns, with a total volume of 51.2 l and a shot spacing of 50 m.

Project SO-101 CONDOR, a study of Chilean offshore natural disasters and ocean environmental research, was carried out in 1995 aboard R/V Sonne. This cruise recovered seismic profiles off the central Chilean forearc.

A research cruise of R/V AGOR Vidal Gormaz was carried out in 2002, as part of the FONDEF Project DOOI104 "Submarine Gas Hydrates: A New Source of Energy for the Twenty-First Century". The primary aim was to locate gas hydrates in sediments along the Chilean margin between 32° and 40°S, at water depths ranging from 200 to 5,000 m (Contardo et al. 2008). A cluster containing four SG-1 sleeve guns with an approximate volume of 40 cubic inches each was used as the seismic source, and a shot spacing of 50 m.

The research cruise VG06 of February 2006 aboard R/V Vidal Gormaz acquired reflection seismic data along the Chilean forearc as part of a second FONDEF project on gas hydrates, the target area being 34°–37°S at 200–3,000 m water depths. The University of Aarhus (Denmark) provided a 600-m-long streamer with 96 channels and an array of four sleeve guns with a total volume of 160 cubic inches. In all, 58 seismic profiles were shot covering an overall length of about 2,350 km (Diaz-Naveas 2007).

Heat flow calculations

Along the central–south Chile continental margin and in similar settings worldwide, commonly occurring BSRs are probably the most widely used indicators for the presence of natural gas hydrates. The reflection is caused by the acoustic impedance contrast between sediments containing gas hydrate and free gas below the gas hydrate stability zone (e.g. Berndt et al. 2004). Thus, BSR imaging of the lower boundary of gas hydrate stability is associated with negative polarity, as can be identified in the seismic sections used in this study (e.g. reflectors imaged in yellow in Fig. 2a and c). Because the

stability of gas hydrates is controlled by temperature and pressure conditions (e.g. Grevemeyer et al. 2003), this can serve to calculate the steady-state heat flow q (mW m^{-2}) by using the following formula:

$$q = \frac{T_z - T_0}{\int\limits_{0}^{z} \frac{\mathrm{d}z'}{k(z')}} \tag{1}$$

where T_z and T_0 are the temperatures at the BSR and the seafloor respectively (Villinger et al. 2010), k is the thermal conductivity and z denotes the BSR depth.

The BSR and the seafloor depths were obtained from the seismic profiles collected during the cruises mentioned above. Seafloor temperatures were taken from CTD measurements off Chile from the World Ocean Data Base (http://www.nodc.noaa.gov/). Thermal conductivity for the southern sector of the study area was taken to be $k=1.25$ W mK^{-1}, based on drillcore data from ODP Leg 141 (Behrmann et al. 1992; Grevemeyer and Villinger 2001). For the central and northern sectors, thermal conductivity was taken to be $k=0.85$ W mK^{-1}, based on ODP Leg 202 drillcore data (Grevemeyer et al. 2003; Mix et al. 2003). The differences reflect compositional variations of the sediments and, more importantly, a higher degree of shallow diagenesis in the vicinity of the Chile Triple Junction (see Behrmann et al. 1994). Temperature at the depth of the BSR, T_z, is calculated by using the dissociation temperature–pressure function (Dickens and Quinby-Hunt 1994):

$$1/T = 3.79 \times 10^{-3} - 2.83 \times 10^{-4}(\log p) \tag{2}$$

where p is the hydrostatic pressure (MPa) and T the temperature (Kelvin). Gas in the system is assumed to be pure methane, with a pore water salinity of 35 g l^{-1}. Hydrostatic and lithostatic pressures and depth were calculated by converting the measured TWT (two way travel time) at the BSR using a velocity–depth function derived from the seismic data (Kaul et al. 2000) or, where available, data from ODP drillholes (e.g. Behrmann et al. 1992). To convert water-column TWT into depth, a seawater compressional wave velocity of 1,500 m s^{-1} was used.

Results

A key observation is that the BSR delineating the inferred base of gas hydrates occurs mostly along the 2,000 m water depth contour and is typically located between about 90–630 meters below seafloor (mbsf). For a given water depth, the depth of the BSR below seafloor increases from south to north
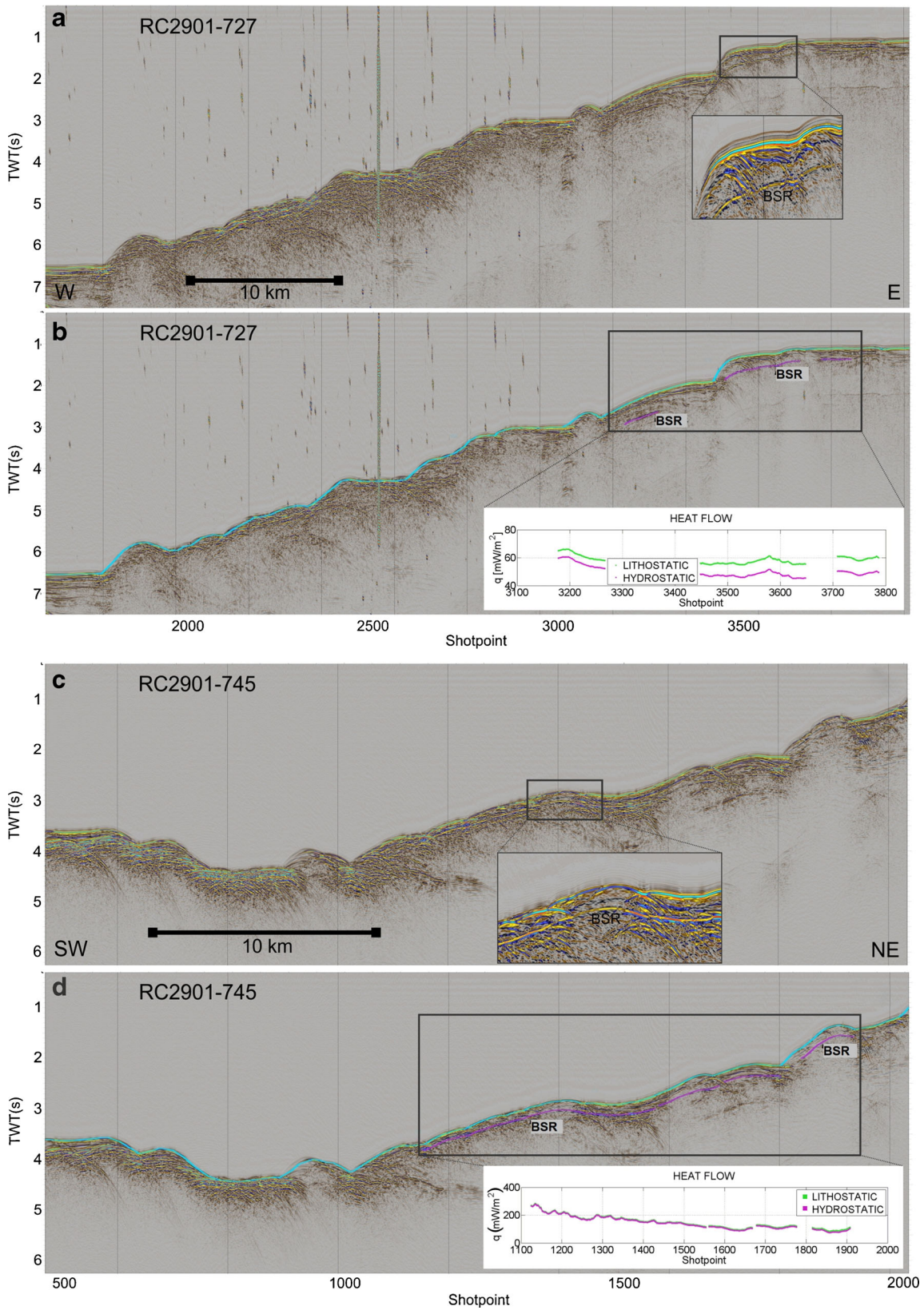
Fig. 2 Two examples of BSR identification. **a** Profile RC2901-727, north sector of study area, zoom showing reverse polarity of BSR (*yellow*). **b** Interpretation of profile RC2901-727 (*purple* BSR), and evaluation of heat flow pattern (*lower right*). **c**, **d** Profile RC2901-745, south sector of study area

in the whole study area (compare Figs. 3a and 4a). The deepest occurrences below seafloor are in deeper waters (>2,000 m) in the northern sector of the study area offshore Valparaiso to Valdivia (33°S–40°S; Fig. 3a). Generally, the BSR shallows upslope above the 2,000 m bathymetric contour in the northern sector, as can be clearly seen in the colour-coded BSR depths (mbsf) reported in Fig. 3a.

On individual seismic profiles in the northern sector of the study area, BSR depth is about 0.3–0.5 s TWT beneath the seafloor. In the three examples given in Fig. 5a–c, this corresponds to heat flows of 30–48 mW m^{-2} for profile SO161-34 (Fig. 5a), 38–60 mW m^{-2} for profile RC 2901-727 (Fig. 5b), and ca. 50 mW m^{-2} for profile RC 2901-731 (Fig. 5c). These values are indicative of conductive heat transfer through forearcs underlain by a relatively old and, therefore, cold subducting oceanic plate. In map view, most of the forearc between 33°S and 40°S is dominated by low heat flow (generally <60 mW m^{-2}).

Distinct deviations from this pattern are rare, and occur at about 35°20′S (offshore Talca), 36°00′S (NW of Concepción) and 38°30′S (SW of Mocha Island). Here heat flow locally increases along section to ca. 90 mW m^{-2}, which is about twice the regional background. The first anomaly is spatially related to a major normal fault scarp (Fig. 6, left-hand panels). The BSR is uplifted on both sides of the fault, and disappears where its projection would intersect the fault plane. BSR uplift is indicative of increased heat flow around the fault trace, and BSR disappearance may be due to inhibition of gas hydrate formation in a zone of vigorous fluid flow along the fault. In the case of the second anomaly (Fig. 6, right-hand panels), the BSR uplift and increased heat flow can be connected to an east-dipping blind thrust that transects the accretionary wedge at depth beneath the forearc cover sediments. The thrust is clearly inactive, as shown by the lack of offset strata in overlying sediments. It may still act as a conduit for fluids from depth, however, creating a local regime of advective heat transfer.

Regarding the third anomaly, the increased heat flow values SW of Mocha Island (Fig. 3b) are in the headscarp area of the southernmost of three large embayments in the forearc slope, where large-scale failure of the forearc slope caused three megascale submarine landslides in the last 600,000 years. The slide that created the southern embayment has a minimum estimated age of 560,000 years and has removed an approx. 500-m-thick section of sediments from the area of increased heat flow (Geersen et al. 2011b). Two explanations are possible for the locally increased heat flow: (1) the headwall of the slide may be an area of fluid advection, or (2) sliding has led to a perturbation of the geothermal gradient in the forearc, which still persists today. On the basis of the available data, it is not possible to decide between these
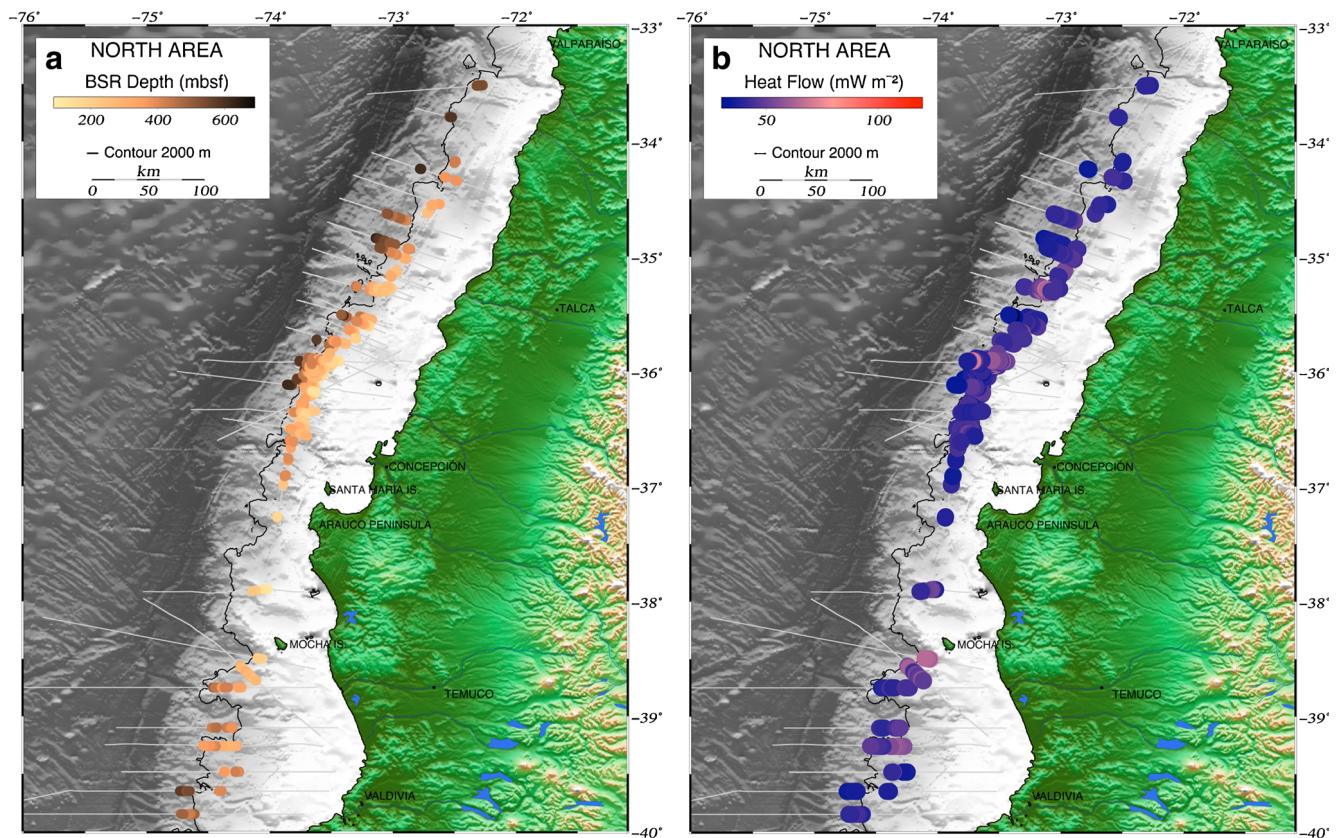

Fig. 3 Large-scale colour-coded results for the northern sector of the study area, based on all seismic profiles available for that sector: a BSR depth (mbsf) and b heat flow (mW m^{-2}). See text for description
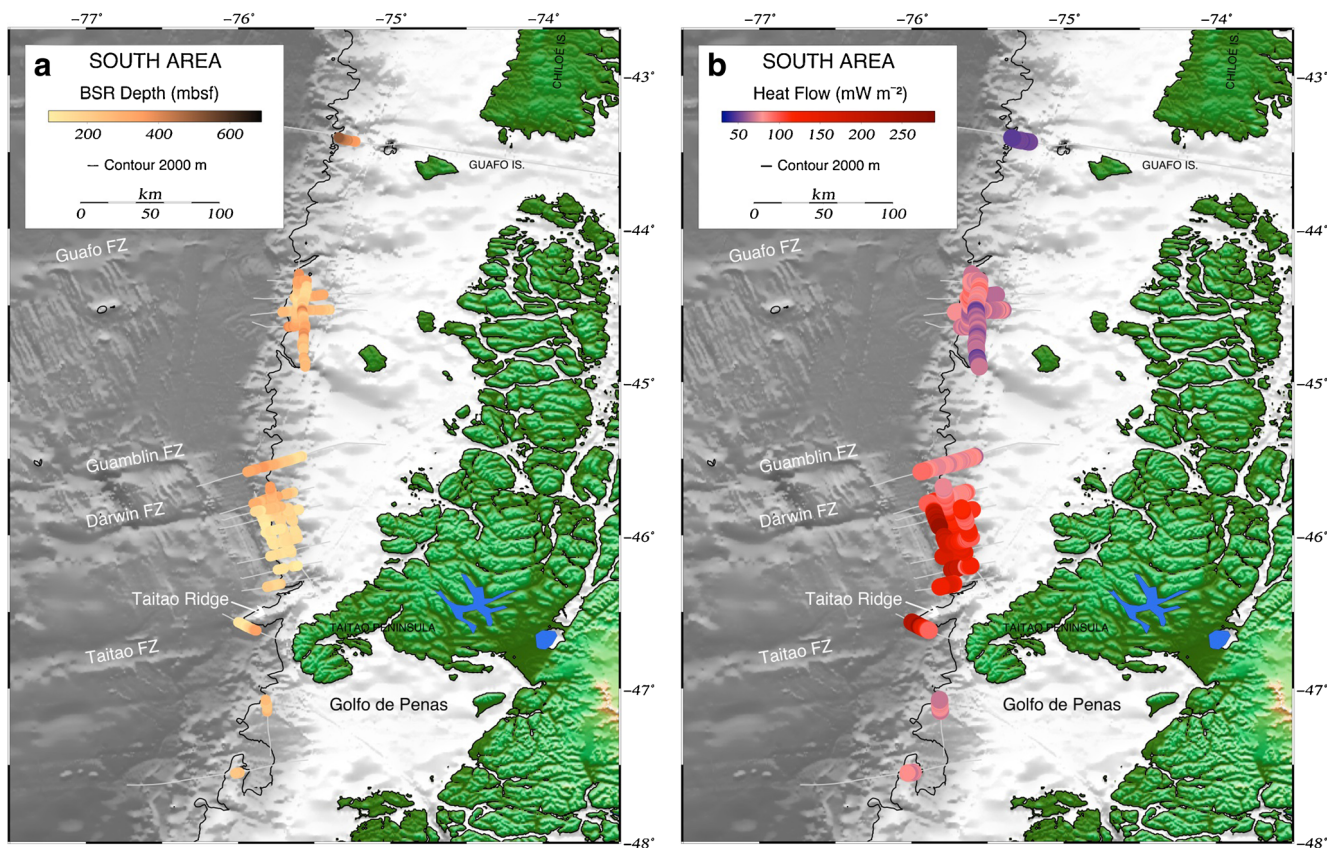
Fig. 4 Large-scale colour-coded results for the southern sector of the study area, based on all seismic profiles available for that sector: **a** BSR depth (mbsf) and **b** heat flow (mW m^{-2}). See text for description

scenarios, but fluid advection and resulting high pore fluid pressures are one major cause for forearc failure discussed in the literature (e.g. Kayen and Lee 1991; Mienert et al. 1998; Behrmann and Meissl 2012). Because BSRs are absent around the central and northern slope embayments of Geersen et al. (2011b), it is impossible to assess the heat flow there and relate it to processes of forearc failure (compare Fig. 3b of this study and Fig. 2 of Geersen et al. 2011b).

In the southern part of the study area between 43°20′S and 47°20′S, the BSR depths below seafloor are generally much larger, irrespective of water depth (see Fig. 3a). Again, BSR occurrence is concentrated along the 2,000 m isobath, mostly slightly above this water depth. Maximum BSR depth is about 500 mbsf in deep water along the seismic profile seawards of Guafo Island at 43°20′S (Fig. 4a). Here the BSR shallows upslope, as one would expect in a regime of constant heat flow along the cross section (compare Fig. 4a and b). Heat flow is low (average of 50 mW m^{-2}) and similar to that of the northern part of the study area (see above).

Between 44°S and 45°S the segment of the Nazca Plate between the Guafo and Guamblin fracture zones is subducted beneath the forearc. Here a cluster of BSRs identified along several seismic profiles shows variable depths, albeit generally shallower than 300 mbsf (Fig. 4a). This corresponds to heat flow values generally not exceeding 100 mW m^{-2}, with an

average of 75 mW m^{-2} (Fig. 4b). The example illustrated in Fig. 5d shows an almost continuous BSR along seismic profile RC 2901-738 on the middle forearc slope along strike of the continental margin, the computed heat flow being about 80–100 mW m^{-2}. These higher values are here tentatively explained by the fact that the Nazca Plate oceanic crust being subducted landwards of the Guafo and Guamblin fracture zones is much younger than that being subducted further north (Fig. 1a). South of the landward projection of the Guamblin Fracture Zone, a narrow segment of young Nazca Plate crust is being subducted north of the Darwin Fracture Zone (Fig. 1a). Heat flow values computed from the downslope increasing BSR depths (Fig. 4a) generally lie above 100 mW m^{-2} (Fig. 4b).

South of the Darwin Fracture Zone, the data reveal a pronounced change in BSR characteristics. Here the actively spreading Chile Ridge is subducted beneath the southern Chile forearc. Figure 4a shows that BSR depth decreases southwards along strike of the plate boundary, and also shoals with decreasing water depth. Heat flow is much higher than further northwards, reaching peak values of almost 300 mW m^{-2} (Fig. 4b) at, for example, the western, seaward end of seismic profile RC 2901-745 (Fig. 5e). This is where the eastern flank of the Chile Ridge is today subducting, and the peak values occur at the toe of the accretionary wedge where active deformation and
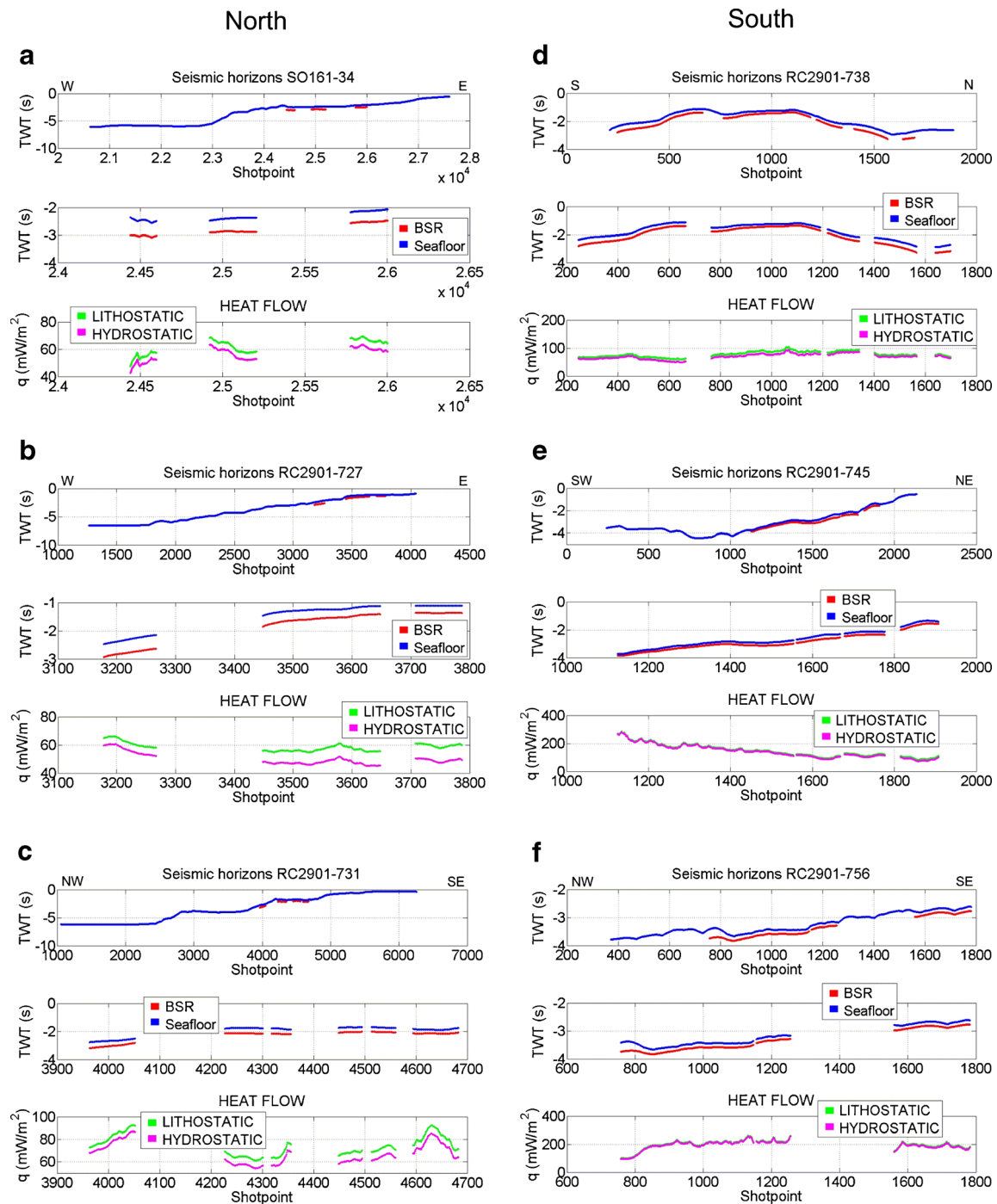
North

South

Fig. 5 Examples of calculated heat flow for the northern (**a**–**c**, profiles SO161-34, RC2901-727, RC2901-731) and southern (**d**–**f**, profiles RC2901-738, RC2901-745, RC2901-756) parts of the study area. In each diagram, the upper and middle boxes show the seismic horizons identified for the seafloor (*blue*) and the BSR (*red*), and the lower box the computed heat flow based on assumed lithostatic and hydrostatic pressure

associated fluid flow are most intense. Further upslope heat flow decreases steadily to about 100 mW m^{-2}, probably reflecting the underlying Patagonian forearc basement that is not yet being heated by the subducting oceanic crust. The data for seismic profile RC 2901-756 (Fig. 5f), a strike line that leads gently upslope in a southward direction, show that heat flow along strike of the forearc is generally about 200 mW m^{-2} on the lower

forearc slope. Along seismic profile RC 2901-751 (Fig. 7), heat flow is high (ca. 200 mW m^{-2}) above the projected spreading axis of the subducted Chile Ridge. Geothermal gradients measured here by temperature logging in a borehole at ODP Site 863 are as high as 100 °C per km (see Behrmann et al. 1992). Landwards of a major active normal fault that offsets strata and the seafloor, heat flow decreases to about 100 mW m^{-2}.
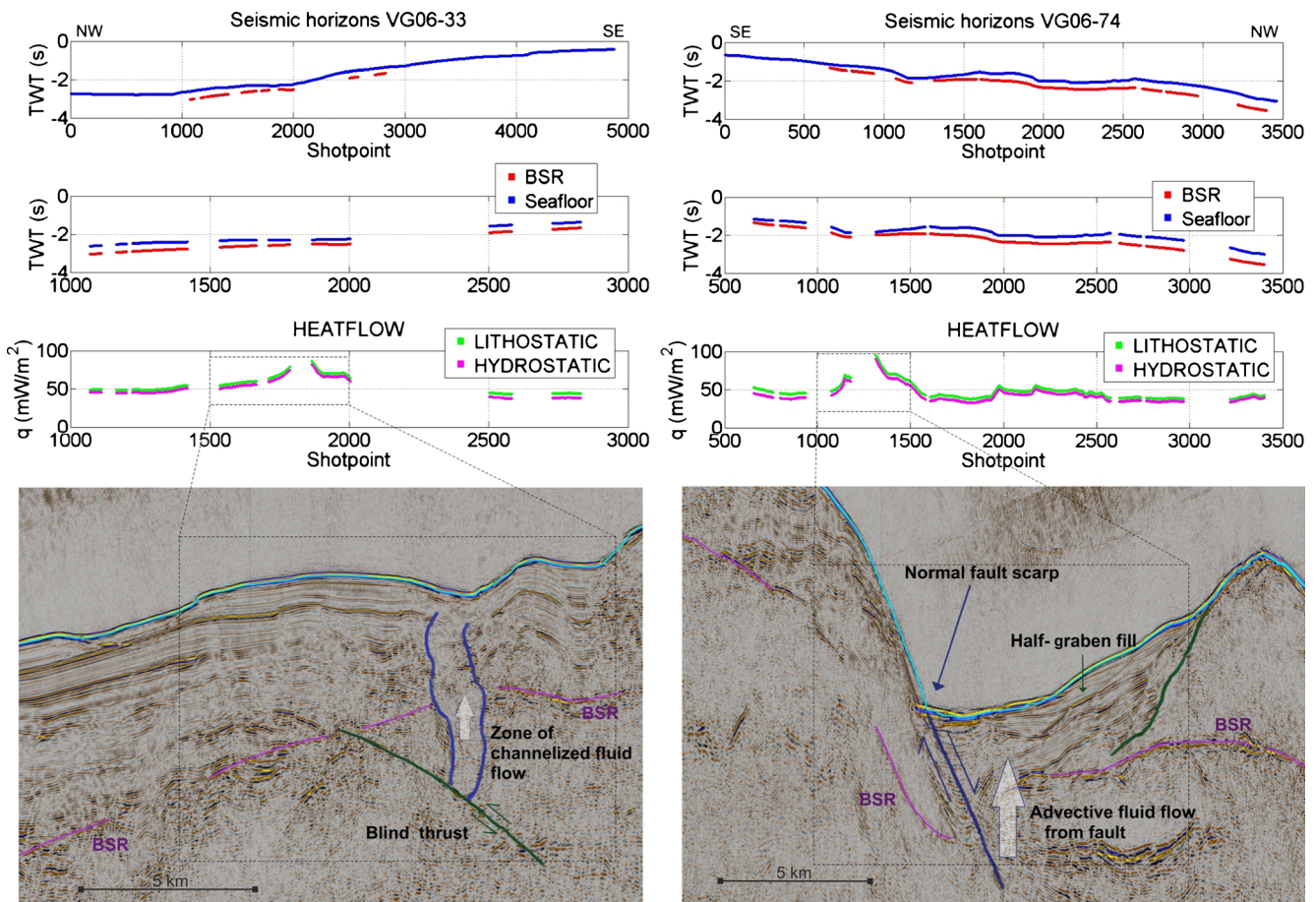
Fig. 6 Two examples of seismic profiles showing local positive anomalies of heat flow and associated tectonic structures on the forearc off Concepción, northern sector of study area. *Left* Profile VG06-33, showing BSR uplift above a blind thrust at depth. *Right* Profile VG06-74, showing BSR uplift and related elevated heat flow through half-graben sediment fill in the hanging wall of a normal fault

This is similar to that observed in the upslope part of seismic profile RC 2901-745 further north. Heat flow across Taitao Ridge, which has been interpreted as an ophiolite recently accreted to the upper plate, is well above 100 mW m^{-2}, attesting to the active tectonic nature of this environment. South of the Taitao Fracture Zone and seawards of the Golfo de Penas, heat flow computed from BSR depth is much lower (cf. southern-most data points on Fig. 4a and b), plausibly reflecting the subduction of oceanic crust of the ca. 7-Ma-old Antarctic Plate long after the passage of the Chile Ridge.

Discussion

Uncertainties in heat flow estimates

BSR-based computations of crustal heat flow need to consider uncertainties regarding underlying assumptions of gas hydrate composition, and the quality and measurement accuracy of parameters like thermal conductivity and acoustic velocity. As Brown et al. (1996) pointed out, gas hydrate stability responsible for the BSR location along the southern Chile margin is probably best explained by a more or less pure water–methane mixture. This, together with the methane-dominated gas signature of the ODP drillcores (Behrmann et al. 1992; Mix et al. 2003), speaks for a biogenic and/or thermogenic methane source of the hydrates. An important calibration for thermal conductivity and compressional wave velocity of forearc rocks is usually provided by information from boreholes, which is available for the study area from two legs of the Ocean Drilling Program (Behrmann et al. 1992; Mix et al. 2003). As pointed out above, thermal conductivities measured on rocks in the southern sector (ODP Leg 141; Behrmann et al. 1992) were higher than those in the central and northern sectors (Grevemeyer et al. 2003; Mix et al. 2003). The differences primarily reflect compositional variations of the sediments and, more importantly, a higher degree of shallow diagenesis in the vicinity of the Chile Triple Junction (see Behrmann et al. 1994).

Compressional wave velocities were taken mainly from the seismic records and errors are probably limited, especially at locations showing shallow BSRs. In the Chile Triple Junction area, drilling during ODP Leg 141 (Behrmann et al. 1992) intersected highly indurated sedimentary rocks with

Fig. 7 Seismic profile RC 2901-751, with BSR indicative of high heat flow above the projected spreading axis of the subducted Chile Ridge. *Upper panel* Interpreted seismic profile. *Lower panels* Computed heat flow based on the seismic horizons identified for the seafloor (*blue*) and the BSR (*red*)
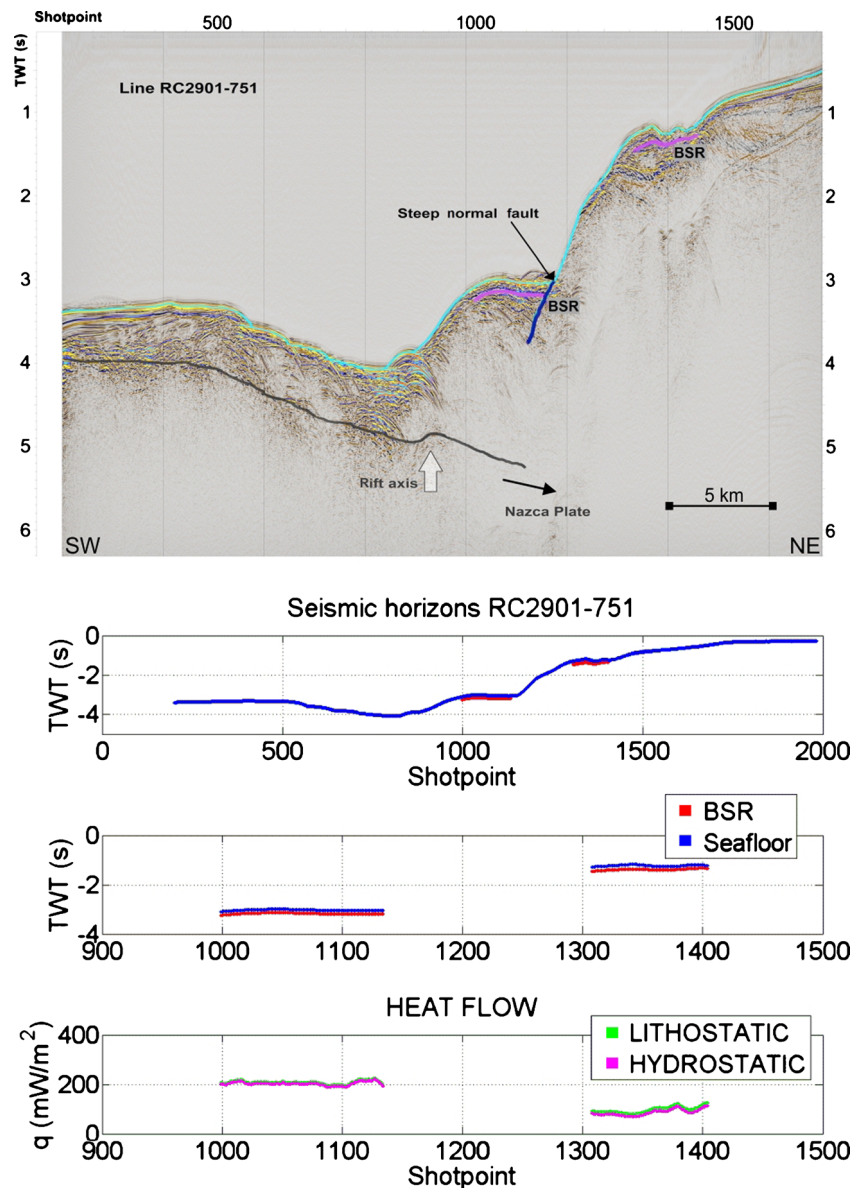
anomalously high compressional wave velocities at ODP Site 859 (seismic profile RC 2901-745; Fig. 5e) and Site 863 (seismic profile RC 2901-751; Fig. 7). It is difficult to accurately assess errors and discrepancies relative to the information from seismic sections. However, heat flow calculations from these two profiles may be considered as maximum estimates, as compressional wave velocity information extracted from the two seismic sections yields values lower than those measured on ODP Leg 141 drillcores (see Behrmann et al. 1992).

Ocean bottom water temperatures were taken from the World Ocean Data Base, as outlined above in the section describing the database. Local and regional variations, and variations with depth were fully accounted for in the computations. For example, typical measured seafloor temperatures are 4.2 °C at 800 m, 2.7 °C at 1,500 m and 1.8 °C at 2,500 m

water depths at 36° southern latitude. Grevemeyer and Villinger (2001) pointed out that, in more general terms, heat flow calculations from BSR alone can contain uncertainties on the order of 20%. Calibrations by borehole temperature or heat probe measurements can reduce this uncertainty. In the present study this was accomplished by using direct measurements of thermal conductivity from drillcores and of temperature from drillholes, as outlined above in the materials and methods section.

BSR occurrence and water depth window

One important feature of the present findings is the distinct distribution of BSRs with respect to water depth along the Chile margin, i.e. BSR occurrence is mostly at about 2,000 m water depth. Moreover, a visual check of Figs. 3 and 4 shows

that the BSRs occur mostly in areas of very rough topography. Rough topography on the forearc is partly due to canyon incision but, much more importantly, to deformation in the vicinity of actively moving faults. For the northern part of the study area, Geersen et al. (2011a; see their Figs. 4, 5 and 7) reported that the transition from rough to smooth seafloor is typically at about 2,000 m water depth, which corresponds to 2.5–3 s TWT. While the actively deforming frontal accretionary prism is mainly located at 3,000 m water depth or more (see Fig. 8 of Geersen et al. 2011a), the forearc slope landwards from there is modified by numerous out-of-sequence thrust ridges and normal fault scarps, which are expressions of localized deformation where the slope sediment cover is underlain by older basement rock.

In the southern part of the study area, BSR occurrence is within the same water depth window (Fig. 4) and the upper, landward limit of rough topography is somewhat above the 2,000 m isobath. In the reflection seismic profiles crossing this part of the forearc, accreted strata with evidence for strong deformation occur at water depths well above 2,000 m (see Figs. 2b and 7 of the present study and, for example, Figs. 2 and 3 of Behrmann and Kopf 2001), and define a common spatial occurrence of zones of active deformation and BSRs. In principle this means that the accreted and faulted strata of the forearc are the major methane source along the whole length of the southern Chile forearc. However, the organic carbon content of the forearc and accreted trench strata is commonly rather low (ca. 0.5% or less; Behrmann et al. 1992; Mix et al. 2003), implying a very efficient process of

Fig. 8 Present-day forearc heat flow as a function of the age of subducted Nazca and Antarctic plate segments at the trench between 44°S and 48°S (mean heat flow for each segment between fracture zones, and one sigma standard deviation), with evidence of an exponential decay in heat flow with increasing age of the subducting plate. The two mean values for the crustal age of 7 Ma refer to the average heat flows through the subducting Nazca (*N*) and Antarctic (*A*) plates. See text for discussion

methane migration from depth and concentration beneath the BSR (also see below).

Evidently, deformation and associated fracturing and increase in permeability probably is the key agent in facilitating methane migration from depth. In many cases this migration may be diffuse if viewed at a large scale, but the evidence from Fig. 6 suggests that it may also be individual faults that aid in channelling the fluid flow and heat flux from the forearc. In this case heat flow intensity may be roughly twice as high as the local average on both sides of the faults. The presence of seep structures (Klaucke et al. 2012) is further independent evidence that fluid flow through the forearc strata may in places be focused.

N–S gradient in BSR continuity

The data reveal that BSR occurrence is strong and laterally persistent in the south of the study area, and weaker and much more patchy in the north (compare Figs. 2 and 5). Organic carbon contents of sediments along the whole margin are relatively low, and the fill of the Chile Trench is characterized by rapidly settling, coarser terrigenous and hemipelagic sediments (Heberer et al. 2010; Geersen et al. 2011b). Indeed, there is no evidence of more slowly settling, finer-grained organic carbon-rich pelagic sediments on the subducting Nazca Plate in the northern sector of the study area, which could serve as a powerful methane source at depth and fuel gas hydrate formation near the seafloor. This is consistent with the weaker and more patchy BSR signatures in this sector.

For the immediate surroundings of the Chile Triple Junction in the south of the study area where heat flow is much higher, Brown et al. (1996) argued that the coherent BSR may result from an upward migration of the base of gas hydrate stability by about 300 m. BSR migration would cause amalgamation of isolated gas hydrate patches into one, highly reflective and continuous layer. This process would be driven by the rising geothermal gradient as the eastern flank of the Chile Ridge is becoming subducted. However, rapid upward migration of the base of the hydrate stability field would tend to leave traces such as multiple BSRs, which do not occur anywhere in the seismic sections studied. Also, the absence of multiple BSRs makes it less likely that upward BSR migration has created a non-steady state situation, which would have made calculation of heat flow from BSR depth difficult. An arguably more straightforward explanation is that vigorous fluid advection in this regime of high heat flow leads to higher methane and water flux from depth and, thus, a stronger and more continuous BSR. In some of the cores taken in ODP Leg 141 drillholes, higher hydrocarbons were detected (Behrmann et al. 1992), attesting to a contribution of thermogenic methane from depth to this part of the forearc.

The strong and continuous BSR in seismic profile RC 2901-738 (Fig. 5d) occurs in a heat flow regime of about
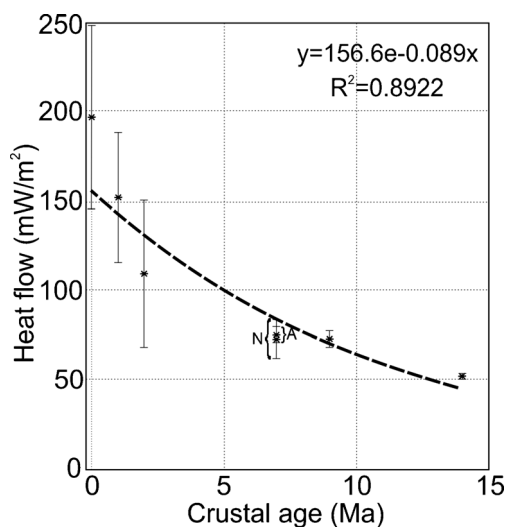
100 mW m^{-2} (Figs. 4b, 5d). This is roughly twice the average heat flow observed further north, where BSR occurrence is discontinuous. This implies that enhanced gas hydrate formation above a BSR driven by elevated heat and fluid flux from depth may already be possible at the 100 mW m^{-2} level, and would not require the strongly elevated heat flow (200–300 mW m^{-2}) observed immediately above the subducting spreading ridge further south (Figs. 4b, 5e, 5f, 7). The effect of BSR patchiness vs. continuity on assessments of gas hydrates as an energy resource (e.g. Burwicz et al. 2011) remains to be analyzed in detail. The present dataset is in principle suitable for such work (see, for example, Vargas Cordero et al. 2010b). Viewed at a larger scale and entirely qualitatively, it seems that there could be a direct link between heat flow intensity and the efficiency of gas hydrate formation in forearc sediments.

Large-scale tectonics and forearc heat flow

It is obvious from the results of this study that the subduction of the Chile Ridge and its associated oceanic spreading centre causes a major heat flow anomaly in the forearc of the overriding South American Plate. The size of the anomaly and that of the subducting spreading ridge segment between the Darwin and Taitao fracture zones correspond well (Fig. 4b). However, average heat flow in the overriding plate is not as high as one would expect above zero-age oceanic lithosphere based on thermal and subsidence models (e.g. Stein and Stein 1992). Initial heat flow predicted by Stein and Stein (1992) would be about 280–300 mW m^{-2}, and not on average 200 mW m^{-2} as shown in Fig. 8. Such deviations of heat flow intensities are known in subduction trench settings (e.g. Grevemeyer et al. 2005), and have been attributed to the cooling effect of hydrothermal circulation through normal fault systems in the subducting oceanic plate. Grevemeyer et al. (2005) argued that this effect is largely controlled by the presence or absence of a sedimentary blanket of the oceanic crust. As new oceanic crust around spreading centres is heavily faulted and not covered by sediments, the effect documented at the Chile Triple Junction may then in fact be used to quantify the cooling effect of hydrothermal circulation in this kind of tectonic setting. Indeed, this cooling effect would be strong enough to diminish heat flow from the subducting Nazca oceanic slab by as much as one third, a value derived by comparing the average 280–300 mW m^{-2} from published models (e.g. Stein and Stein 1992) with the average 200 mW m^{-2} observed above the subducting Chile Ridge (Fig. 8). This would weaken the thermal anomaly in the overriding plate accordingly. Plotting average heat flow in the forearc above older subducted Nazca and Antarctica crust (Fig. 8), there is evidently an exponential decay of this signal with time, leading to heat flow through the forearc of about 50 mW m^{-2} above 14-Ma-old subducted crust. This value is still well below the heat flow levels expected from models or heat flow measurements on open oceanic plates (Stein and Stein 1992), and implies that much of the heat generated by magmatic activity at the spreading ridge in the Nazca and Antarctic crust is removed more or less instantaneously by hydrothermal cooling. In the north of the study area where much older oceanic crust of the Nazca Plate is being subducted, the regional low values for heat flow (30–60 mW m^{-2}) come much closer to expected surface heat flow in older oceanic or continental crust (e.g. Davies and Davies 2010).

Conclusions

The findings and interpretations discussed above lead to the following main conclusions:

1. On the Chile forearc between 33° and 47° southern latitude, close spatiotemporal links exist between large-scale tectonic features and heat flow intensity. In the south, the forearc is heated from beneath by the subducting Chile Ridge, causing an approx. fourfold increase in heat flow. Absolute values and their comparison to global models and data, however, also show that there must be cooling of the crust formed at the Chile spreading ridge shortly after its formation, and before being subducted. Further north, where older Nazca Plate lithosphere is subducted beneath the South American continent, surface heat flow (30–60 mW m^{-2}) more closely matches global average values for oceanic and continental crust.

2. In the south of the study area in the vicinity of the Chile Triple Junction, the BSR marking inferred gas hydrate occurrence is continuous and strong. Further north BSRs are widespread but patchy. Rising heat flow above a subducting spreading ridge may generate a powerful methane source at depth in the subduction zone. Vigorous fluid flux then creates a strong and continuous BSR. This study provides evidence that heat flow of 100 mW m^{-2}, which is about two to three times the large-scale average of 30–60 mW m^{-2}, may already be sufficient to drive this process.

3. There is a spatial linkage between BSR and, thus, inferred gas hydrate occurrence and active deformation in the study area. Accreted and faulted strata of the forearc are the major methane source along the whole length of the southern Chile forearc. Deformation and associated fracturing and increase in permeability probably is the key agent in facilitating methane migration from depth. As these sediments are relatively poor in organic carbon, there must be a very efficient process of methane migration from depth and concentration beneath the BSR. Much of the methane migration is probably diffuse, but increased heat flow in the vicinity of individual faults implies that these can act as channels for deep-rooted fluids and heat.

References

Angermann D, Klotz J, Reigber C (1999) Space-geodetic estimation of the Nazca-South America Euler vector. Earth Planet Sci Lett 171: 329–334. doi:10.1016/S0012-821X(99)00173-9

Bangs NL, Brown KM (1995) Regional heat flow in the vicinity of the Chile Triple Junction constrained by the depth of the bottom simulating reflector. In: Lewis SD, Behrmann JH, Musgrave RJ et al. (eds) Proc ODP Sci Results 141:253–258

Bangs NL, Cande SC (1997) Episodic development of a convergent margin inferred from structures and processes along the southern Chile margin. Tectonics 16:489–503. doi:10.1029/97TC00494

Bangs NL, Sawyer DS, Golovchenko X (1993) Free gas at the base of the gas hydrate zone in the vicinity of the Chile triple junction. Geology 21:905–908

Behrmann JH, Kopf A (2001) Balance of tectonically accreted and subducted sediment at the Chile Triple Junction. Int J Earth Sci 90: 753–768

Behrmann JH, Meissl S (2012) Submarine landslides, Gulf of Mexico continental slope: insights into transport processes from fabrics and geotechnical data. In: Yamada Y, Kawamura K, Ikehara K, Ogawa Y, Urgeles R, Mosher D, Chaytor J, Strasser M (eds) Submarine mass movements and their consequences. Springer, Heidelberg, pp 463–474. doi:10.1007/978-94-007-2162-1

Behrmann JH, Lewis SD, Musgrave R, Bangs N, Bodén P, Brown K, Collombat H, Didenko AN, Didyk BM, Froelich PN, Golovchenko X, Forsythe R, Kurnosov V, Lindsley-Griffin N, Marsaglia K, Osozawa S, Prior D, Sawyer D, Scholl D, Spiegler D, Strand K, Takahashi K, Torres M, Vega-Faundez M, Vergara H, Waseda A (1992) Chile Triple Junction. Proc ODP Init Rep A 141:1–708

Behrmann JH, Lewis SD, Cande S, Leg ODP, 141 Scientific Party (1994) Tectonics and geology of spreading ridge subduction at the Chile Triple Junction; a synthesis of results from Leg 141 of the Ocean Drilling Program. Geol Rdsch 83:832–852

Berndt C, Bünz S, Clayton T, Mienert J, Saunders M (2004) Seismic character of bottom simulating reflectors: examples from the mid-Norwegian margin. Mar Petrol Geol 21:723–733

Bohm M, Luth S, Echtler H, Asch G, Bataille K, Bruhn C, Rietbrock A, Wigger P (2002) The Southern Andes between 36 degrees and 40 degrees S latitude: seismicity and average seismic velocities. Tectonophysics 356:275–289

Brown KM, Bangs NL, Froelich PN, Kvenvolden KA (1996) The nature, distribution, and origin of gas hydrate in the Chile Triple Junction region. Earth Planet Sci Lett 139:471–483

Burwicz EB, Rüpke LH, Wallmann K (2011) Estimation of the global amount of submarine gas hydrates formed via microbial methane formation based on numerical reaction-transport modeling and a novel parameterization of Holocene sedimentation. Geochim Cosmochim Acta 75:4562–4576. doi:10.1016/j.gca.2011.05.029

Campos J, Hatzfeld D, Madariaga R, Lopez G, Kausel E, Zollo A, Iannacone G, Fromm R, Barrientos S, Lyon-Caen H (2002) A seismological study of the 1835 seismic gap in south-central Chile. Phys Earth Planet Interiors 132:177–195. doi:10.1016/S0031-9201(02)00051-1

Comte D, Eisenberg A, Lorca E, Pardo M, Ponce L, Saragoni R, Singh SK, Suarez G (1986) The 1985 central Chile earthuake: a repeat of previous great earthquakes in the region? Science 233:449–453. doi:10.1126/science.233.4762.449

Contardo X, Cembrano J, Jensen A, Díaz-Naveas J (2008) Tectono-sedimentary evolution of marine slope basins in the Chilean forearc (33°30′–36°50′S): insights into their link with the subduction process. Tectonophysics 459:206–218

Contreras-Reyes E, Flueh ER, Grevemeyer I (2010) Tectonic control on sediment accretion and subduction off south central Chile: implications for coseismic rupture processes of the 1960 and 2010 megathrust earthquakes. Tectonics 29, TC6018. doi:10.1029/2010TC002734

Davies JH, Davies DR (2010) Earth's surface heat flux. Solid Earth 1:5–24

Diaz-Naveas J (1999) Sediment subduction and accretion at the Chilean convergent margin between 35° and 40°S. PhD Dissertation, University of Kiel, Kiel

Diaz-Naveas J (2007) Preliminary seismic and bathymetric results of VG06 cruise off Central Chile. In: Abstr Vol Worksh Science and Technology Issues in Methane Hydrate R&D, 5–9 March 2006, Kauai, Hawaii, p 53

Dickens GR, Quinby-Hunt MS (1994) Methane hydrate stability in seawater. Geophys Res Lett 21:2115–2118

Froelich PN, Kvenvolden KA, Torres ME, Waseda A, Didyk BM Lorenson TD (1995) Geochemical evidence for gas hydrate in sediment near the Chile triple junction. In: Lewis SD, Behrmann JH, Musgrave RJ et al. (eds) Proc ODP Sci Results 141:279–286

Ganguly N, Spence GD, Chapman NR, Hyndman RD (2000) Heat flow variations from bottom simulating reflectors on the Cascadia margin. Mar Geol 164:53–68

Geersen J, Behrmann JH, Völker D, Krastel S, Ranero CR, Diaz-Naveas J, Weinrebe W (2011a) Active tectonics of the South Chilean marine fore arc (35°S-40°S). Tectonics 30, TC3006. doi:10.1029/2010TC002777

Geersen J, Voelker D, Behrmann JH, Reichert C, Krastel S (2011b) Pleistocene giant slope failures offshore Arauco Peninsula, Southern Chile. J Geol Soc 168:1237–1248

Geersen J, Völker D, Behrmann JH, Kläschen D, Weinrebe W, Krastel S, Reichert C (2013) Seismic rupture during the 1960 Great Chile and the 2010 Maule earthquakes limited by a giant Pleistocene submarine slope failure. Terra Nova 25:472–477

Grevemeyer I, Villinger H (2001) Gas hydrate stability and the assessment of heat flow through continental margins. Geophys J Int 145: 647–660

Grevemeyer I, Diaz-Naveaz JL, Ranero CR, Villinger HW (2003) Heat flow over the descending Nazca plate in Central Chile, 32°S to 41°S: observations from ODP Leg 202 and the occurrence of natural gas hydrates. Earth Planet Sci Lett 213:285–298

Grevemeyer I, Kaul N, Diaz-Naveas JL, Villinger HW, Ranero CR, Reichert C (2005) Heat flow and bending-related faulting at subduction trenches: case studies offshore of Nicaragua and Central Chile. Earth Planet Sci Lett 236:238–248. doi:10.1016/j.epsl.2005.04.048

Grevemeyer I, Kaul N, Díaz-Naveas JL (2006) Geothermal evidence for fluid flow through the gas hydrate stability field off Central Chile - transient flow related to large subduction zone earthquakes? Geophys J Int 166:461–468

Haberland C, Rietbrock A, Lange D, Bataille K, Hofmann S (2006) Interaction between forearc and oceanic plate at the South-Central Chilean margin as seen in local seismic data. Geophys Res Lett 33, L23302. doi:10.1029/2006GL028189

Hackney RI, Echtler HP, Franz G, Götze H-J, Lucassen F, Marchenko D, Melnick D, Meyer U, Schmidt S, Tasárová Z, Tassara A, Wiedecke S (2006) The segmented overriding plate and coupling at the South-Central Chilean margin (36–42°S). In: Oncken O, Chong G, Franz G, Giese P, Götze H-J, Ramos VA, Strecker MR, Wigger P (eds) The Andes – active subduction orogeny. Springer, Berlin, pp 355–374

Heberer B, Roeser G, Behrmann JH, Rahn M, Kopf A (2010) Holocene sediments from the Southern Chile Trench: a record of active margin magmatism, tectonics, and paleoseismicity. J Geol Soc 167:539–553. doi:10.1144/0016-76492009-015

Hyndman RD, Spence GD (1992) A seismic study of methane hydrate marine bottom-simulating-reflectors. J Geophys Res 97:6683–6698

Kaul N, Rosenberger A, Villinger H (2000) Comparison of measured and BSR-derived heat flow values, Makran accretionary prism, Pakistan. Mar Geol 164:37–51

Kayen RE, Lee HJ (1991) Pleistocene Slope Instability of gas hydrate-laden sediment on the Beaufort Sea Margin. Mar Geotechnol 10:125–141

Klaucke I, Weinrebe W, Linke P, Kläschen D, Bialas J (2012) Sidescan sonar imagery of widespread fossil and active cold seeps along the central Chilean continental margin. Geo-Mar Lett 32(5/6):489–499. doi:10.1007/s00367-012-0283-1

Kukowski N, Oncken O (2006) Subduction erosion – the "normal" mode of fore-arc material transfer along the Chilean Margin? In: Oncken O, Chong G, Franz G, Giese P, Götze H-J, Ramos VA, Strecker MR, Wigger P (eds) The Andes – active subduction orogeny. Springer, Berlin, pp 217–236

Kvenvolden KA (1998) A primer on the geological occurrence of gas hydrate. In: Henriet J-P, Mienert J (eds) Gas hydrates. Relevance to world margin stability and climate change. Geol Soc Spec Publ 137:9–30

Lomnitz C (1970) Major earthquakes and tsunamis in Chile during the period 1535 to 1955. Geol Rdsch 59:938–960. doi:10.1007/BF02042278

Maksymowicz A (2013) Reestablishment of an accretionary prism after the subduction of a spreading ridge—constraints by a geometric model for the Golfo de Penas, Chile. Geo-Mar Lett 33(5):345–355. doi:10.1007/s00367-013-0331-5

Mienert J, Posewang J, Baumann M (1998) Gas hydrates along the northeastern Atlantic margin: possible hydrate-bound margin instabilities and possible release of methane. In: Henriet J-P, Mienert J (eds) Gas hydrates. Relevance to world margin stability and climate change. Geol Soc Spec Publ 137:275–291

Milkov AV (2004) Global estimates of hydrate-bound gas in marine sediments: how much is really out there? Earth-Sci Rev 66:183–197

Mix AC, Tiedemann R, Blum P et al (2003) Proc Ocean Drilling Program Initial Reports, vol 202. Ocean Drilling Program, College Station, TX

Morales E (2003) Methane hydrates in the Chilean continental margin. Electron J Biotechnol 6(2). http://ejb.ucv.cl/content/vol6/issue2/issues/1/

Rehak K, Strecker MR, Echtler HP (2008) Morphotectonic segmentation of an active forearc, 37°–41°S, Chile. Geomorphology 94:98–116

Reichert C, Schreckenberger N, SPOC Team (2002) Fahrtbericht SONNE - Fahrt SO-161 Leg 2&3 SPOC, Subduktionsprozesse vor Chile - BMBF-Forschungsvorhaben 03G0161A-Valparaíso 16.10.2001-Valparaíso 29.11.2001. Bundesanst für Geowiss und Rohstoffe, Hannover

Ruegg JC, Rudloff A, Vigny C, Madariaga R, de Chabalier JB, Campos J, Kausel E, Barrientos S, Dimitrov D (2009) Interseismic strain accumulation measured by GPS in the seismic gap between Constitución and Concepción in Chile. Phys Earth Planet Interiors 175:78–85. doi:10.1016/j.pepi.2008.02.015

Stein CA, Stein S (1992) A model for the global variation in oceanic depth and heat flow with lithospheric age. Nature 359:123–129

Tasárová Z (2007) Towards understanding the lithospheric structure of the southern Chilean subduction zone (36°S–42°S) and its role in the gravity field. Geophys J Int 170:995–1014

Tebbens SF, Cande SC (1997) Southeast Pacific tectonic evolution from early Oligocene to Present. J Geophys Res Solid Earth 102:12061–12084. doi:10.1029/96JB02582

Vargas Cordero I (2009) Gas hydrate occurrence and morphostructures along the Chilean margin. Dissertation. University of Trieste, Trieste

Vargas Cordero I, Tinivella U, Accaino F, Loreto MF, Fanucci F, Reichert C (2010a) Analyses of bottom simulating reflections offshore Arauco and Coyhaique (Chile). Geo-Mar Lett 30(3/4):271–281. doi:10.1007/s00367-009-0171-5

Vargas Cordero I, Tinivella U, Accaino F, Loreto MF, Fanucci F (2010b) Thermal state and concentration of gas hydrate and free gas of Coyhaique, Chilean Margin (44°30′S). Mar Petrol Geol 27:1148–1156. doi:10.1016/j.marpetgeo.2010.02.011

Vargas Cordero I, Tinivella U, Accaino F, Fanucci F, Loreto MF, Lascano ME, Reichert C (2011) Basal and frontal accretion processes versus BSR characteristics along the Chilean margin. J Geol Res 2011:846101. doi:10.1155/2011/846101

Villinger H, Tréhu AM, Grevemeyer I (2010) Seafloor marine heat flux measurements and estimation of heat flux from seismic observations of bottom simulating reflectors. In: Riedel M, Willoughby EC, Chopra S (eds) Geophysical characterization of gas hydrates. Society of Exploration Geophysicists, Tulsa, OK, pp 279–300

Völker D, Wiedicke M, Ladage S, Gaedicke C, Reichert C, Rauch K, Kramer W, Heubeck C (2006) Latitudinal variation in sedimentary processes in the Peru-Chile Trench off Central Chile. In: Oncken O, Chong G, Franz G, Giese P, Götze H-J, Ramos VA, Strecker MR, Wigger P (eds) The Andes – active subduction orogeny. Springer, Berlin, pp 193–216

Völker D, Geersen J, Behrmann JH, Weinrebe WR (2012) Submarine mass wasting off southern central Chile: distribution and possible mechanisms of slope failure at an active continental margin. In: Yamada Y, Kawamura K, Ikehara K, Ogawa Y, Urgeles R, Mosher D, Chaytor J, Strasser M (eds) Submarine mass movements and their consequences. Springer, Heidelberg, pp 379–389. doi:10.1007/978-94-007-2162-3_34

von Huene R, Corválan J, Flueh ER, Hinz K, Korstgard J, Ranero CR, Weinrebe W, Scientists CONDOR (1997) Tectonic control of the subducting Juan Fernández Ridge on the Andean margin near Valparaiso, Chile. Tectonics 16:474–488

3. MANUSCRIPT #2

Villar-Muñoz, L.; Bento, J.P.; Klaeschen, D.; Tinivella, U.; Vargas-Cordero, I.; Behrmann, J.H. 2018. A first estimation of gas hydrates offshore Patagonia (Chile). Marine and Petroleum Geology. 96: 232-239. doi: 10.1016/j.marpetgeo.2018.06.002.
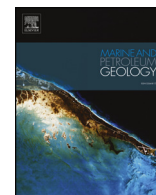
Research paper

A first estimation of gas hydrates offshore Patagonia (Chile)

Lucía Villar-Muñoz[a,*], Joaquim P. Bento[b], Dirk Klaeschen[a], Umberta Tinivella[c], Iván de la Cruz Vargas-Cordero[d], Jan H. Behrmann[a]

[a] GEOMAR Helmholtz Centre for Ocean Research, Wischhofstr. 1-3, 24148, Kiel, Germany
[b] Escuela de Ciencias del Mar, Pontificia Universidad Católica de Valparaíso, Av. Altamirano 1480, 2360007, Valparaíso, Chile
[c] OGS Istituto Nazionale di Oceanografia e di Geofisica Sperimentale, Borgo Grotta Gigante 42/C, 34010, Sgonico, Italy
[d] Universidad Andres Bello, Quillota 980, 2531015, Viña del Mar, Chile

ABSTRACT

In many places along the central and southern Chilean active continental margin sedimentary successions covering the forearc contain methane hydrate, resulting from a mixture of biogenic and thermogenic processes. Here, we report the spatial distribution of gas hydrate in the accretionary prism and forearc sediments offshore western Patagonia (50°S and 57°S), landward of the Antarctica-South America plate boundary. Knowledge of the forearc structure here is limited, owing to the small number of reflection seismic profiles available, lack of high-resolution bathymetry data and the absence of scientific drillholes. However bottom-simulating reflectors (BSR) indicative of gas hydrate occur regionally extensive below about one third of the forearc slope, between about 280 and 630 m below sea floor. BSR-derived heat flow was calculated at about 30 and 70 mWm^{-2}. These are typical values above subduction zones of oceanic crust older than 10 Ma, where vigorous fluid flow above young and hot subducting oceanic crust has leveled off. To move towards an estimate of gas hydrate present in the sediments, the velocity model was converted into a gas-phase concentration model using data from one of the seismic sections. Average thickness of gas hydrate is about 290 m, and average concentrations estimated are in a range of 3.4%–10%. If we use the minimum value of 3.4%, the amount of methane present in the region is about $3.0 \times 10^{13}\,m^3$ at standard pressure-temperature conditions. We conclude that the Pacific forearc of Patagonia area is an important reservoir of methane hydrates and we propose this area be considered as a potential methane hydrate concentrated zone and a key area to be investigated in the future.

1. Introduction

In 1988, on board the R/V CONRAD cruise RC2901, seismic marine data acquired along the Chilean continental margin identified gas hydrate presence through the detection of a well-known reflector called bottom simulating reflector (BSR). After this discovery, several published seismic profiles from Valparaíso to Taitao (33° S and 47° S, respectively) have been analyzed and used to determine the spatial distribution and concentration of hydrates (e.g. Froelich et al., 1995; Brown et al., 1996; Grevemeyer and Villinger, 2001; Grevemeyer et al., 2003; Vargas-Cordero et al., 2010, 2011, 2016, 2017; Villar-Muñoz et al., 2014). However, south of Taitao Peninsula across the Antarctic-South America and the Antarctic-Scotia plate boundaries only few seismic profiles are currently available. The severe wind and wave conditions prevailing here make it difficult to complete good quality geophysical surveying. In addition to the potential as a future energy resource (e.g. Collett and Kuuskraa, 1998) gas hydrate deposits in

sediments at seismically active continental margins may present a serious geological hazard because of the risk of destabilization by abrupt events such as earthquakes (e.g. Boobalan and Ramanujam, 2013) and submarine slope failure (e.g. Dillon et al., 1998). Also processes acting on much larger time scales such as the hydrostatic pressure reduction caused by tectonic uplift, or melting of ice sheets, in response to global warming (e.g. Nisbet, 1990; Bratton, 1999) may be relevant. Therefore, it is important to attempt an assessment of the amount of gas hydrate present at the Patagonian Pacific margin, as it is affected by all short and long timescale processes mentioned above. At convergent plate margins basaltic oceanic crust overlain by thick successions of highly porous and fluid-saturated sediments are being subducted beneath a less dense plate. The accretion of sediment, onto the overriding plate during subduction at oceanic trenches, creates an accretionary prism that may change through geological time, and it is an important process in the evolution of continental margins leading to mountain building and intense deformation, inducing a system of vigorous fluid flow and

---

hydrocarbon formation and migration (e.g. Behrmann et al., 1994). The methane is accumulated and frozen out in the form of gas hydrates in some areas, from the deformation front up to the forearc basin, which can be easily identified in seismic profiles as a prominent BSR (e.g. Hyndman and Spence, 1992). The BSR marks the base of the gas stability zone, and its depth is a constrained by pressure and temperature in the subsurface.

Furthermore, in subduction zones, fluids play a key role in the nucleation and rupture propagation of earthquakes (Sibson, 1973), and are a major agent of advective heat transfer from depth to the Earth's surface. However, direct measurements of the heat transfer are logistically demanding, requiring drillholes or heat probes. Using the stability relations of gas hydrates, geothermal gradients can be constrained by BSR depth and regional variations along the Chilean margin (e.g. Grevemeyer et al., 2003; Vargas-Cordero et al., 2010, 2017; Villar-Muñoz et al., 2014) have been documented previously.

In this paper, we study the western Patagonian region in terms of BSR identification, characterization and perform an estimation of methane reservoir. We chose this region because the accreted sedimentary section is thick, forearc deformation is strong, and documentation of BSR in seismic sections is widespread (Polonia et al., 1999, 2007; Polonia and Torelli, 2007; Rubio et al., 2000; Loreto et al., 2007). However, it has been no evaluation with respect to regional heat flow, nor a semi-quantitative estimation of the gas volume. Here, we intend to advance on the Patagonian region between approximately 50° and 57° southern latitudes by conducting such an analysis.

2. Geological setting

The Patagonian study area is located in the southernmost tip of South America (Fig. 1) and is a tectonically complex area (Pelayo and Wiens, 1989), where not only the Antarctic and South American plates are involved, but also the Scotia plate plays an important role in the tectonic. In the north of the studied area, the Antarctic plate is being subducted beneath the South American plate at a rate of 1.9 cmyr^{-1} (Cisterna and Vera, 2008), and the Chilean trench represents the limits of these plates. In the middle area, close to the Evangelistas lighthouse, the Magallanes-Fagnano fault system intersects the Chile trench defining a triple point between Antarctic, South American and Scotia plates, named as the Fuegian Triple Junction (FTJ) (Polonia et al., 2001), and it is interpreted to be an instable and diffused area of deformation (Forsyth, 1975; Cunningham, 1993). Finally, south of FTJ, the Antarctic plate is subducting below the Scotia plate at a rate of 1.3 cmyr^{-1} and in turn the Scotian plate is subducting beneath the South American plate at a rate of 0.7 cmyr^{-1} (Cisterna and Vera, 2008). The convergence direction of the Antarctic plate is almost margin-perpendicular around 52° S and becomes progressively more oblique toward the south (over 60° at ~ 57° S), due to the counterclockwise rotation of the Patagonian orocline (Cunningham, 1993). Despite that the seismicity is smaller and less frequent than in the north of Chile, it has been recorded two major earthquakes in the region (Martinic, 1988, 2006; Cisterna and Vera, 2008): in 1879 (~ 7.5 M) and, seventy years later, in 1949 (7.5 M). During the last episode, were observed landslides, big waves and anomalous currents.

Plate convergence in southern Chile is marked by a large volume of incoming sediments, and this region was classified as a typical accretionary margin by von Huene and Scholl (1991). The present day accretionary prism is interpreted to be post late Miocene in age (Polonia et al., 1999). A well-defined and locally broad late Miocene accretionary prism is growing at the toe of the continental basement (Cande and Leslie, 1986). In the northern part of the study area, between 50° and 53° S, the prism is very narrow and characterized by intense
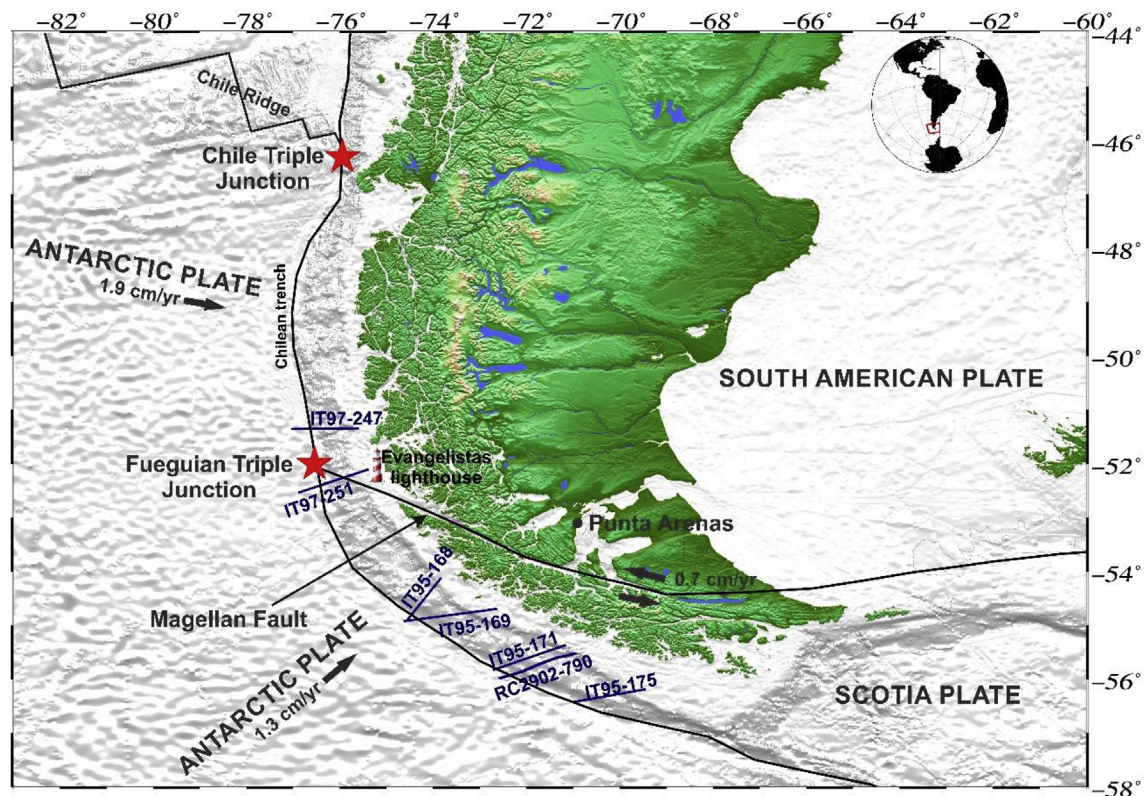

Fig. 1. Location map of the study area offshore Chile, the bathymetry being based on GEBCO_08 Grid (version 20091120, http://www.gebco.net). Tectonic setting of the Nazca, Antarctic, Scotia and South American plates: black lines show the plate boundaries, blue lines correspond to navigation tracks of the studied seismic profiles, and red stars mark a triple junction of the plates. (For interpretation of the references to colour in this figure legend, the reader is referred to the Web version of this article.)

deformation of prism sediments (Loreto, 2005), the décollement level is very shallow, the wedge taper is generally larger than 15°, and frontal thrusts, if present, are seaward vergent. In the southern part, between 53° and 57° S, the deformation style is notably different. Here, the prism is locally very large, its sediment shows clear deformational structures (folds and faults), the taper is 7°–19°, the décollement is deep and subhorizontal, sediments are locally proto-deformed at the trench along seaward and landward vergent thrusts, and a large and undeformed forearc basin is present (Polonia et al., 1999, 2001; Loreto, 2005). Inside the accretionary complex a well-developed BSR at about 0.5 s TWT below the seafloor is imaged. In contrast to a positive seafloor reflection, the BSR has a negative reflection coefficient, and this suggests that it corresponds to a transition between gas hydrates bearing (above) and free gas bearing (below) sediments. Mainly in the southern area, the BSR is extraordinarily continuous where the landward vergence structures are well developed, indicating presence of overpressured fluids (Polonia et al., 1999; Loreto et al., 2007).

3. Geophysical data and processing

The seven seismic reflection profiles presented in this paper were collected during three geophysical cruises offshore southern Chile (western Patagonia). The locations of all seismic profiles are given in Fig. 1.

The seismic profile RC2902-790 was obtained aboard R/V R.D. CONRAD (1988) using a 240-channel digital streamer with 12.5 m group spacing and offsets up to 3300 m recorded 15 s of data. This profile was described by Rubio et al. (2000) and analyzed in this paper. The velocity seismic field was obtained by using iteratively grid based reflection tomography pre-stack depth migration; details about the procedure is described in Woodward et al. (2008).

The remaining profiles were acquired by two cruises aboard the Italian R/V OGS-EXPLORA in 1995 and 1997, IT95 (lines 247 and 251) and IT97 (lines 168, 169, 171 and 175) using 120-channels of a 3000 m long streamer and a seismic source consisted of a 36 air-gun array fired every 50 m. These Italian profiles were described by Polonia et al. (1999), Polonia and Torelli (2007) Polonia et al. (2007) and Loreto et al. (2007).

3.1. Heat flow calculations

Commonly occurring BSRs are probably the most widely used indicators for the presence of natural gas hydrates. The BSR is associated with the acoustic interface between overlying sediment containing gas hydrate, which increases compressional seismic velocity, and underlying sediment containing free gas, which decreases compressional seismic velocity (e.g. Hyndman and Spence, 1992). Thus, BSR imaging of the lower boundary of gas hydrate stability presents a negative polarity, as identified in the seismic sections used in this study (Fig. 2). Because the stability of gas hydrates is controlled by temperature and pressure conditions (e.g. Grevemeyer et al., 2003), this can serve to calculate the steady-state heat flow (q, expressed in mWm^{-2}) by using the following formula:

$$q = \frac{T_z - T_0}{\int_0^z \frac{dz'}{k(z')}}$$

(1)

where T_z and T_0 are the temperatures at the BSR and the seafloor respectively (Villinger et al., 2010), k is the thermal conductivity and z denotes the BSR depth. The BSR and the seafloor depths were obtained from the seismic profiles collected during the cruises mentioned above. Seafloor temperatures were taken from CTD measurements off Chile from the World Ocean Data Base (http://www.nodc.noaa.gov/). Thermal conductivity for the studied area was assumed to be $k = 0.85$ WmK^{-1}, based on ODP Leg 202 drill core data (Grevemeyer et al.,

2003; Mix et al., 2003) and because of sediments on the overriding plate in the research area are not modified by an anomalous heat flow produced by a subducting spreading ridge, as occur in the south-central Chilean margin (Villar-Muñoz et al., 2014). Temperature at the depth of the BSR, T_z, is calculated by using the dissociation temperature-pressure function (Dickens and Quinby-Hunt, 1994):

$$1/T = 3.79 \times 10^{-3} - 2.83 \times (\log p)$$

(2)

where p is the hydrostatic pressure (MPa) and T the temperature (K). Gas in the system is assumed to be pure methane, with a pore water salinity of 35 gl^{-1}. To convert water-column TWT into depth, a seawater compressional wave velocity of 1500 ms^{-1} was used.

3.2. Gas hydrate concentration

The method for estimating gas hydrate and free gas concentrations consists of comparing seismic velocities with theoretical velocity curves in absence of gas hydrate and free gas, which have been considered as background velocity. We followed a modified Domenico's approach in order to reproduce the velocity field in the absence of gas, i.e. full water saturation (Tinivella and Carcione, 2001; Tinivella, 2002). A qualitative estimate of concentrations was obtained by comparing the theoretical velocity for full-water saturation to the seismic velocity, estimated by the velocity analysis. A quantitative estimate was obtained by fitting the theoretical velocity to the experimental velocity, increasing the parameters of the theoretical model related to the gas-phase concentrations. The method can model two main distributions to calculate the concentrations of free gas in the pore space: uniform distribution (gas and water in pore space) and patchy distribution (all gas in patches without water). In our case, we considered initial porosity just below the seafloor equal to 50% (Diemer and Forsythe, 1995) and bottom water temperature equal 2.2 °C (Grevemeyer and Villinger, 2001). The other parameters are supposed in agreement with Vargas-Cordero et al. (2010); in particular, the porosity (ϕ) versus depth (z, km) was evaluated considering the following equation:

$$\phi = 0.50 - 0.80\,z + 0.25\,z^2$$

(3)

4. Results

4.1. Heat flow

A key observation is that the BSR, delineating the base of gas hydrates, mostly was identified around the 2000 m water depth contour and is typically located between 286 and 632 m below sea floor (mbsf) (Fig. 3a). Note that the profile IT97-251 (the second line from north to south) has no evidence of BSR.

At the beginning of profile IT95-169 (~55°S), we can observe the darkest point, around 2100 m water depth, which marks the deepest BSR identified: 632 mbsf. On the other hand, the bright shallowest BSR was distinguished in the southernmost profile, IT95-175 (~57°S): 286 mbsf. In both profiles, available literature information was used. BSR-derived heat flow calculations along the profiles are 33–67 mWm^{-2} (Fig. 3b). These are heat flow values indicative of conductive heat transfer through forearcs underlain by a relatively old (> 10 Ma), and, therefore, cold downgoing oceanic plate. In map view, it is clear that most of the forearc between 51°S and 57°S is dominated by low (i.e. generally < 60 mWm^{-2}) heat flow. So, the values of BSR-derived heat flow are in agreement with the geological environment of the study area and the available direct measurements, confirming the reliability of our velocity models obtained by seismic data analysis and used to estimate gas hydrate and free gas concentrations.

We also detected a weak reflector below the BSR in the seismic profile RC2902-790, around the trace number 1200 and 2200, which could be interpreted as the base of free gas reflector, the so-called BGR
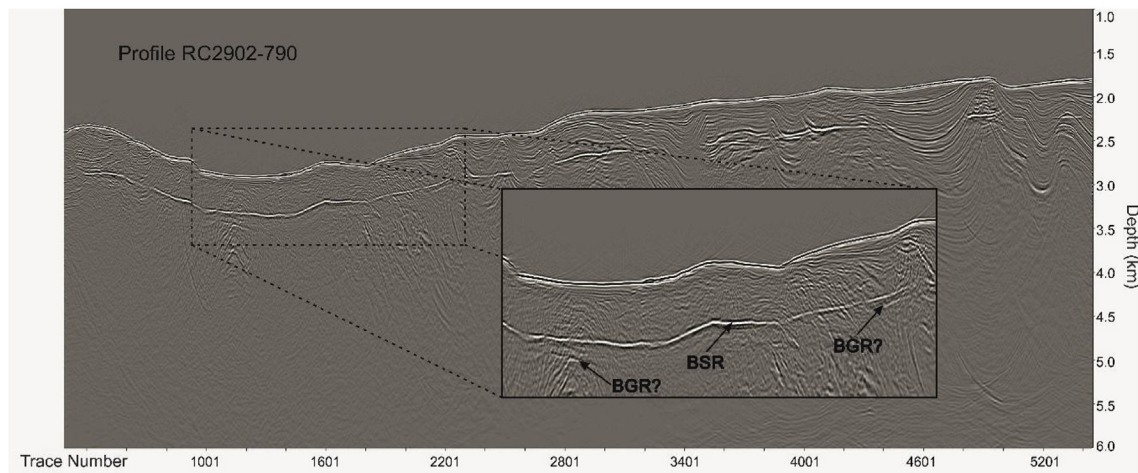
Fig. 2. Example of BSR identification. Profile RC2902-790, south sector of study area. Zoom showing reverse polarity of BSR. The reflector was identified below the BSR and interpreted as BGR. See text for details.

(see zoom section on Fig. 2).

4.2. Seismic velocity model and gas hydrate concentration

The final velocity model of the RC2902-790 seismic profile shows that the layer above the BSR is characterized by high velocity (1800–2200 ms^{-1}), with respect to the normal compacted marine sediments, which can be associated to gas hydrate presence. A layer below the BSR shows sectors with a velocities (1600–1700 ms^{-1}), that could be associated to free gas presence (Fig. 4). Note that these velocities are lower than expected for water saturated sediments at this depth, but relatively higher than expected for free gas bearing sediments (i.e., Tinivella and Carcione, 2001). Probably, the identified layer below the BSR is constituted by an average of free gas and water-bearing sediments and the real base of the free gas layer is not be detected by seismic data due to low resolution of the data.

The velocity field was translated in terms of gas hydrate and free gas concentrations as described in the previous section (Fig. 5). Because of our analysis is mainly qualitative due to a lack of well data, we considered the average hydrate concentration, evaluating also the average BSR depth at each CDP. The average gas hydrate concentration (Fig. 6) indicates the hydrate presence below the seafloor: the average thickness of gas hydrate layer across the seismic line is 287 m and the average hydrate concentration is about 3.4% of total volume. The highest gas hydrate concentrations are located at CDP 7000 (see also Fig. 5) and

between CDPs 9000 to 9500, reaching a value of about 10% of total volume, in correspondence of the part of the section where the BSR is strongest (see zoom section on Fig. 2). Lower gas hydrate concentrations are located between CDPs 7500 to 9000 (about 5% of total volume). Note that this last part of the seismic line in Fig. 4 is characterized by presence of faults, which can favor the escape of fluids.

The BSR observed into studied seismic profiles varies in continuity and amplitude (Fig. 7). Over the accretionary prism, we calculated that the BSR is present in an average of 36% of the analyzed total area, increasing its continuity and amplitude from north to south. Note that over the seismic profile IT97-251, which is located near to the FTJ (see Fig. 1), the BSR was absent.

4.3. Estimation of gas hydrates

To provide a basis for the estimate of methane stored in the studied region, bulk estimate of hydrate concentration was calculated using the following values: 3.4% of the total volume (blue dashed line in Fig. 6) at 50% porosity between 286 and 632 mbsf (from Fig. 3a), free gas layer thicknesses 284 m (red dashed line in Fig. 6) and a total projected area of about 53,000 km^2. From this, methane budget just from hydrates is 3.03×10^{13} m^3 at standard pressure-temperature conditions.
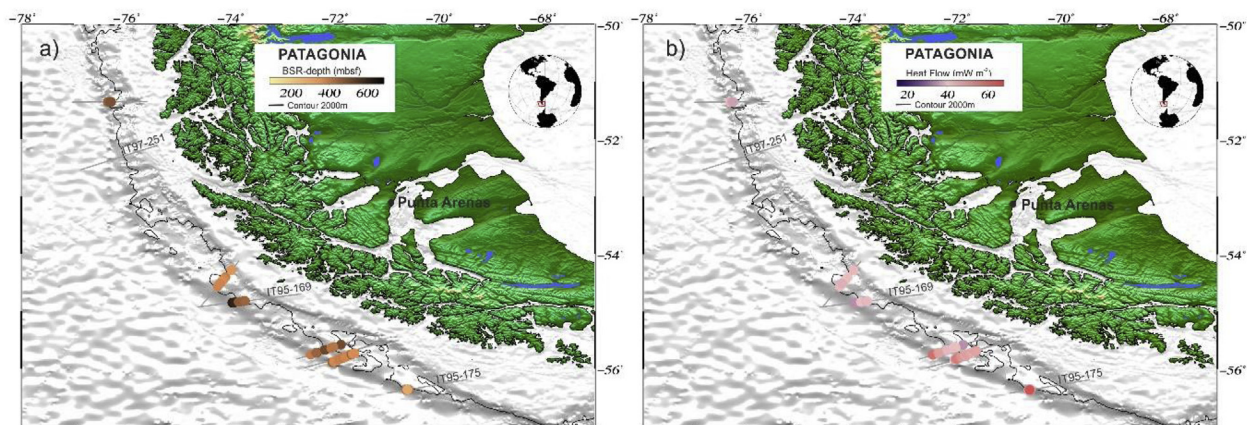

Fig. 3. Colour-coded results of BSR identification in all seismic lines of the study area. (a) BSR depth in meters below sea floor (mbsf) (b) Heat flow in mWm^{-2}. Solid line correspond to 2000 m isobath. See text for description. (For interpretation of the references to colour in this figure legend, the reader is referred to the Web version of this article.)
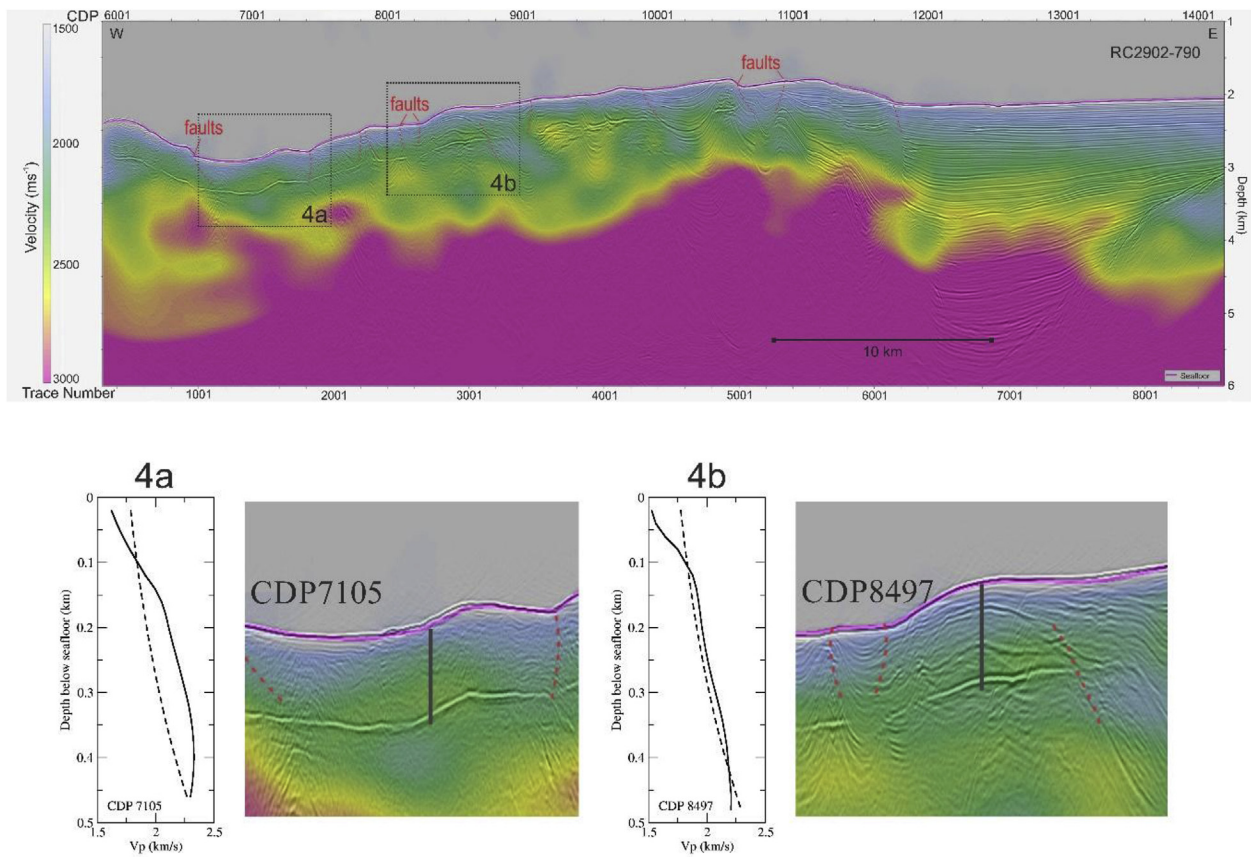
Fig. 4. Top: pre-stack depth migration section of the RC2903-790, in which the main faults are indicated (broken red lines); the seismic velocity is over imposed. The blow-ups indicate a detail of the seismic section. Panels 4a and 4b reported the seismic (solid lines) and modeled (broken lines) velocities at the CDPs 7105 and 8497 respectively. Their position is indicated as black lines in the blow-ups. The discrepancies between the seismic and modeled velocities are interpreted as caused by hydrate presence. See text for details. (For interpretation of the references to colour in this figure legend, the reader is referred to the Web version of this article.)

5. Discussion

The Chilean margin is one of the key area for gas hydrate studies since a significant amount of methane is suggested to be trapped in the marine sediments as indicated in global climate change modeling (IPCC, 2014). Moreover, two major earthquakes had been registered in the study area suggesting a tectonically active region. Considering this, we hypothesize a new earthquake in the future, due to an existing seismic gap, capable to destabilize the hydrate bearing reservoir, and induce methane release into the ocean. (e.g, Ruppel and Kessler, 2016).

In terms of a development on a larger timescale, today it is assumed that in the worst case climate change scenario, with a steady warming of the ocean of 3 °C, around 85% of the methane trapped in the sea floor could be released into the water column, and part of it could reach the atmosphere (Bollmann et al., 2010). One of the expected consequences due to global warming could be the sea level rise due to melting of polar ice caps and glacial ice (IPCC, 2014); so, the inevitable increase of the pressure at the sea floor is foreseen. The increase in pressure, however, would not be sufficient to counteract the effect of temperature increase that can dissociate the methane hydrates (i.e., Bratton, 1999; Ruppel and Kessler, 2016). For example, a sea-level rise of 10 m could slow down the methane-hydrate dissociation caused by a warming of 1 °C only by a few decades (Bollmann et al., 2010). One major goal of the current gas hydrate research is to provide more precise input parameters, in particular the volume of methane trapped in the marine sediments as hydrates from geophysical studies, in order to optimize global climate change models.

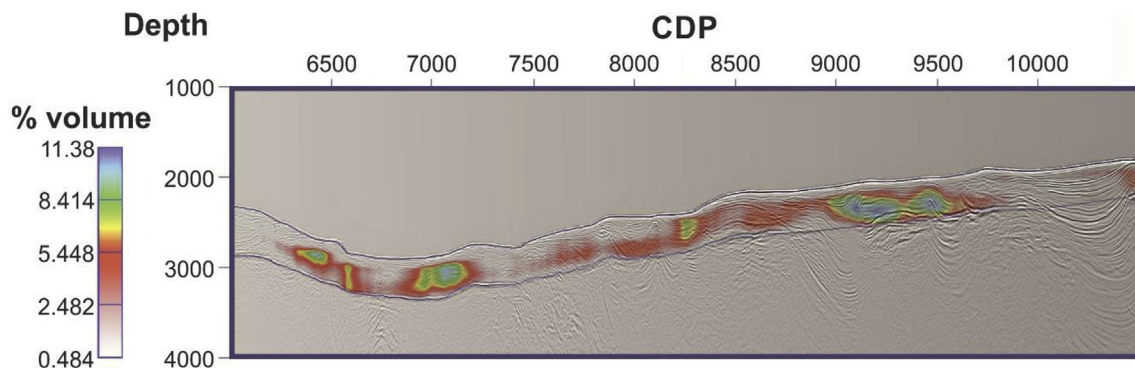In this context, few seismic lines were analyzed to study the

Fig. 5. Gas hydrate concentration model extracted from the velocity models in the southern sectors of the study area. See text for details.
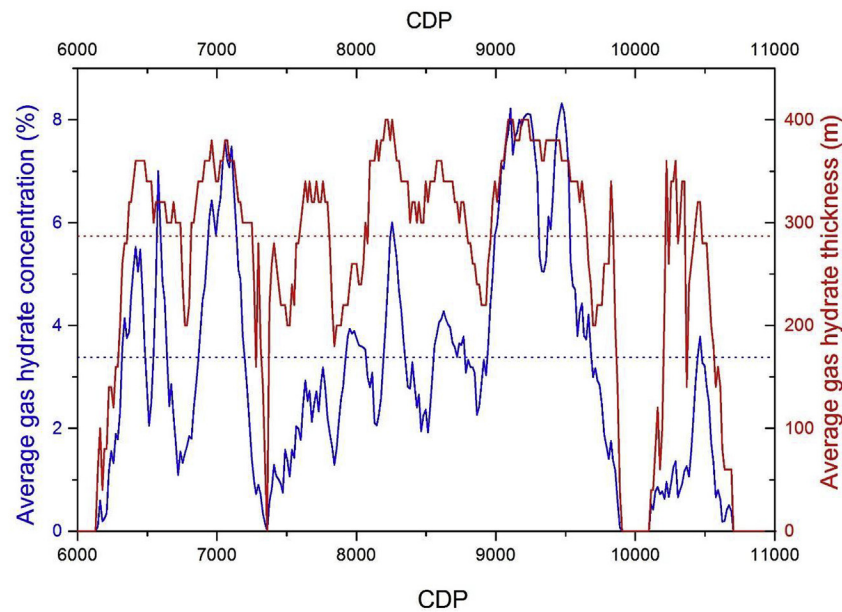
Fig. 6. Average gas hydrate concentration (solid blue line) and average gas hydrate thickness (solid red line) across the seismic line. The global average values are indicated with dashed lines. (For interpretation of the references to colour in this figure legend, the reader is referred to the Web version of this article.)

relationship between the gas hydrate system and geological setting along the southern Chilean margin. Our analysis points out that seismic character of the BSR (continuity and amplitude) is strongly variable showing an increase toward south (Fig. 7). In the northern part of the study area (50°–53° S), the prism is very narrow and characterized by intense deformation of prism sediments (Loreto, 2005) making it difficult for the hydrate to form and, thus, be expressed by a BSR. On the contrary, in the southern part between 53° and 57° S, we observe a wide and thicker prism, and its sedimentary sections show clear deformational structures (folds and faults), which promote formation and preservation of methane hydrates (Vargas-Cordero et al., 2011).

The stronger BSR was identified on seismic profile IT95-171, described by Loreto (2005), where a deep décollement, located near the top of the oceanic crust, is shown. Thus, nearly all of the about 2.5 km thick trench sedimentary section is being frontally accreted, increasing fluid circulation in the sediment layers by progressive loading, and stimulating methane hydrate formation. Another clear example of a large accretionary prism is observed on the profile RC2902-790, where a continuous and strong BSR is identified (Fig. 2).

On the other hand, profile IT97-251 (Fig. 7), close to the FTJ, has no evidence of a BSR in the whole section, maybe due to the Magallanes-Fagnano fault system, where deeper fluids could escape to the water column, making hydrate formation more difficult. This is an instable and diffuse area of deformation (Forsyth, 1975; Cunningham, 1993) related with the Magellan-Fagnano fault system. Although this line shows a 12 km wide accretionary prism, it contains sediments poorly stratified and intensely deformed by fractures and seaward dipping discontinuities (Loreto et al., 2007). Besides, this prism is underlain by a shallow main décollement level, probably preventing fluid circulation and/or fluid trapping in the sediments.

Finally, the estimated total gas volume in this work is comparable with recent estimations made in Japan (Bo et al., 2018; Taladay et al., 2017) and based on the large amount of gas hydrates founded in the Patagonian area, we propose that this area should be considered as a methane hydrate concentrated zone (MHCZ). Many efforts need to be made to improve the knowledge of this area because of its strategic relevance. In fact, if a massive destabilization occurs, caused by natural factors (e.g. submarine sliding, earthquake-induced deformation, or global warming), significant amounts of methane can be released into the oceans and, as suggested by several authors, into the atmosphere

(e.g. Ruppel and Kessler, 2016).

6. Conclusions

The results of this search for gas hydrate in the Patagonian Pacific margin lead us to conclude that:

(1) The hydrate layer is typically located between about 280 and 630 mbsf, and values of BSR-derived crustal heat flow are around 30–70 mWm^{-2}. These are typical values above subduction zones of oceanic crust older than 10 Ma.
(2) The RC2902-790 seismic profile shows that the layer above the BSR is characterized by high velocity (1800–2200 ms^{-1}), associated to gas hydrate presence, and below the BSR shows sectors with velocities characterized by values of about 1600–1700 ms^{-1} that could be related to free gas presence.
(3) The BSR increases its continuity and amplitude from north to south and is present in an average of 36% of the total forearc area.
(4) Estimates of the average thickness of the gas hydrate layer are about 290 m and the average hydrate concentration is about 3.4% of total volume.
(5) From these estimates, and using a porosity of 50% in a total projected area of 53,000 km^2, the estimated methane budget just from gas hydrates is about 3×10^{13} m^3 at standard pressure-temperature conditions.
(6) Sudden or slow release of this amount of methane in the event of gas hydrate dissociation presents a sizeable geological risk that warrants further, more detailed assessment.
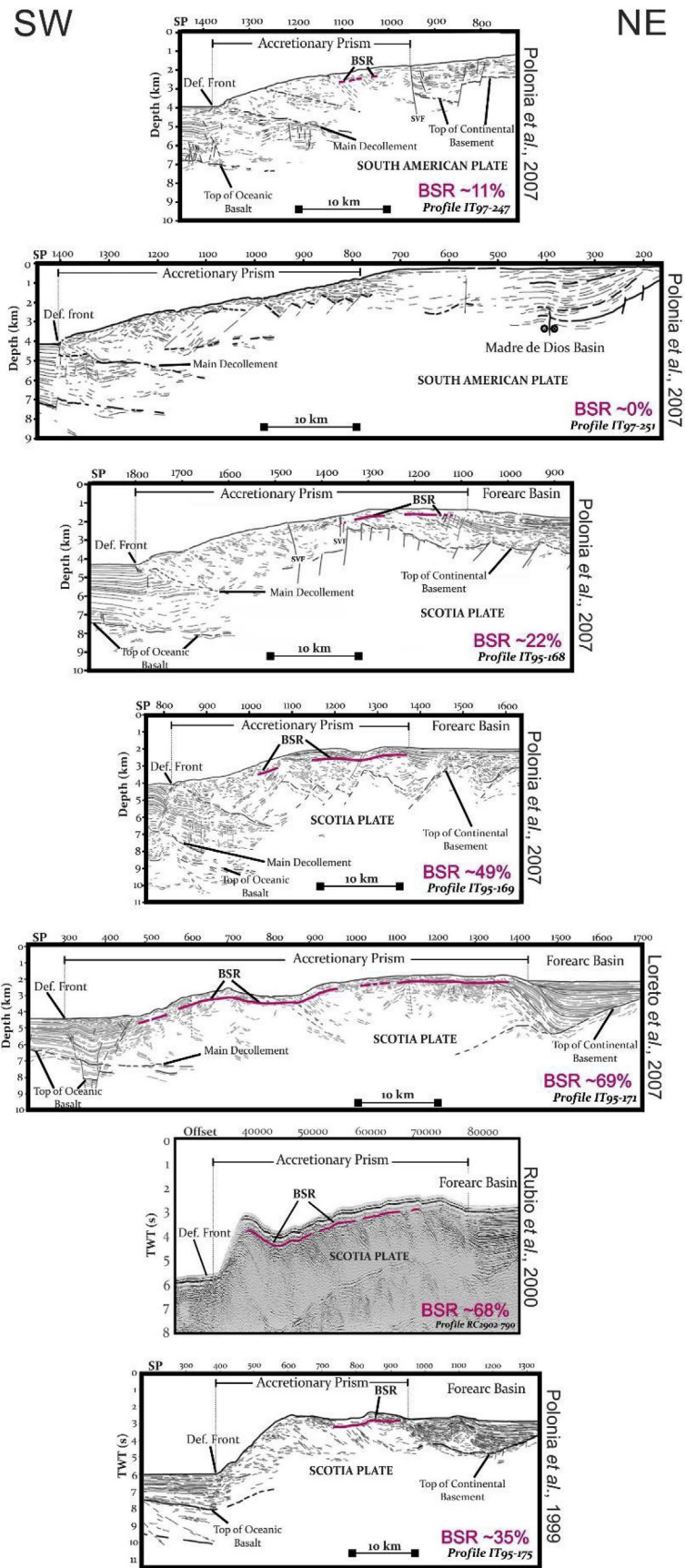(7) We propose the Pacific margin of Patagonia be considered as a MHCZ.

Fig. 7. Result of the BSR average in the study area. Diagrams show the seven seismic profiles studied in this work, from north to south. Pink lines mark the BSR identified by different authors inside the accretionary prism, starting in the Deformation Front (Def. Front) up to the Forearc Basin. (For interpretation of the references to colour in this figure legend, the reader is referred to the Web version of this article.)

References

Behrmann, J.H., Lewis, S.D., Cande, S.C., 1994. Tectonics and geology of spreading ridge subduction at the Chile Triple Junction: a synthesis of results from Leg 141 of the Ocean Drilling Program ODP Leg 141 Scientific Party. Geol. Rundsch. 83, 832–852.

Bo, Y.Y., Lee, G.H., Kang, N.K., Yoo, D.G., Lee, J.Y., 2018. Deterministic estimation of gas-hydrate resource volume in a small area of the Ulleung Basin, East Sea (Japan Sea) from rock physics modeling and pre-stack inversion. Mar. Petrol. Geol. 92, 597–608.

Bollmann, M., Bosch, T., Colijin, F., Ebinghaus, R., Froese, R., Güssow, K., et al., 2010. World Ocean Review. Living with the Ocean. Maribus GmbH, Hamburg 236 p.

Boobalan, A.J., Ramanujam, N., 2013. Triggering mechanism of gas hydrate dissociation and subsequent sub marine landslide and ocean wide Tsunami after Great Sumatra-Andaman 2004 earthquake. Arch. Appl. Sci. Res. 5, 105–110.

Bratton, J.F., 1999. Clathrate eustasy: methane hydrate melting as a mechanism for geologically rapid sea-level fall. Geology 27, 915–918.

Brown, K.M., Bangs, N.L., Froelich, P.N., Kvenvolden, K.A., 1996. The nature, distribution, and origin of gas hydrate in the Chile Triple Junction region. Earth Planet Sci. Lett. 139, 471–483.

Cande, S.C., Leslie, R.B., 1986. Late Cenozoic tectonics of the southern Chile trench. J. Geophys. Res. 91, 471–496.

Cisterna, A., Vera, E., 2008. Sismos históricos y recientes en Magallanes. Magallania 36 (1), 43–51.

Collett, T.S., Kuuskraa, V.A., 1998. Hydrates contain vast store of world gas resources. Oil Gas J. 96 (19), 90–95.

Cunningham, W.D., 1993. Strike-slip faults in the southernmost Andes and the development of the Patagonian orocline. Tectonics 12, 169–186.

Diemer, J.A., Forsythe, R., 1995. Grain size variations within slope facies recovered from the Chile Margin Triple Junction. In: Lewis, S.D., Behrmann, J.H., Musgrave, R.J. (Eds.), Proc ODP, Sci Results 141. Ocean Drilling Program, College Station, Texas.

Dickens, G.R., Quinby-Hunt, M.S., 1994. Methane hydrate stability in seawater. Geophys. Res. Lett. 21, 2115–2118.

Dillon, W.P., Danforth, W.W., Hutchinson, D.R., Drury, R.M., Taylor, H.H., Booth, J.S., 1998. In: Henriet, J.-P., Mieneat (Eds.), Gas Hydrates: Relevance to World Margin Stability and Climate Change. J. Geol. Soc. Special Publications 137, London, pp. 293–302.

Forsyth, D.W., 1975. Fault plane solutions and tectonics of the South Atlantic and Scotia Sea. Journal of Geophysical 80, 1429–1443.

Froelich, P.N., Kvenvolden, K.A., Torres, M.E., Waseda, A., Didyk, B.M., Lorenson, T.D., 1995. Geochemical evidence for gas hydrate in sediment near the Chile triple junction. In: Lewis, S.D., Behrmann, J.H., Musgrave, R.J. (Eds.), Proc ODP Scientific Results 141, pp. 279–286.

Grevemeyer, I., Villinger, H., 2001. Gas hydrate stability and the assessment of heat flow through continental margins. Geophys. J. Int. 145, 647–660.

Grevemeyer, I., Diaz-Naveaz, J.L., Ranero, C.R., Villinger, H.W., 2003. Heat flow over the descending Nazca plate in Central Chile, 32°S to 41°S: observations from ODP Leg 202 and the occurrence of natural gas hydrates. Earth Planet Sci. Lett. 213, 285–298.

Hyndman, R.D., Spence, G.D., 1992. A seismic study of methane hydrate marine bottom-simulating-reflectors. J. Geophys. Res. 97, 6683–6698.

IPCC, 2014. Climate Change 2014: Synthesis Report. Contribution of Working Groups I, II and III to the Fifth Assessment Report of the Intergovernmental Panel on Climate Change. Core Writing Team, R.K. Pachauri and L.A. Meyer, Geneva 151 p.

Loreto, M.F., 2005. Analisi dei processi di subduzione della Placca Antartica al largo della Terra del Fuoco (Cile Meridionale). PhD thesis. University of Parma, Dip. of Earth Science.

Loreto, M.F., Tinivella, U., Ranero, C., 2007. Evidence for fluid circulation, overpressure and tectonic style along the Southern Chilean margin. Tectonophysics 429, 183–200.

Martinic, M., 1988. El gran temblor de tierra de 1879 en la Patagonia Austral. Rev. Patagónica 30–31.

Martinic, M., 2006. Documentos inéditos para la historia de Magallanes. El fallido intento colonizador en Muñoz Gomero 1969-1971. Magallania 34 (2), 119–124.

Mix, A.C., Tiedemann, R., Blum, P., et al., 2003. In: Proceedings of the Ocean Drilling Program, Initial Reports, No 202.

Nisbet, E.G., 1990. The end of the ice age. Can. J. Earth Sci. 27 (1), 148–157.

Pelayo, A.M., Wiens, D.A., 1989. Seismotectonics and relative plate motion in the Scotia Sea region. J. Geophys. Res. 94, 7293–7320.

Polonia, A., Brancolini, G., Torelli, L., Vera, E., 1999. Structural variability at the active continental margin off southernmost Chile. Geodynamics 27, 289–307.

Polonia, A., Brancolini, G., Torelli, L., 2001. The accretionary complex of southernmost Chile from the strait of Magellan to the Drake passage. Terra Antarct. 8 (2), 87–98.

Polonia, A., Torelli, L., 2007. Antarctic/Scotia plate convergence off southernmost Chile. Geol. Acta 5, 295–306.

Polonia, A., Torelli, L., Brancolini, G., Loreto, M.F., 2007. Tectonic accretion versus erosion along the southern Chile trench: oblique subduction and margin segmentation. Tectonics 26, TC3005.

Rubio, E., Torné, M., Vera, E., Díaz, A., 2000. Crustal structure of the southernmost Chilean margin from seismic and gravity data. Tectonophysics 323, 39–60.

Ruppel, C.D., Kessler, J.D., 2016. The interaction of climate change and methane hydrates. Rev. Geophys. 55, 126–168.

Sibson, R.H., 1973. Interactions between temperature and pore fluid pressure during earthquake faulting - a mechanism for partial or total stress relief. Nature 243, 66–68.

Taladay, K., Boston, B., Moore, G.F., 2017. Gas-in-place estimate for potential gas hydrate concentrated zone in the Kumano Basin, Nankai Trough Forearc, Japan. Energies 10, 1552.

Tinivella, U., Carcione, J.M., 2001. Estimation of gas-hydrate concentration and free-gas saturation from log and seismic data. Lead. Edge 20, 200–203.

Tinivella, U., 2002. The seismic response to overpressure versus gas 638 hydrate and free gas concentration. J. Seismic Explor. 11, 283–305.

Vargas-Cordero, I., Tinivella, U., Accaino, F., Loreto, M.F., Fanucci, F., Reichert, C., 2010. Analyses of bottom simulating reflections offshore Arauco and Coyhaique (Chile). Geo Mar. Lett. 30, 271–281.

Vargas-Cordero, I., Tinivella, U., Accaino, F., Fanucci, F., Loreto, M.F., Lascano, M.E., Reichert, C., 2011. Basal and frontal accretion processes versus BSR characteristics along the Chilean Margin. J. Geol. Res. 2011, 1–10.

Vargas-Cordero, I., Tinivella, U., Villar-Muñoz, L., Giustiniani, M., 2016. Gas hydrate and free gas estimation from seismic analysis offshore Chiloé island (Chile). Andean Geol. 43 (10), 263–274.

Vargas-Cordero, I., Tinivella, U., Villar-Muñoz, L., 2017. Gas hydrate and free gas concentrations in two sites inside the Chilean Margin (Itata and Valdivia Offshores). Energies 10 (12), 2154.

Villinger, H., Tréhu, A.M., Grevemeyer, I., 2010. Seafloor marine heat flux measurements and estimation of heat flux from seismic observations of bottom simulating reflectors. In: Riedel, M., Willoughby, E.C., Chopra, S. (Eds.), Geophysical Characterization of Gas Hydrates. Society of Exploration Geophysicists, Tulsa, pp. 279–300.

Villar-Muñoz, L., Behrmann, J.H., Diaz-Naveas, J., Klaeschen, D., Karstens, J., 2014. Heat flow in the southern Chile forearc controlled by large-scale tectonic processes. Geo Mar. Lett. 34, 185–198.

von Huene, R., Scholl, D.V., 1991. Observations at convergent margins concerning sediment subduction, subduction erosion, and the growth of continental crust. Rev. Geophys. 29, 279–316.

Woodward, M.J., Nichols, D., Zdraveva, O., Whitfield, P., Johns, T., 2008. A decade of tomography. Geophysics 73, VE5–VE11.

4. MANUSCRIPT #3

Villar-Muñoz, L.; Vargas-Cordero, I.; Bento, J.P.; Tinivella, U.; Fernandoy, F.; Giustiniani, M.; Behrmann, J.H.; Calderón-Díaz, S. 2019. Gas Hydrate Estimate in an Area of Deformation and High Heat Flow at the Chile Triple Junction. Geosciences. 9: 28. doi: 10.3390/geosciences9010028.

Article

Gas Hydrate Estimate in an Area of Deformation and High Heat Flow at the Chile Triple Junction

Lucía Villar-Muñoz [1],*, Iván Vargas-Cordero [2] , Joaquim P. Bento [3] , Umberta Tinivella [4] , Francisco Fernandoy [2,5] , Michela Giustiniani [4] , Jan H. Behrmann [1] and Sergio Calderón-Díaz [2]

[1]   GEOMAR Helmholtz Centre for Ocean Research, Wischhofstr. 1-3, 24148 Kiel, Germany; jbehrmann@geomar.de

[2]   Facultad de Ingeniería, Universidad Andrés Bello, Quillota 980, Viña del Mar 2531015, Chile; ivan.vargas@unab.cl (I.V.-C.); francisco.fernandoy@unab.cl (F.F.); sergio.calderon@unab.cl (S.C.-D.)

[3]   Escuela de Ciencias del Mar, Pontificia Universidad Católica de Valparaíso, Av. Altamirano 1480, Valparaíso 2340000, Chile; jnettojunior@gmail.com

[4]   Istituto Nazionale di Oceanografia e di Geofisica Sperimentale (OGS), Borgo grotta gigante 42/c, 34010 Sgonico, Italy; utinivella@inogs.it (U.T.); mgiustiniani@inogs.it (M.G.)

[5]   Centro de Investigación Para la Sustentabilidad (CIS), Universidad Andrés Bello, República 252, Santiago 8370134, Chile

*   Correspondence: lucia.villar@gmail.com; Tel.: +56-9-5226-4461

check for updates

Abstract: Large amounts of gas hydrate are present in marine sediments offshore Taitao Peninsula, near the Chile Triple Junction. Here, marine sediments on the forearc contain carbon that is converted to methane in a regime of very high heat flow and intense rock deformation above the downgoing oceanic spreading ridge separating the Nazca and Antarctic plates. This regime enables vigorous fluid migration. Here, we present an analysis of the spatial distribution, concentration, estimate of gas-phases (gas hydrate and free gas) and geothermal gradients in the accretionary prism, and forearc sediments offshore Taitao (45.5°–47° S). Velocity analysis of Seismic Profile RC2901-751 indicates gas hydrate concentration values <10% of the total rock volume and extremely high geothermal gradients (<190 °C·km^{-1}). Gas hydrates are located in shallow sediments (90–280 m below the seafloor). The large amount of hydrate and free gas estimated (7.21 × 10^{11} m^3 and 4.1 × 10^{10} m^3; respectively), the high seismicity, the mechanically unstable nature of the sediments, and the anomalous conditions of the geothermal gradient set the stage for potentially massive releases of methane to the ocean, mainly through hydrate dissociation and/or migration directly to the seabed through faults. We conclude that the Chile Triple Junction is an important methane seepage area and should be the focus of novel geological, oceanographic, and ecological research.

Keywords: BSR; gas hydrate; methane; seepage; active margin; Chile Triple Junction

1. Introduction

Gas hydrate is a crystalline ice-like solid formed by a mixture of water and gasses, mainly methane, giving place to a clathrate structure [1,2] that can be stored in the pore space of marine sediments under low temperature (<25 °C) and high pressure (>0.6 MPa) conditions. Methane gas may be produced biogenically at shallow depths or may migrate from a deeper source through advective transport along pathways such as fracture networks, faults, or shear zones (e.g., [3]). Since the gas hydrates are rich in methane, 1 m^3 of hydrate will yield 0.8 m^3 of water and 164 m^3 of methane at standard pressure and temperature (STP: 0 °C, 0.101325 Mpa) conditions [4], and a significant amount of hydrate

represents unconventional and potential energy resources [5]. Moreover, gas hydrates play a part in global climate change, geo-hazards, and potential drilling hazards (e.g., [6–10]).

It is possible to identify gas hydrates in marine sediments using seismic profiles. The main indicator is the so-called Bottom Simulating Reflector (BSR), whose presence is related to the impedance contrast between high velocity gas hydrate-bearing and the underlying low velocity free gas layer [11–14]. Gas hydrate occurrences along the Chilean margin have been reported in many places by analysing the available seismic profiles (e.g., [11,14–27]), as well as more recently by direct identification of cold seeps emitting methane at the seafloor [28–34]. The first discovery of a seepage area was in 2004, offshore Concepción. Afterwards, other bathyal seep sites were identified, mainly by the presence of typical seep communities: (a) off the Limarí River at ~30° S (~1000 m water depth); (b) off El Quisco at 33° S (~340 m water depth); and c) off the Taitao Peninsula at ~46° S (~600 m water depth) [30–37].

Cold seeps sites are found in both active and passive margins and are related to the expulsion of methane-rich fluids. Chemosynthetic communities have been observed along active margins characterized by a well-developed accretionary prism, and along tectonically erosive margins [38]. The Chile Triple Junction (CTJ) area is a spectacular example of tectonic erosion (e.g., [39]). Even though many investigations are associated with seepage identification and gas expulsion quantification (gas bubbles) (e.g., [29,38,40–42]), there are few cases where the objective was to estimate the size of the gas source, as concentrations of gas hydrate and free gas [43].

Furthermore, the studies that report estimates of gas hydrates concentrations along the Chilean margin are scarce, even though, in the last decades, gas-phase concentrations have been estimated by fitting modelled velocity with theoretical velocity in the absence of gas [44]. These estimates reach an average of 15% and 1% of the total volume of gas hydrate and free gas concentrations, respectively [22,24,25,27]. A recent investigation of the southernmost Chilean continental margin showed that a regionally extensive methane hydrate reservoir, characterized by high gas hydrate and free gas concentrations, is present in the Patagonian marine sediments [27]. This could be an important natural resource for Chile, but because of the hydrate decomposition, this also potentially poses a great environmental threat.

On the other hand, the Chilean south-central margin is one of the tectonically most active regions on Earth, with very large and mega-scale earthquakes occurring every 130 and 300 years, respectively [45]. The margin segment close to the CTJ is characterized by high seismicity [46,47] that may trigger submarine sediments sliding and eventual gas hydrate dissociation. Some authors suggest that large subduction zone earthquakes have the potential to trigger hydrocarbon seepage to the ocean and possibly to the atmosphere (e.g., [29,48]). In this context, known gas hydrate quantities stored beneath marine sediments play an important role in the geohazard assessment. Besides, in subduction zones such as the Chilean margin, fluids play a key role in the nucleation and rupture propagation of earthquakes [49], and are a major agent of advective heat transfer from depth to the Earth's surface. For this reason, it is crucial to know the pathways where methane-rich fluids could migrate. The release of this methane stored in the forearc wedge could have consequences for the ocean and atmosphere systems, and the destabilized gas hydrate-bearing sediments are a formidable geohazard, in the form of submarine slumps, induced earthquakes, and tsunamis (e.g., [2,6,50–54]).

The particularity of the Chilean margin close to the CTJ, with anomalous heat flow and high seismicity, together with the presence of hydrothermal systems (e.g., [55]) and possible seafloor seeps, offers a unique scenario to study hydrate deposits. The aim of this study is to characterize and estimate the methane concentrations (hydrate and free gas phases) stored in the marine sediments in order to understand the potential amount of this gas that could be released through these natural pathways, likely affecting the geochemical properties of the seawater and, consequently, the marine ecology.

Geological Setting

The CTJ (Figure 1) is the site of the intersection of three tectonic plates: Nazca, Antarctic, and South America [39,56,57]. Here, the Chile Rise (CR), an active spreading centre, is being subducted beneath the South American continental margin. Ridge subduction began near Tierra del Fuego ~14 million years ago (Ma) and then migrated northwards to its current position north of the Taitao Peninsula (e.g., [15]). The Nazca plate subducts beneath South America in an ENE direction at a rate of about 70 km·Ma^{-1} north of the CTJ, and the Antarctic plate subducts in an ESE direction at about 20 km·Ma^{-1} south of the CTJ (e.g., [56]). The CR spreading rate has been estimated to have been about 70 km·Ma^{-1} over the past 5 Ma, but within the last 1 Ma, it has slowed down to about 60 km·Ma^{-1} (e.g., [58]).
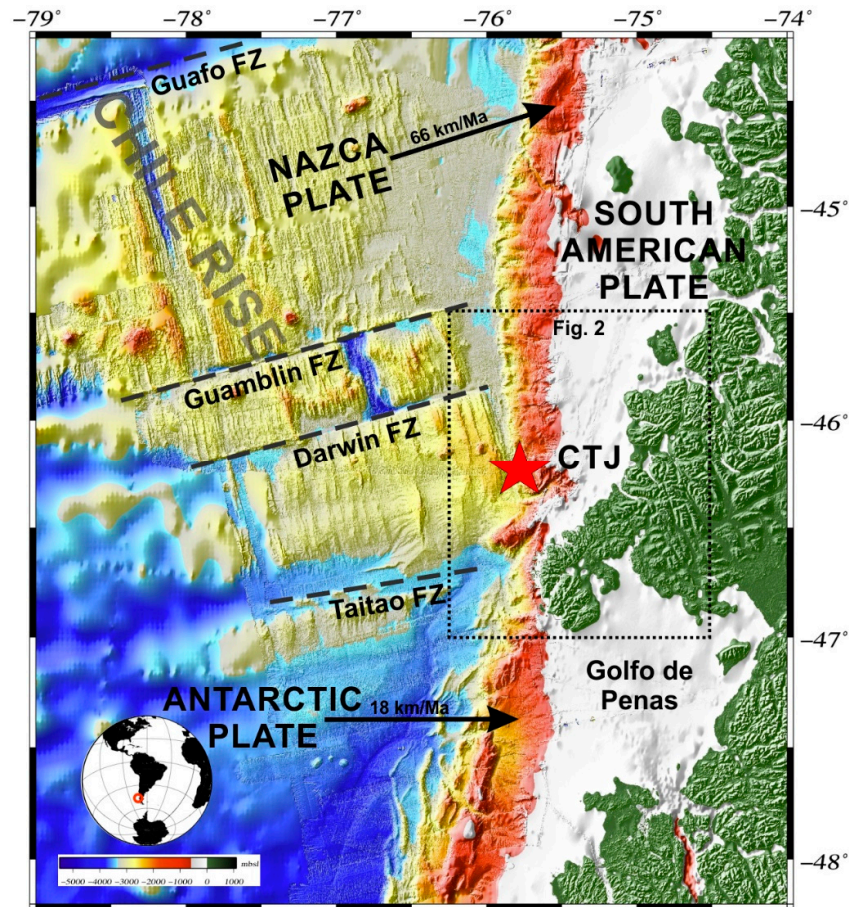

Figure 1. Location map of the study area offshore Taitao Peninsula. The bathymetry is based on GEBCO_08 Grid (version 20091120, http://www.gebco.net) and integrated with the IFREMER grid (cruise of the R/V L'Atalante, 1997). Tectonic setting of the Nazca, Antarctic, and South American plates: dashed black lines show the main Fracture Zones (FZ), red star marks a triple junction of the plates (CTJ), and dashed square corresponds to Figure 2.
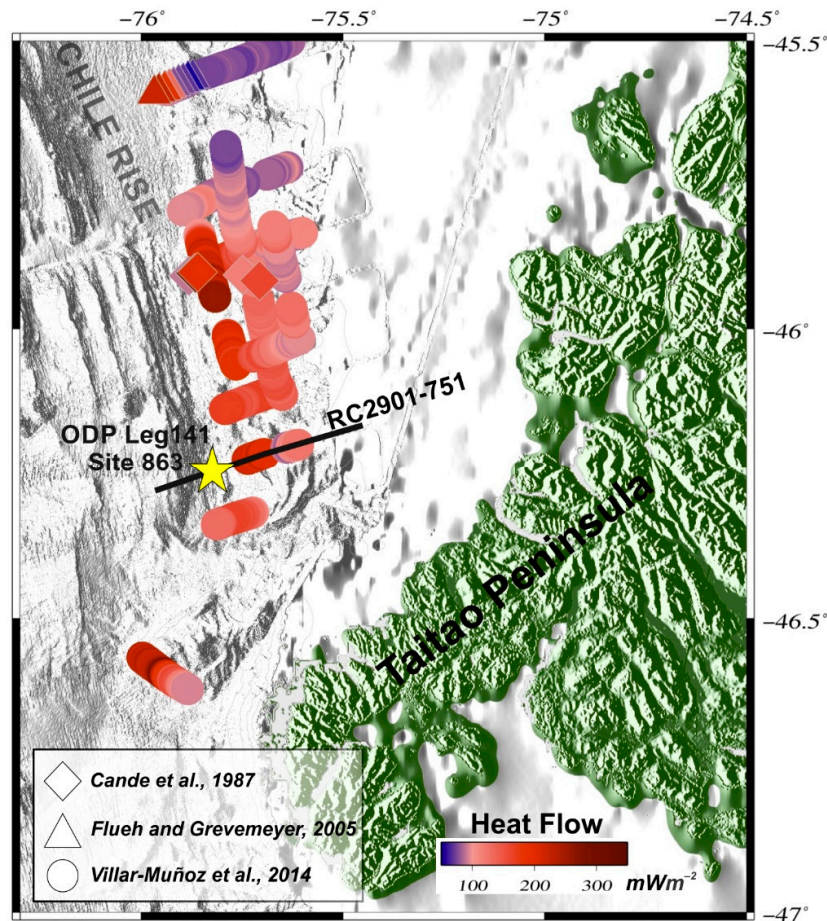
Figure 2. Heat flow (in m·Wm^{-2}) large-scale colour-coded based on BSR-derived heat flow and heat probes available for the area studied (after [26]). See text for description.

Close to the CTJ, the gas hydrate environment has peculiar characteristics relative to hydrate occurrences elsewhere. In fact, the ridge-trench collision perturbs pressure and temperature (PT) conditions within the sediment where hydrates have formed [11]. Excessively high heat flow, higher than 250 m·Wm^{-2}, was estimated above practically zero-age subducted crust (Figure 2). This is based on heat flow values derived from the depth of gas hydrate bottom-simulating reflectors [26,59] and direct measurements during the last decades [57,60].

The BSR-derived heat flow values are in general agreement with probe and borehole measurements [61]. Besides, high temperature gradients of 80–100 °C·km^{-1} were obtained at the toe of the continental wedge (e.g., Site 863 in Figure 2), just above the subducted zero-age crust [55]. The thermal anomaly in the region varies rapidly due to the presence of a strong convective circulation [62].

More recently, explorative work at the seafloor close to the CTJ has provided evidence for a sediment-hosted hydrothermal source near (~50 km) a methane-rich cold-seep area [63]. Advective methane transport operates within 5 km of the toe of the accretionary prism [59,64]. However, in the interior regions of the wedge, free gas migration and in situ gas production (within the hydrate stability region) build-up the hydrate [15], and BSR-depth towards the trench appears to rise in the sediments in proximity of the spreading ridge [15,26].

Moreover, gas at the base of the hydrate layer at the CTJ could also be produced from hydrate dissociation when changes in PT conditions shift the zone of hydrate stability upward, not only due to the accumulation of overburden, but also due to changes in PT conditions associated with active ridge

subduction [11]. Increasing heat flow, associated with the approach of the CR, may have caused the base of the hydrate stability field to migrate ~300 m upwards in the sediments [15].

In this complex region, we find both active margin tectonic regimes: subduction erosion and subduction accretion occurring in close proximity (e.g., [65]). Bourgois et al [66] assumes that the tectonic evolution of the Chile margin in the area reflects the evolution of the tectonic regime at depth: subduction erosion from 5–5.3 to 1.5–1.6 Ma, followed by subduction accretion since 1.5–1.6 Ma. [67], indicates that subduction accretion occurring today along the pre-subduction segment is linked to a dramatic post-glacial increase in trench sediment supply. From evidence found by drilling at Ocean Drilling Program (ODP) Site 863 (Figure 2) at the CTJ proper, it was concluded that accretion ceased in late Pliocene, and presently, the small frontal accretionary prism is undergoing tectonic erosion [39,55].

2. Materials and Methods

2.1. Database

The analyzed seismic line was acquired in 1988 onboard the vessel R/V Robert Conrad within the framework of the project entitled "Paleogene geomagnetic polarity timescale" for Empresa Nacional del Petroleo (ENAP). The seismic profile was acquired using an air gun array with a size of 0.062 m^3. The shot spacing was approximately 50 m, and the streamer length was 3000 m and included 236 channels with an intertrace of 12.5 m. The seismic line RC2901-751 analyzed in this study was modelled to estimate gas hydrate and free gas concentrations.

During ODP Leg 141, the Site 863 located a few km south of the CTJ was drilled along the profile RC2901-751 in an area where the axis of the spreading ridge is subducting at 50 ka (Figure 2). Porosity and temperature data were obtained from this site.

2.2. Methods

The processing was performed using open source Seismic Unix software and codes ad-hoc [68] and includes a tested method reported in several studies [14,22,24,25,27,43,69]: (a) BSR identification, (b) seismic velocity modelling, (c) gas-phases estimates, and (d) geothermal gradient estimation.

(a) BSR identification: a stacking section was obtained by using standard processing (i.e. geometry arrangement, spherical divergence, velocity analysis, normal-moveout corrections, stacking, and filtering). The objective was to identify the BSR in a selected part of the stacking section. Once the BSR was recognized, the seismic velocity was modelled.

(b) Seismic velocity modelling: An in-depth velocity model was obtained using the Kirchhoff Pre-stack Depth migration (PreSDM) iteratively with a layer stripping approach (details in [70,71]). This approach uses the output of the PreSDM, the common image gathers (CIGs) [71]. In the seismic profile, three layers were modelled: the first between the seawater level and the seafloor reflector (SF layer); the second between the seafloor and the BSR (BSR layer); and the third between the BSR and the Base of Free Gas (BGR layer). It started with an initial constant velocity model equal to 1480 ms^{-1}. After four iterations, the SF reflector in the CIGs was flat, suggesting that the migration velocity was correct. The correct migration for BSR and BGR was reached after 25 and 15 iterations, respectively. Below the BGR, a velocity gradient was included and, to improve the migration result, the final velocity model was smoothed. Finally, band-pass filtering and mixing were applied to improve the final PreSDM image. The sensitivity was considered a depth error equal to 2.5% proposed by [22] after a sensitive test.

(c) Gas-phases estimates: Once the final velocity model had been built, it was converted into gas hydrate and free gas concentrations. At first, a qualitative estimate was performed, comparing the modelled velocity curves against theoretical curves in the absence of gas. Afterwards, positive anomalies were associated with gas hydrate presence, while negative anomalies were related to free gas presence. Modified Hamilton's curves [72] were adopted to estimate the theoretical velocity curves in the absence of hydrates and free gas or full water saturated sediments [73]. Gas hydrates and free

gas concentrations were modified until the velocity model fitted the theoretical model, to obtain a quantitative estimate. The resultant is a concentration model in terms of total volume (for more details see [44]). Regarding the sensitivity, errors for gas hydrate and free gas estimates were assumed to be equal to 1.2% and 0.3% of volume, respectively. These errors were evaluated by [74], who performed a sensitive test to determine the influence of each parameter on the estimation of gas hydrate and free gas content. In fact, the main error was related to the assumptions of sediment properties.

(d) Geothermal gradient estimation: The geothermal gradient, indispensable to calculating the theoretical BSR-depth, was estimated using the following relation:

$$dT/dZ = (T_{BSR} - T_{SEA})/(Z_{BSR} - Z_{SEA}), \tag{1}$$

where BSR and seafloor depths (Z_{BSR}, Z_{SEA}) were extracted from the PreSDM section. Seafloor temperatures (T_{SEA}) were based on measurements from CTD data collected during ODP Leg 141 [75], while BSR temperatures (T_{BSR}) were based on the dissociation temperature-pressure function of gas hydrates [4]. Our estimation only considers methane because ethane concentration is negligible [22]. With regard to sensitivity, an error of depth equal to 2.5% was considered for seismic data [22].

3. Results

3.1. BSR Identification

The Kirchhoff PreSDM section (Figure 3) shows:

(a) A normal fault at a distance of 7 km representing the boundary between the lower and upper part of the continental rise and slope, respectively. Moreover, evidence of slip affecting the seafloor, as shallow faults and fractures, is registered from 8 to 15 km of distance;

(b) A strong and almost continuous BSR on the section that only gets weak or null where faults and fractures appear. Below the BSR, it is possible to recognize a weak but continuous reflector interpreted as BGR and, so, a free gas layer with a thickness of about 70 m;

(c) A variable depth of the BSR ranging between 80 and 150 m below seafloor (mbsf). The maximum depth of BSR was detected at about 2200 meters below sea level (mbsl) from 0 to 6 km, while the minimum depth (about 80 mbsf) was identified upwards (from 7 to 16 km). From 16 to 21 km of distance (in the "uplift part" of Figure 3), the BSR depth increases, reaching a depth of 150 mbsf.

3.2. Seismic Velocity Model

Above the BSR, a layer with a velocity ranging from 1650 to 1740 m/s was identified, while below the BSR, the velocity decreases from 1288 to 1550 m/s. Besides, below the BSR, the velocity decreases upwards (from 15 to 21 km of distance; see Figure 3 dark blue color), reaching its minimum value. An opposite velocity trend was observed above the BSR; in fact, when the velocity increases above the BSR (from 10 to 21 km of distance), the minimum velocity values are found below it. The BSR depth increases to the east, as shown by the velocity curves in Figure 3.
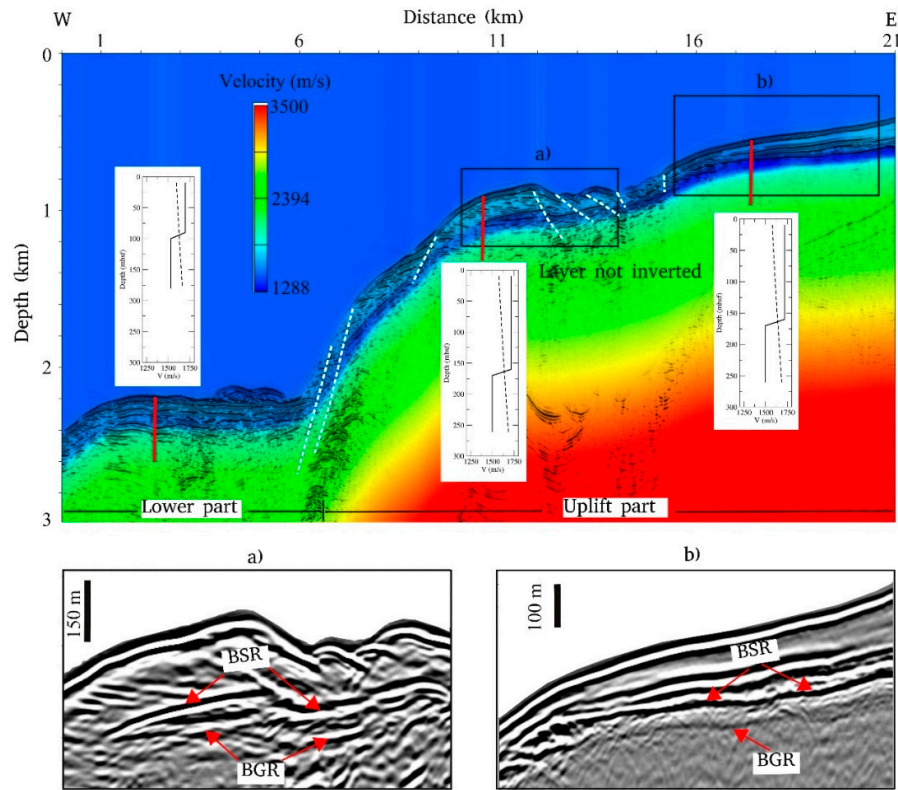
Figure 3. Velocity model superimposed in the Kirchhoff PreSDM section. The three inserts show the modelled velocity curves (solid black lines) and the theoretical curves in the absence of hydrates and free gas (dashed black lines) along the velocity model. Below, the rectangles indicate the position of the zooms in panel (a) and (b), in which red arrows indicate BSR and BGR (if present). The white dotted lines indicate faults and fractures.

3.3. Gas-Phases Estimates

High gas hydrates concentrations areas are located from 7 to 14 km of distance at approximately 1000 mbsl, reaching values ranging between 7 and 10% of total volume. Low gas hydrates concentrations regions (with values from 1 to 3% of total volume) are located from 1 to 6 km of distance at 2200 mbsl and from 15 to 20 km of distance at 600 mbsl (Figure 4). At shallow water depths, from 15 to 20 km of distance, high free gas concentrations were estimated, with values up to 0.8% of total volume. Note that hydrate and free gas concentrations show an opposite trend. In fact, from 7 to 14 km of distance, where gas hydrate concentrations increase (above the BSR), free gas concentrations decrease (see Top and Bottom panels in Figure 4). On the other hand, from 15 to 20 km of distance, where gas hydrate concentrations decrease, free gas concentrations increase.
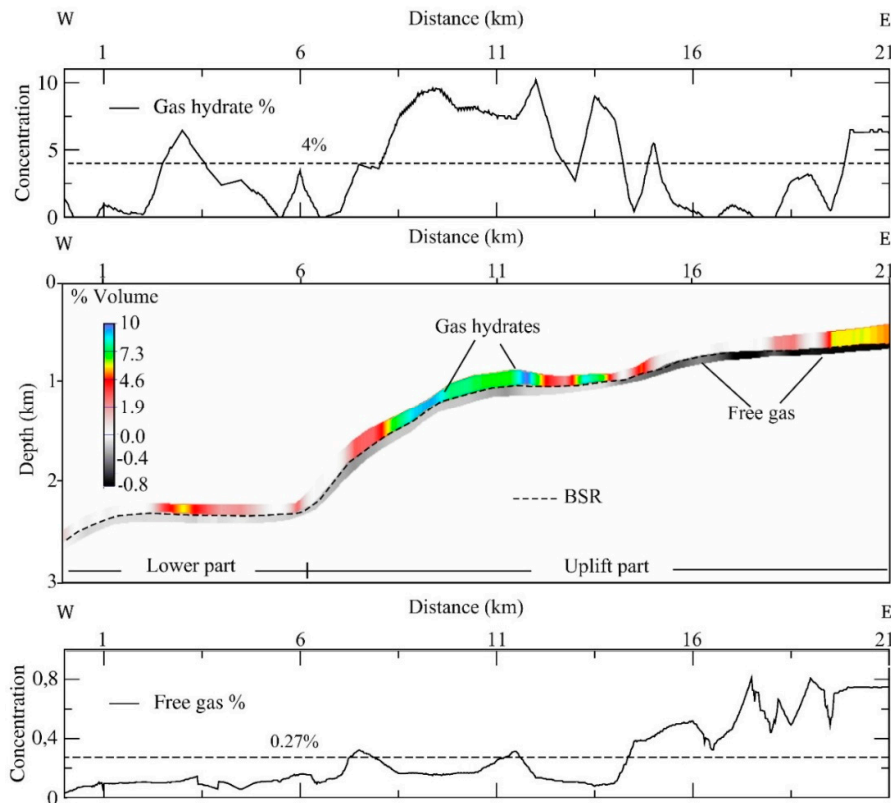
Figure 4. Gas hydrate and free gas concentration models and profiles relative to RC2901-751 seismic profile. Top panel: gas hydrate concentration values. Middle panel: gas-phase concentration model. Bottom panel: free gas concentration values. Dashed lines in the top and bottom panels correspond to the average gas hydrate and free gas concentrations, respectively.

3.4. Geothermal Gradient

The anomalous geothermal gradients calculated are variable in the seismic profile, ranging between 35 to 190 °C/km (Figure 5). The geothermal gradient increases towards the west (Figure 5), and the maximum values are at 2200 mbsl (see Figure 3). The minimum values were calculated on the east side of the profile (Figure 5) in correspondence of a water depth ranging from 600 to 1000 m. There are two isolated peaks (at ~9 and ~14 km of distance) of about 125 and 170 °C/km (Figure 5).
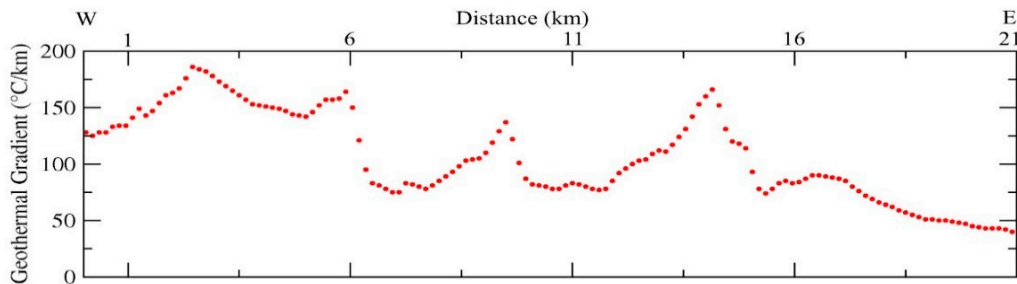

Figure 5. Geothermal gradient of the seismic profile RC2901-751. See text for details.

3.5. Gas Hydrate and Free Gas Volume at Standard Temperature and Pressure Conditions

In order to estimate the amount of methane stored in the marine sediments close to the CTJ region, bulk estimates of hydrate and free gas concentrations at standard temperature and pressure (STP) conditions were calculated using the following values:

- For gas hydrate: 4% of the total volume (dashed line in the upper panel of Figure 4), 50% porosity, thickness of the gas hydrate layer equal to 108 m, and a total projected area of about 2300 km^2. Considering these assumptions, the methane budget is 7.21 $\times$ 10^{11} m^3 at STP conditions;
- For free gas: 0.27% of the total volume (dashed line in the lower section of Figure 4), 50% porosity, thickness of the free gas layer equal to 85 m, and a total projected area of about 2300 km^2. Considering these assumptions, the methane budget from gas hydrates is 4.1 $\times$ 10^{10} m^3 at STP conditions.

The projected area was delimited based on the multi-resolution gridded Global Multi-Resolution Topography (GMRT) Synthesis [76] data and it comprises a part of the continental slope. The area was visually identified as the region that begins at the shelf break in the seaward edge of the shelf until it merges with the deep ocean floor at approximately 3000–3400 mbsl. All analyses were conducted with the open source Quantum Gis 3.4 (Qgis) and Generic Mapping Tools 5.4.4 (GMT) projects.

The free gas-volume expansion ratio was calculated using the Peng-Robinson equation of state [77], applying the methodology explained by [78]. Here, we assume that free gas is only composed of methane and it is located just below the gas hydrate stability zone. We divided the area containing free gas into five sub-areas to better assess the in-situ geothermal and pressure conditions and variations of the volume expansion ratios. Table 1 shows the free gas volume at in-situ and STP conditions. The rate of free gas volume expansion was calculated to estimate the volume of free gas content at STP conditions. The area was subdivided into five different regions, and at each one, pressure and temperature were calculated according to the corresponding geothermal gradient.

Table 1. Free gas volume at in-situ and STP conditions.

Interval (mbsl)	Area (m^2)	Temperature (K)	Pressure (MPa)	Volume in-situ (m^3)	Volume STP (m^3)	Volume Expansion Ratio
500–1000	4.19 $\times$ 10^8	285.8	7.6	4.25 $\times$ 10^7	3.69 $\times$ 10^9	86.8
1000–1500	4.37 $\times$ 10^8	289.7	12.7	4.44 $\times$ 10^7	6.71 $\times$ 10^9	151.2
1500–2000	5.59 $\times$ 10^8	291.0	17.7	5.68 $\times$ 10^7	1.20 $\times$ 10^{10}	212.2
2000–2500	3.69 $\times$ 10^8	291.5	22.8	3.75 $\times$ 10^7	9.90 $\times$ 10^9	263.9
2500–3000	2.79 $\times$ 10^8	292.1	27.9	2.84 $\times$ 10^7	8.67 $\times$ 10^9	305.5
Total	2.06 $\times$ 10^9			2.10 $\times$ 10^8	4.10 $\times$ 10^{10}	

4. Discussion

The seismic section showed evidence of active tectonics; in fact, a large normal fault zone located at 7 km of distance represents the boundary between the western and eastern sectors (Lower and Uplift part in the Figure 3). Morphological features close to the normal fault can be associated with active tectonic extension and uplift processes above the subducting CR seafloor spreading centre [39]. Further upslope deformation is characterized by normal faults and fractures with small offsets affecting shallow sediments (Figure 3). The weak seismic character of BSR in the seaward (westward sector) is related to low free gas concentrations, while in the uplifted landward (eastward sector), a continuous and strong BSR can be related to high free gas concentrations up to 0.8% (Figure 4). These values are consistent with free gas concentrations reported by [11] along Seismic Line 745, located northward of this study area. A shallow BSR depth (average ~100 mbsf) can be explained by a high heat flow (average > 200 mW/m^2) and geothermal gradient (average ~90 °C/km), as reported by [26] and in agreement with this study. In addition, vertical and lateral velocity variations above and below the BSR can be associated with gas hydrate and free gas presence and their concentration changes. Maximum velocity values above the BSR (up to 1740 m/s) can correspond to high gas hydrate concentrations, whereas low velocities below the BSR (around 1290 m/s) are related to high free gas concentrations (Figures 3 and 4). In fact, this low velocity can only be explained with free gas presence.

The gas-phase concentration distribution is in general agreement with heat flow reported by [26]. Moreover, low concentrations of gas hydrate and free gas coincide with high values of heat flow and geothermal gradients close to the Chile trench and the plate boundary (Figures 2 and 5), while

high concentrations of gas hydrate and free gas are associated with a low heat flow and geothermal gradient further up the continental slope. A similar pattern was also recognized by [22] on the Chilean continental slope around 44° S.

The observation that both gas hydrate and free gas concentrations in the sediments have lower values close to the trench in the CTJ area could be explained as a result of gas hydrate dissociation and free gas migration in a regime of fluid advection under high heat flow conditions [59]. High heat flow is caused by the subduction of the Chile Rise [11,26,57,59,60], and geothermal fluids are supplied from deeper strata [67] that are undergoing deformation, anomalous compaction, and de-watering (e.g., [55,65]). The highest values of heat flow are located close to the heat source near the trench (Figures 2 and 5). We assume that in this area, the advective heat transfer in a regime of rising heat flow can change the pressure-temperature conditions, causing gas hydrate dissociation in the past and likely in the present. Low concentrations of free gas close to the trench (~0.1% of total volume), can be explained due to a variable production. Here, the dissociated hydrates is released as free gas and can migrate up into the hydrate stability zone, giving place to gas hydrate formation in higher areas (from 7 to 14 km of distance in Figure 4), increasing gas hydrate concentrations (~8% of total volume). However, active faults and fractures in the lower forearc can destroy stratigraphic seals and, consequently, impede free gas storage (e.g., [26,43]) above the subducting spreading ridge. This may explain the low concentrations of gas hydrate and free gas layers calculated close to the trench and high concentrations in shallow waters, where the lower values of heat flow were found, and deformation is less prevalent (Figures 3 and 4). Note, however, that low concentrations of gas hydrate and free gas were also found close to faults and fractures because of the enhancement of fluid-escape (Figures 3 and 4). Therefore, high heat flow due to spreading ridge subduction, tectonic faulting, and vigorous fluid advection at the leading edge of the overriding South American plate may indeed be a major factor for hydrate and gas reservoir distribution offshore Taitao Peninsula. Moreover, the highest value of free gas concentration, located in the shallower part of the accretionary wedge (~16 km of distance; Figure 4), can be explained by the upward migration of gas towards an impermeable hydrate layer, forming a structural trap [22]. Note also that this sector is characterized by the absence of faults that could act as pathways for upward fluid migration.

The anomalous heat flow close to the CTJ changes the stable PT conditions for the gas hydrate, promotes its dissociation and fluid escapes. The dissolved methane from gas hydrates could enter into the ocean through fluid ventings or as gas bubbles [79]. Some of the dissolved methane is diluted and oxidized as it rises through the ocean interior. However, an increase in gas methane entering the ocean above seawater saturation could lead to methane reaching the ocean surface mixed layer and being transported to the atmosphere via sea-air exchange [80].

A question worth discussing here is whether some of the methane in gas hydrates in the lower continental slope may in fact have been formed by abiotic processes (e.g., [81]) during the formation of serpentinite from ultramafic rocks. This can be valid for hydrates present in sediments just above the youngest crust of the CR subducted (near the trench), where active serpentinization and methane venting can initiate, develop, and survive, as was observed in similar regions (e.g., [82]). ODP Site 863 (see Figure 2 and [55]) is located on the seismic line presented in this study, right above the subducting oceanic spreading ridge. Pore waters squeezed from the drill cores recovered at ODP Site 863 show very high pH values up to 10.5, especially at drillhole depths greater than 600 meters below the sea floor. Along with the concentration profiles of F, B, Cl, and SO_4, this suggests that the pore fluids could be created from a sequence of reactions involving Mg-depleted fluids (see Figure 6 and description on p. 406 of [55]). This can be taken as an indication of metasomatic alteration in the serpentinized peridotite of the oceanic mantle (e.g., [83,84]) belonging to the downgoing plate at depth. Recently, Suess et al. [85] has shown that gas hydrates involving abiotically formed methane might be formed in sediment drifts overlying altered oceanic crust and mantle in slow-spreading environments. It is possible to envisage a similar scenario here, with the difference that the sediments of the lowermost

continental slope are not directly sedimented above the spreading ridge, but are tectonically thrusted over the downgoing plate.

Finally, the estimated volume of gas hydrate calculated in the present study was lower than the values calculated in other regions along the Chilean margin (e.g., [27]). We hypothesize that this can be explained by the following reasons: (a) limited sediment accumulation due to the shortening of the wedge close to the CTJ, which causes unfavourable conditions for the formation of gas hydrates [11,39]; (b) the presence of faults and fractures that can locally promote fluid escape and prevent gas hydrate formation (e.g., [43,85]); (c) faults identified in the seismic profile (Figure 3) cross the transition layer of the gas hydrate phase and serve as pipes that drain water and methane to the seafloor (e.g., [85]); (d) the CTJ is characterised by an anomalous thermal state (e.g., [26]) that inhibits the formation of gas hydrates, by changing the gas hydrate stability zone.

5. Conclusions

The results of this research for the gas hydrate in the margin close to the Chile Triple Junction lead us to conclude that:

- The values for gas hydrate concentration are lower than 10% of the total rock volume. The highest concentrations are calculated in shallower waters, where the geothermal gradient is low and deformation is less prevalent;
- The amount of hydrate and free gas estimated over the studied area were 7.21×10^{11} m^3 and 4.1×10^{10} m^3, respectively;
- An inverse correlation between gas-phase concentrations and geothermal gradient is recognized. Low gas hydrate and free gas concentrations coincide with high values of geothermal gradients over the studied area;
- An extremely high geothermal gradient close to the trench was calculated, reaching values up to $190\ °C \cdot km^{-1}$, caused by the subduction of the CR at the CTJ, altering the stable PT conditions for the gas hydrate, which promotes its dissociation and upward migration, and fluid escapes;
- High heat flow, tectonic faulting, and vigorous fluid advection may be important factors for hydrate and gas reservoir distribution offshore Taitao Peninsula;
- The CTJ is an important methane seepage area and should be the focus of novel geological, oceanographic, and ecological research.

Author Contributions: Conceptualization, L.V.-M. and I.V.-C.; formal analysis, L.V.-M. and I.V.-C.; funding acquisition, I.V.-C.; investigation, L.V.-M. and I.V.-C.; methodology, L.V.-M., I.V.-C., J.P.B., U.T., F.F., M.G., and S.C.; software, L.V.-M., I.V.-C., J.P.B., and U.T.; supervision, J.H.B.; visualization, L.V.-M. and J.P.B.; writing—original draft, L.V.-M.; writing—review & editing, I.V.-C., J.P.B., U.T., F.F., M.G., J.H.B., and S.C.

Conflicts of Interest: The authors declare no conflict of interest. The funders had no role in the design of the study; in the collection, analyses, or interpretation of data; in the writing of the manuscript, or in the decision to publish the results.

References

1. Sloan, E.D. Fundamental principles and applications of natural gas hydrates. *Nature* **2003**, *426*, 353–363. [CrossRef] [PubMed]
2. Sloan, E.D.; Koh, C. *Clathrate Hydrates of Natural Gases*, 3rd ed.; CRC Press: Boca Raton, FL, USA, 2007; 752p.
3. Schmidt, M.; Hensen, C.; Morz, T.; Müller, C.; Grevemeyer, I.; Wallmann, K.; Mau, S.; Kaul, N. Methane hydrate accumulation in Mound 11 mud volcano, Costa Rica forearc. *Mar. Geol.* **2005**, *216*, 77–94. [CrossRef]
4. Sloan, E.D. *Clathrate Hydrates of Natural Gases*, 2nd ed.; CRC Press: Boca Raton, FL, USA, 1998; 705p.

5. Milkov, A.V. Global estimates of hydrate-bound gas in marine sediments: How much is really out there? *Earth-Sci. Rev.* **2004**, *66*, 183–197. [CrossRef]

6. Crutchley, G.J.; Mountjoy, J.J.; Pecher, I.A.; Gorman, A.R.; Henrys, S.A. Submarine Slope Instabilities Coincident with Shallow Gas Hydrate Systems: Insights from New Zealand Examples. In *Submarine Mass Movements and their Consequences*; Advances in Natural and Technological Hazards Research; Lamarche, G., Mountjoy, J., Bull, S., Hubble, T., Krastel, S., Lane, E., Micallef, A., Moscardelli, L., Mueller, C., Pecher, I., Eds.; Springer: Cham, Switzerland, 2016; 41p.

7. Hovland, M.; Orange, D.; Bjorkum, P.A.; Gudmestad, O.T. Gas hydrate and seeps-effects on slope stability: The "hydraulic model". In Proceedings of the Eleventh International Offshore and Polar Engineering Conference, Stavanger, Norway, 17–22 June 2001; Volume 1, pp. 471–476.

8. Kretschmer, K.; Biastoch, A.; Rüpke, L.; Burwicz, E. Modeling the fate of methane hydrates under global warming. *Glob. Biogeochem. Cycles* **2015**, *29*, 610–625. [CrossRef]

9. Mountjoy, J.J.; Pecher, I.; Henrys, S.; Crutchley, G.; Barnes, P.M.; Plaza-Faverola, A. Shallow methane hydrate system controls ongoing, downslope sediment transport in a low-velocity active submarine landslide complex, Hikurangi Margin, New Zealand. *Geochem. Geophys. Geosyst.* **2014**, *15*, 4137–4156. [CrossRef]

10. Ruppel, C.D.; Kessler, J.D. The interaction of climate change and methane hydrates. *Rev. Geophys.* **2017**, *55*, 126–168. [CrossRef]

11. Bangs, N.L.; Sawyer, D.S.; Golovchenko, X. Free gas at the base of the gas hydrate zone in the vicinity of the Chile triple Junction. *Geology* **1993**, *21*, 905–908. [CrossRef]

12. Hyndman, R.D.; Spence, G.D. A seismic study of methane hydrate marine bottom-simulating-reflectors. *J. Geophys. Res.* **1992**, *97*, 6683–6698. [CrossRef]

13. Kvenvolden, K.A. Comparison of marine gas hydrates in sediments of an active and passive continental margin. *Mar. Pet. Geol.* **1985**, *2*, 65–70. [CrossRef]

14. Vargas-Cordero, I.; Tinivella, U.; Accaino, F.; Loreto, M.F.; Fanucci, F.; Reichert, C. Analyses of bottom simulating reflections offshore Arauco and Coyhaique (Chile). *Geo-Mar. Lett.* **2010**, *30*, 271–281. [CrossRef]

15. Brown, K.M.; Bangs, N.L.; Froelich, P.N.; Kvenvolden, K.A. The nature, distribution, and origin of gas hydrate in the Chile Triple Junction region. *Earth Planet. Sci. Lett.* **1996**, *139*, 471–483. [CrossRef]

16. Grevemeyer, I.; Kaul, N.; Díaz-Naveas, J.L. Geothermal evidence for fluid flow through the gas hydrate stability field off Central Chile-transient flow related to large subduction zone earthquakes? *Geophys. J. Int.* **2006**, *166*, 461–468. [CrossRef]

17. Loreto, M.F.; Tinivella, U.; Ranero, C. Evidence for fluid circulation, overpressure and tectonic style along the Southern Chilean margin. *Tectonophysics* **2007**, *429*, 183–200. [CrossRef]

18. Polonia, A.; Brancolini, G.; Torelli, L.; Vera, E. Structural variability at the active continental margin off southernmost Chile. *J. Geodyn.* **1999**, *27*, 289–307. [CrossRef]

19. Polonia, A.; Brancolini, G.; Torelli, L. The accretionary complex of southernmost Chile from the strait of Magellan to the Drake passage. *Terra Antarct.* **2001**, *8*, 87–98.

20. Polonia, A.; Torelli, L. Antarctic/Scotia plate convergence off southernmost Chile. *Geol. Acta* **2007**, *5*, 295–306.

21. Polonia, A.; Torelli, L.; Brancolini, G.; Loreto, M.F. Tectonic accretion versus erosion along the southern Chile trench: Oblique subduction and margin segmentation. *Tectonics* **2007**, *26*, TC3005. [CrossRef]

22. Vargas-Cordero, I.; Tinivella, U.; Accaino, F.; Loreto, M.F.; Fanucci, F. Thermal state and concentration of gas hydrate and free gas of Coyhaique, Chilean Margin (44° 30′ S). *Mar. Pet. Geol.* **2010**, *27*, 1148–1156. [CrossRef]

23. Vargas-Cordero, I.; Tinivella, U.; Accaino, F.; Fanucci, F.; Loreto, M.F.; Lascano, M.E.; Reichert, C. Basal and Frontal Accretion Processes versus BSR Characteristics along the Chilean Margin. *J. Geol. Res.* **2011**, *2011*, 1–10. [CrossRef]

24. Vargas-Cordero, I.; Tinivella, U.; Villar-Muñoz, L.; Giustiniani, M. Gas hydrate and free gas estimation from seismic analysis offshore Chiloé island (Chile). *Andean Geol.* **2016**, *43*, 263–274. [CrossRef]

25. Vargas-Cordero, I.; Tinivella, U.; Villar-Muñoz, L. Gas Hydrate and Free Gas Concentrations in Two Sites inside the Chilean Margin (Itata and Valdivia Offshores). *Energies* **2017**, *10*, 2154. [CrossRef]

26. Villar-Muñoz, L.; Behrmann, J.H.; Diaz-Naveas, J.; Klaeschen, D.; Karstens, J. Heat flow in the southern Chile forearc controlled by large-scale tectonic processes. *Geo-Mar. Lett.* **2014**, *34*, 185–198. [CrossRef]

27. Villar-Muñoz, L.; Bento, J.P.; Klaeschen, D.; Tinivella, U.; Vargas-Cordero, I.; Behrmann, J.H. A first estimation of gas hydrates offshore Patagonia (Chile). *Mar. Pet. Geol.* **2018**, *96*, 232–239. [CrossRef]

28. Coffin, R.; Pohlman, J.; Gardner, J.; Downer, R.; Wood, W.; Hamdan, L.; Walker, S.; Plummerg, R.; Gettrus, J.; Diaz, J. Methane hydrate exploration on the mid Chilean coast: A geochemical and geophysical survey. *J. Pet. Sci. Eng.* **2007**, *56*, 32–41. [CrossRef]

29. Geersen, J.; Scholz, F.; Linke, P.; Schmidt, M.; Lange, D.; Behrmann, J.H.; Volker, D.; Hensen, C. Fault zone controlled seafloor methane seepage in the rupture area of the 2010 Maule earthquake, Central Chile. *Geochem. Geophys. Geosyst.* **2016**, *17*, 4802–4813. [CrossRef]

30. Jessen, G.L.; Pantoja, S.; Gutierrez, M.A.; Quinones, R.A.; Gonzalez, R.R.; Sellanes, J.; Kellermann, M.Y.; Hinrichs, K.U. Methane in shallow cold seeps at Mocha Island off central Chile. *Cont. Shelf Res.* **2011**, *31*, 574–581. [CrossRef]

31. Sellanes, J.; Quiroga, E.; Gallardo, V. First direct evidence of methane seepage and associated chemosynthetic communities in the bathyal zone off Chile. *J. Mar. Biol. Assoc. UK* **2004**, *84*, 1065–1066. [CrossRef]

32. Sellanes, J.; Krylova, E. A new species of Calyptogena (Bivalvia, Vesicomyidae) from a recently discovered methane seepage area off Concepción Bay, Chile (36S). *J. Mar. Biol. Assoc. UK* **2005**, *85*, 969–976. [CrossRef]

33. Sellanes, J.; Quiroga, E.; Neira, C. Megafaunal community structure and trophic relationships of the recently discovered Concepción Methane Seep Area (Chile, 36S). *ICES J. Mar. Sci.* **2008**, *65*, 1102–1111. [CrossRef]

34. Scholz, F.; Hensen, C.; Schmidt, M.; Geersen, J. Submarine weathering of silicate minerals and the extent of pore water freshening at active continental margins. *Geochim. Cosmochim. Acta* **2013**, *100*, 200–216. [CrossRef]

35. German, C.R.; Shank, T.M.; Lilley, M.D.; Lupton, J.E.; Blackman, D.K.; Brown, K.M.; Baumberger, T.; FrühGreen, G.; Greene, R.; Saito, M.A.; et al. Hydrothermal Exploration at the Chile Triple Junction—ABE's Last Adventure. In *AGU Fall Meeting Abstracts*; American Geophysical Union: Washington, DC, USA, 2010.

36. Oliver, P.G.; Sellanes, J. New species of Thyasiridae from a methane seepage area off Concepción, Chile. *Zootaxa* **2005**, *1092*, 1–20. [CrossRef]

37. Völker, D.; Geersen, J.; Contreras-Reyes, E.; Sellanes, J.; Pantoja, S.; Rabbel, W.; Thorwart, M.; Reichert, C.; Block, M.; Weinrebe, W.R. Morphology and geology of the continental shelf and upper slope of southern Central Chile (33S–43S). *Int. J. Earth Sci. (Geol. Rundsch.)* **2014**, *103*, 1765. [CrossRef]

38. Olu, K.; Duperret, A.; Sibuet, M.; Foucher, J.P.; Fiala-Medioni, A. Structure and distribution of cold seep communities along the Peruvian active margin: Relationship to geological and fluid patterns. *Mar. Ecol. Prog. Ser.* **1996**, *132*, 109–125. [CrossRef]

39. Behrmann, J.H.; Lewis, S.D.; Cande, S.C. Tectonics and geology of spreading ridge subduction at the Chile Triple Junction: A synthesis of results from Leg 141 of the Ocean Drilling Program. *Geol. Rundsch.* **1994**, *83*, 832–852. [CrossRef]

40. Hillman, J.I.T.; Klaucke, I.; Bialas, J.; Feldman, H.; Drexler, T.; Awwiller, D.; Atgin, O.; Çifçi, G. Gas migration pathways and slope failures in the Danube Fan, Black Sea. *Mar. Pet. Geol.* **2018**, *92*, 1069–1084. [CrossRef]

41. Hovland, M.; Svensen, H.; Forsberg, C.F.; Johansen, H.; Fichler, C.; Fosså, J.H.; Jonsson, R.; Rueslåtten, H. Complex pockmarks with carbonate-ridges off mid-Norway: Products of sediment degassing. *Mar. Geol.* **2005**, *218*, 191–206. [CrossRef]

42. Römer, M.; Sahling, H.; Pape, T.; Bohrmann, G.; Spieß, V. Quantification of gas bubble emissions from submarine hydrocarbon seeps at the Makran continental margin (offshore Pakistan). *J. Geophys. Res.* **2012**, *117*, C10015. [CrossRef]

43. Vargas-Cordero, I.; Tinivella, U.; Villar-Muñoz, L.; Bento, J.P. High Gas Hydrate and Free Gas Concentrations: An Explanation for Seeps Offshore South Mocha Island. *Energies* **2018**, *11*, 3062. [CrossRef]

44. Tinivella, U.; Carcione, J.M. Estimation of gas-hydrate concentration and free-gas saturation from log and seismic data. *Lead Edge* **2001**, *20*, 200–203. [CrossRef]

45. Cisternas, M.; Atwater, B.F.; Torrejón, F.; Sawai, Y.; Machuca, G.; Lagos, M.; Eipert, A.; Youlton, C.; Salgado, I.; Kamataki, T.; et al. Predecessors of the giant 1960 Chile earthquake. *Nature* **2005**, *437*, 404–407. [CrossRef]

46. Agurto-Detzel, H.; Rietbrock, A.; Bataille, K.; Miller, M.; Iwamori, H.; Priestley, K. Seismicity distribution in the vicinity of the Chile Triple Junction, Aysén Region, southern Chile. *J. S. Am. Earth Sci.* **2014**, *51*, 1–11. [CrossRef]

47. Murdie, R.E.; Prior, D.J.; Styles, P.; Flint, S.S.; Pearce, R.G.; Agar, S.M. Seismic responses to ridge-transform subduction: Chile triple junction. *Geology* **1993**, *21*, 1095–1098. [CrossRef]

48. Fischer, D.; Mogollón, J.M.; Strasser, M.; Pape, T.; Bohrmann, G.; Fekete, N.; Spiess, V.; Kasten, S. Subduction zone earthquake as potential trigger of submarine hydrocarbon seepage. *Nat. Geosci.* **2013**, *6*, 647–651. [CrossRef]

49. Sibson, R.H. Interactions between temperature and pore fluid pressure during earthquake faulting—A mechanism for partial or total stress relief. *Nat. Phys. Sci.* **1973**, *243*, 66–68. [CrossRef]

50. Boobalan, A.J.; Ramanujam, N. Triggering mechanism of gas hydrate dissociation and subsequent submarine landslide and ocean wide Tsunami after Great Sumatra-Andaman 2004 earthquake. *Arch. Appl. Sci. Res.* **2013**, *5*, 105–110.

51. Elger, J.; Berndt, C.; Rüpke, L.H.; Krastel, S.; Gross, F.; Geissler, W.H. Submarine slope failures due to pipe structure formation. *Nat. Commun.* **2018**, *9*, 715. [CrossRef] [PubMed]

52. Kvenvolden, K.A. Gas hydrates-geological perspective and global change. *Rev. Geophys.* **1993**, *31*, 173–187. [CrossRef]

53. Waite, W.F.; Santamarina, J.C.; Cortes, D.D.; Dugan, B.; Espinoza, D.N.; Germaine, J.; Jang, J.; Jung, J.W.; Kneafsey, T.J.; Shin, H.; et al. Physical properties of hydrate-bearing sediments. *Rev. Geophys.* **2009**, *47*, RG4003. [CrossRef]

54. Xu, W.; Germanovich, L.N. Excess pore pressure resulting from methane hydrate dissociation in marine sediments: A theoretical approach. *J. Geophys. Res.* **2006**, *111*. [CrossRef]

55. Behrmann, J.H.; Lewis, S.D.; Musgrave, R.; Bangs, N.; Bodén, P.; Brown, K.; Collombat, H.; Didenko, A.N.; Didyk, B.M.; Froelich, P.N.; et al. Chile Triple Junction. In Proc. ODP. *Init. Repts. (Pt. A)* **1992**, *141*, 1–708.

56. Cande, S.C.; Leslie, R.B. Late Cenozoic tectonics of the southern Chile trench. *J. Geophys. Res.* **1986**, *91*, 471–496. [CrossRef]

57. Cande, S.C.; Leslie, R.B.; Parra, J.C.; Hodbart, M. Interaction between the Chile ridge and Chile trench: Geophysical and geothermal evidences. *J. Geophys. Res.* **1987**, *92*, 495–520. [CrossRef]

58. Herron, E.M.; Cande, S.C.; Hall, B.R. An active spreading center collides with a subduction zone: A geophysical survey of the Chile margin triple Junction. *Mem. Geol. Soc. Am.* **1981**, *154*, 683–701.

59. Brown, K.M.; Bangs, N.L.; Marsaglia, K.; Froleich, P.N.; Zheng, Y.; Didyk, B.M.; Prior, D.; Richford, E.L.; Torres, M.; Kumsov, V.B.; et al. A summary of ODP 141 hydrogeologic, geochemical, and thermal results. *Proc. ODP Sci. Results* **1995**, *141*, 363–373.

60. Flueh, E.; Grevemeyer, I. *FS SONNE Cruise Report SO 181 TIPTEQ-from the Incoming Plate to Megathrust Earthquakes. Rep. 06.12.2004–26.02.2005*; Leibniz-Institut für Meereswissenschaften an der University Kiel: Kiel, Germany, 2005; 533p.

61. Völker, D.; Grevemeyer, I.; Stipp, M.; Wang, K.; He, J. Thermal control of the seismogenic zone of southern central Chile. *J. Geophys. Res.* **2011**, *116*, B10305. [CrossRef]

62. Lagabrielle, Y.; Guivel, C.; Maury, R.; Bourgois, J.; Fourcade, S.; Martin, H. Magmatic-tectonic effects of high thermal regime at the site of active ridge subduction: The Chile Triple Junction model. *Tectonophysics* **2000**, *326*, 255–268. [CrossRef]

63. German, C.R.; Ramirez-Llodra, E.; Baker, M.C.; Tyler, P.A. ChEss Scientific Steering Committee. Deep-Water Chemosynthetic Ecosystem Research during the Census of Marine Life Decade and Beyond: A Proposed Deep-Ocean Road Map. *PLoS ONE* **2011**, *6*, e23259. [CrossRef]

64. Bangs, N.L.; Brown, K.M. Regional heat flow in the vicinity of the Chile Triple Junction constrained by the depth of the bottom simulating reflection. *Proc. ODP Sci. Results* **1995**, *141*, 253–259.

65. Behrmann, J.H.; Kopf, A. Balance of tectonically accreted and subducted sediment at the Chile Triple Junction. *Int. J. Earth Sci. (Geol. Rundsch.)* **2001**, *90*, 753–768. [CrossRef]

66. Bourgois, J.; Martin, H.; Lagabrielle, Y.; Le Moigne, J.; Frutos Jara, J. (Chile margin triple junction area) Subduction erosion related to spreading-ridge subduction: Taitao peninsula. *Geology* **1996**, *24*, 723–726. [CrossRef]

67. Bangs, N.L.; Cande, S.C. Episodic development of a convergent margin inferred from structures and processes along the southern Chile margin. *Tectonics* **1997**, *16*, 489–503. [CrossRef]

68. Cohen, J.K.; Stockwell, J.W. *CWP/SU: Seismic Unix Release 4.0: A Free Package for Seismic Research and Processing*; Center for Wave Phenomena, Colorado School of Mines: Golden, CO, USA, 2008; pp. 1–153.

69. Loreto, M.F.; Tinivella, U.; Accaino, F.; Giustiniani, M. Offshore Antarctic Peninsula gas hydrate reservoir characterization by geophysical data analysis. *Energies* **2011**, *4*, 39–56. [CrossRef]

70. Yilmaz, O. *Seismic Data Analysis: Processing, Inversion and Interpretation of Seismic Data*, 2nd ed.; Society of Exploration Geophysicists: Oklahoma, OK, USA, 2001; 2027p.

71. Liu, Z.; Bleistein, N. Migration velocity analysis: Theory and an iterative algorithm. *Geophysics* **1995**, *60*, 142–153. [CrossRef]

72. Hamilton, E.L. Sound velocity gradients in marine sediments. *J. Acoust. Soc. Am.* **1979**, *65*, 909–922. [CrossRef]

73. Tinivella, U. A method for estimating gas hydrate and free gas concentrations in marine sediments. *Bollettino di Geofisica Teorica ed Applicata* **1999**, *40*, 19–30.

74. Tinivella, U. The seismic response to overpressure versus gas 638 hydrate and free gas concentration. *J. Seism. Explor.* **2002**, *11*, 283–305.

75. Grevemeyer, I.; Villinger, H. Gas hydrate stability and the assessment of heat flow through continental margins. *Geophys. J. Int.* **2001**, *145*, 647–660. [CrossRef]

76. Ryan, W.B.F.; Carbotte, S.M.; Coplan, J.O.; O'Hara, S.; Melkonian, A.; Arko, R.; Weissel, R.A.; Ferrini, V.; Goodwillie, A.; Nitsche, F.; et al. Global Multi-Resolution Topography synthesis. *Geochem. Geophys. Geosyst.* **2009**, *10*, Q03014. [CrossRef]

77. Peng, D.; Robinson, D.B. A new two-constant equation of state. *Ind. Eng. Chem. Fundam.* **1976**, *15*, 59–64. [CrossRef]

78. Barth, G. *Methane Gas Volume Expansion Ratios and Ideal Gas Deviation Factors for the Deep Water Bering Sea Basins*; USGS Open-File Report; USGS: Reston, VA, USA, 2005; 1451p.

79. Reeburgh, W.S. Oceanic Methane Biogeochemistry. *Chem. Rev.* **2007**, *107*, 486–513. [CrossRef]

80. Cynar, F.J.; Yayanos, A.A. *Biogeochemistry of Global Change: Radiatively Active Trace Gases*; Oremland, R.S., Ed.; Chapman-Hall: Atlanta, GA, USA, 1993; pp. 551–573.

81. McCollom, T.M. Abiotic methane formation during experimental serpentinization of olivine. *PNAS* **2016**, *113*, 13965–13970. [CrossRef] [PubMed]

82. Johnson, J.E.; Mienert, J.; Plaza-Faverola, A.; Vadakkepuliyambatta, S.; Knies, J.; Bünz, S.; Andreassen, K.; Ferré, B. Abiotic methane from ultraslow-spreading ridges can charge Arctic gas hydrates. *Geology* **2015**, *43*, 371–374. [CrossRef]

83. Bach, W.; Paulick, H.; Garrido, C.J.; Ildefonse, B.; Meurer, W.P.; Humphris, S.E. Unraveling the sequence of serpentinization reactions: Petrography, mineral chemistry, and petrophysics of serpentinites from MAR 15°N (ODP Leg 209, Site 1274). *Geophys. Res. Lett.* **2006**, *33*, 4–7. [CrossRef]

84. Kelley, D.S.; Karson, J.A.; Früh-Green, G.L.; Dana, R.; Yoerger, D.R.; Shank, T.M.; Butterfield, D.A.; Hayes, J.M.; Schrenk, M.O.; Olson, E.J.; et al. A serpentinite-hosted ecosystem: The Lost City hydrothermal vent field. *Science* **2005**, *307*, 1428–1434. [CrossRef] [PubMed]

85. Suess, E.; Torres, M.; Bohrmann, G.; Collier, R.W.; Greinert, J.; Linke, P.; Rehder, G.; Tréhu, A.; Wallmann, K.; Winckler, G.; et al. Gas hydrate destabilization: Enhanced dewatering, benthic material turnover and large methane plumes at the Cascadia convergent margin. *Earth Planet. Sci. Lett.* **1999**, *170*, 1–15. [CrossRef]

5. **SYNTHESIS**

The most important aim of this thesis was to improve the knowledge of gas hydrate reservoirs along the Chilean continental slope, highlighting its spatial distribution, providing volume estimates, and identifying methane hydrate concentrated zones (MHCZ in the following). In addition, there was the aim to refine the understanding of the thermal regime and its effects on the gas hydrate concentration.

The results presented in the three core chapters of this thesis work, and the articles published as a secondary author, yield important advances concerning estimate of gas hydrate and the consequences of the thermal regime on its occurrence along the Chilean margin. In the case of the Patagonia region, for instance, the results from the Manuscript #2 (Chapter 3), provided - for the first time - an estimate of gas hydrate for that region. Gas hydrates are presently one of the most important topics in marine geoscientific investigations along the Chilean margin, particularly with respect of the fact that this margin is one of the tectonically most active plate boundaries on Earth. The geological risk associated with gas hydrate occurrence is related to aspects of future extraction, but also has a global dimension if, for example, the methane is released from a gas hydrate reservoir driven by tectonic activity or processes related to marine slope instability.

Gas hydrate estimation and distribution

Methane hydrate identification is based on the interpretation of subsurface data. For this, multichannel seismic data were used to identify the BSR in more than 100 seismic lines from 33°- 57° S, almost 3000 km along strike of the Pacific coast of Chile. In order to analyze the BSR, standard and advanced processing was performed by using the open-source scientific library called Seismic UNIX (SU, Cohen and

Stockwell, 2008) and ad-hoc codes in selected sections where the BSR was strongest and continuous (e.g. offshore Mocha Island, Chiloé Island, Taitao Peninsula and Patagonia). This allowed recognizing the hydrate layer above the BSR, the free gas layer below it, and in some cases, down to the Base of Free Gas reflector (BGR).

Once a final velocity model was built, it was converted in a gas-phase concentration model (Tinivella 1999; Tinivella et al. 2002) by fitting the theoretical velocity field with the experimental velocity field (Fig.13). A modified Domenico's approach (Domenico, 1977) was used in order to reproduce the velocity field in the absence of gas, or the case of full water saturation.
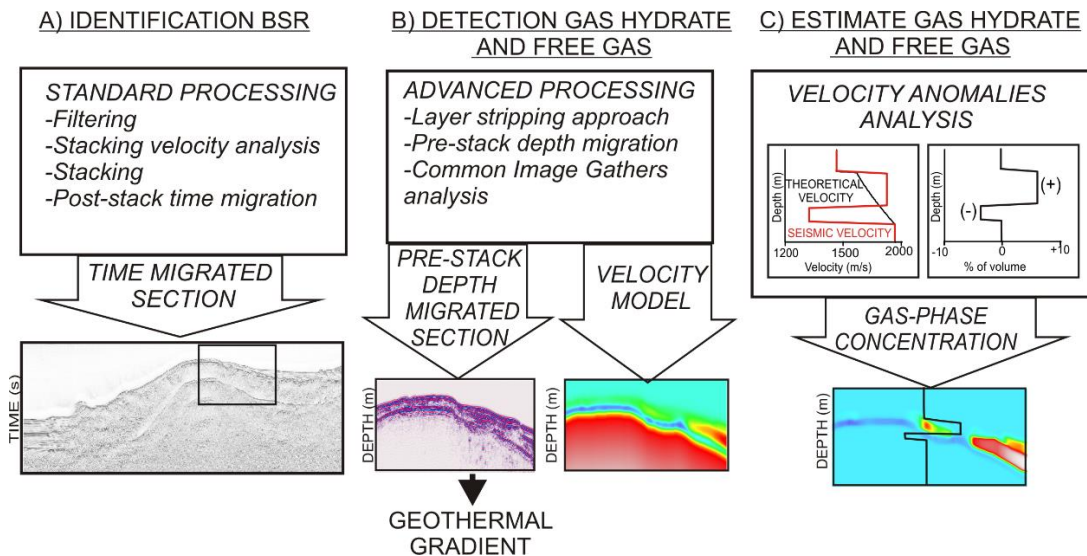
Figure 13: Schematic flow chart of applied processing sequences described by Vargas-Cordero et al, 2010: (A) Standard processing to identify the BSR. The picture shows the stacked section; the square indicates the zoom shown in the other panels. (B) The method used to determine the velocity field. The pictures show the pre-stack depth migration (left) and the velocity model (right). (C) Scheme of velocity anomaly versus gas phase concentration. The picture on the top-left shows an example of the seismic velocity (red line) and reference velocity (black line). On the top-right, the gas hydrate concentration (positive values) and the free gas concentration (negative values) are reported as an example. Bottom: the gas-phase concentration and an example of the velocity profile (black line).

I decided to use a simplified theory, instead of more refined theory (i.e. Carcione et al., 2000; Chand et al. 2004), because of the lack of direct measurements (e.g. borehole information). In fact, in this thesis, the main potential error on gas hydrate estimate is due to assumptions made regarding sediment properties, and not the theoretical model used to determine the theoretical velocity versus hydrate/free gas concentration. This topic is discussed in the next section

Advantages and uncertainties of the estimation method

The main advantage to use SU, an open-source library constantly updated and tested (Colorado School of Mines), is that iteratively uses pre-stack depth migration methods to obtain the velocity model and a good image in depth. This method is very well tested and agreed by the scientific community, and, in fact, the quality of the complex algorithm is comparable to that of commercial software (e.g. PROMAX and ECHOS; Vargas-Cordero et al., 2010, 2016; Tinivella et al., 2001, 2009; Loreto et al., 2011). In effect, the pre-stack depth migration is used to determine the reliability of the velocity model obtained from the traveltime inversion. When the velocity-depth model and the pre-stack depth migration section are consistent, it is implied that we have an accurate velocity field (Kim et al., 1996). The error of the velocity model obtained by using iterative pre-stack depth migration is about 5% (Tinivella et al., 2002; Vargas-Cordero et al., 2010).

The results of the test of sensitivity to calculate hydrate concentrations (Tinivella et al. 2002), indicate that the most important parameters involved are porosity and average density. A variation of ±5% of the porosity and average density is translated in a variation of the gas hydrate concentration of about 1.2% by volume and for free gas estimate are in the order of magnitude of about 0.3% of volume.

The limitation of this methodology is that well data is not available for regions close to the studied areas. The use of well data could have allowed us to better constrain

petrophysical parameters necessary to evaluate the theoretical velocity model and to estimate gas-phase concentration. If there were borehole data, the uncertainties on gas hydrate estimates would be expected to be less than 5%.

In summary, the volume estimative of methane presented in the Manuscript #2 and #3 is limited by the lack of well data. Therefore, the estimates must be used with due caution, and considered qualitatively and not in terms of fully quantitative estimates. Nevertheless, the results might be reasonable and are locally in agreement with other methodically independent studies (e.g. Bangs et al., 1993; Vargas-Cordero, 2010).

The importance of the entire work, despite the uncertainties associated with the method, is to confirm the widespread existence of gas hydrates along the Chilean Pacific margin from Valparaiso (33°S) to Patagonia (57°S), and spotting several methane hydrate concentrated zones (MHCZ). In this study, two extended MHCZ were identified, located offshore Patagonia (54°- 57°S) and Central Chile (35°- 39°S) margin, with hydrate concentrations between 10-20% and layer thicknesses ranging from 200 to 300 m. The high concentrations and thicker layers can be explained because thick sediment sequences are accreted to the overriding plate, at the toe of the wedge and middle forearc, and are affected by deformation processes that promote the methane formation, migration, accumulation and preservation as hydrate in these areas.

Moreover, this thesis presents an overview of the BSR distribution along the slope. It is confirmed that a shallower, strong and continuous BSR around the Chile Triple Junction (CTJ) deepens, weakens and becomes less continuous northwards, which is directly related to the age of the downgoing oceanic plate. Since crustal heat flow along the margin is strongly influenced by the age of the subducted slab, as is

explained in the next paragraphs, these heat flow differences constrain the hydrothermal circulation, and the rates at which methane in the sediment can be generated at depth and migrate into the GHSZ. Besides, high heat flow promotes hydrate dissociation, developing a sediment layer with high free gas concentration below the hydrate layer and, therefore, dropping the seismic velocity values making the BSR stronger. For these reasons, in the area close to the CTJ, with a regime of very high heat flow, vigorous fluid migration and intense rock deformation, we found a strong and continuous BSR in comparison with the BSR located further north of the studied area.

Heat Flow (q)

The technique of using the bottom-simulating reflection (BSR) as a proxy for subsurface temperature was described by Yamano et al. (1982), and, due to the stability of gas hydrates is controlled by temperature and pressure conditions (e.g. Grevemeyer et al. 2003), this can serve to calculate the steady-state heat flow q (mW m^{-2}). The heat flow calculation formula, assuming purely conductive heat transfer, is:

$$q = \frac{T_z - T_0}{\int\limits_0^z \frac{\mathrm{d}z'}{k(z')}}$$

where T_z and T_0 are the temperatures at the BSR and the seafloor respectively (Villinger et al. 2010), k is the thermal conductivity and z denotes the BSR depth.

Advantages and uncertainties of the method

Following the method described by Villinger et al. (2010), the BSR-derived heat flow estimated along the Chilean margin is uncertain because many parameters (i.e.

sediment velocity and density, pore water and gas chemistry, sediment thermal properties, subseafloor pressure, and seafloor temperature) are poorly known and simplifying assumptions were made in the Central and Patagonia regions. Heat flow calculations from BSR alone can contain uncertainties on the order of 20% (Grevemeyer et al., 2001), but calibrations by borehole temperature or heat probe measurements may reduce this uncertainty, as is the case of the CTJ study, where direct measurements of thermal conductivity and downhole temperature from ODP Leg 141 drillholes (Behrmann et al., 1992) were used.

Despite this, heat flow calculation from BSR may still be less accurate than heat probe measurements. However, it is a much more integrative approach, if there is a robust seismic database, as is the case in this thesis. In other words, this allows generating a regional overview of the thermal regime instead of a local view from heat probes techniques, thus avoiding time-consuming of the local survey.

In this thesis, the estimated heat flow along the Chilean margin is between one-third to two-thirds of the expected global mean for crust of that age (e.g. Stein, 2003) and the values are in agreement with direct measurements (e.g. Cande et al., 1987; Flueh et al., 2005; Grevemeyer et al., 2005). These low values are related to the increased hydrothermal circulation of cold seawater resulting from flexing and normal faulting of the oceanic plate prior to subduction (e.g. Yamano et al., 1990; Langseth and Silver, 1996; Grevemeyer et al., 2005). This, in addition to faults and fractures on the overriding plate that facilitate the entry of cold seawater, allows cooling the forearc and in turn outputting warmer water in discharges areas.

In the Central Chile (33° - 40° S) and Patagonia (51°- 57° S) study areas, the average heat flow is about 40 mW m^{-2}, but there are probably fluid discharge areas characterized by relative high heat flow values (>70 mW m^{-2}), in close proximity of

areas with high intensity of deformation and faulting. The better example of such a circulation system is close to Mocha Island (~38.5° S), where a high and variable heat flow (60 - 100 mW m^{-2}) was estimated, probably related to high supply of deep fluids channeled by faults and fractures characteristic of the area (for details, see Vargas-Cordero et al., 2018).

The most anomalous BSR-derived heat flow values obtained in this thesis work are located around the CTJ (~46 °S), where the subduction of the oceanic spreading center causes a major heat flow anomaly in the forearc of the overriding South American Plate. The results are in agreement with the high heat flow values previously estimated and measured in the same area (e.g. Bangs et al., 1995; Cande et al., 1987; Flueh et al., 2005). Here, the presence of cold seeps and hydrothermal vents is reported in the literature (e.g. German et al., 2010; Völker et al., 2014), and there is intense deformation above the downgoing oceanic spreading centre separating the Nazca and Antarctic plates (e.g. Behrmann et al., 2001).

It is well known that hydrothermal circulation exists on the flanks of oceanic spreading centers, and measurements indicate that circulation of crustal fluids is largely constrained to the uppermost 200 m of igneous crust (Fisher et al., 1990), where permeability is high. Thus, on one side there is an incoming oceanic spreading ridge already cooled by this circulation, and on the other side, there is a cover of overriding deformed, accreted and faulted strata of the forearc, where cold seawater may enter deep into the accreted sediments cooling the entire system (Fig. 14).
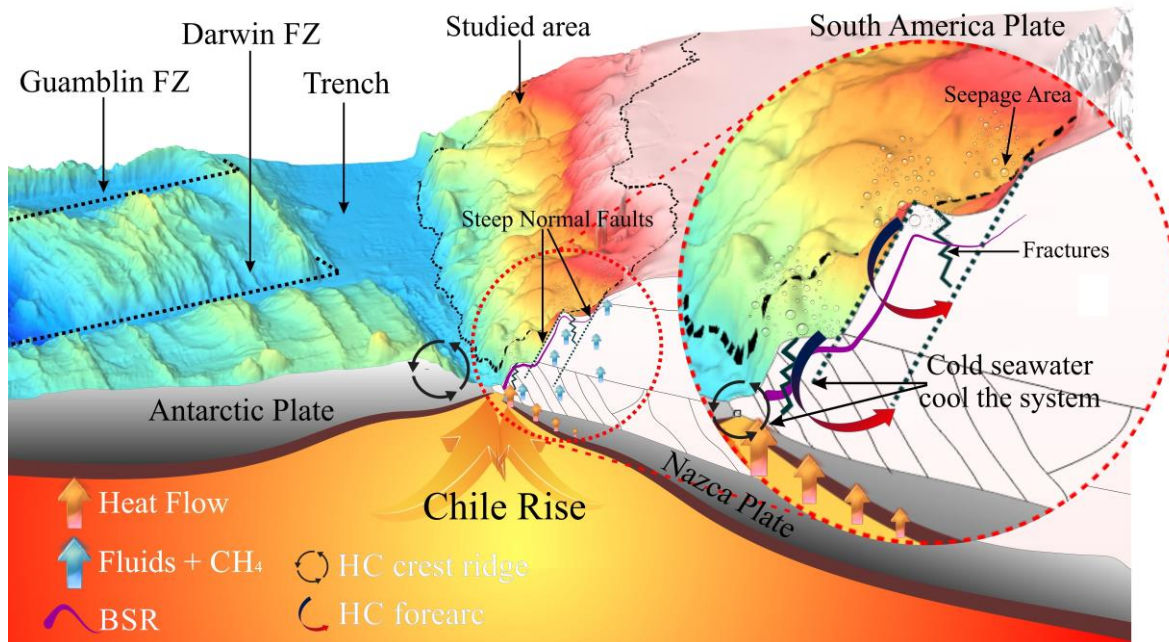
Figure 14: Schematic cross section from the subduction of the Chile Rise. The picture shows the two geofluid systems (HC: Hydrothermal Circulation). Both processes decrease the heat flow estimated in the margin close to the Chile Triple Junction. Dashed black polygon corresponds to the studied area in Chapter 4. Faults are reported by Behrmann et al. (1994).

There is a clear discrepancy between predicted models of heat flow in young oceanic lithosphere (<10 Ma ; e.g. Stein et al., 1992, 1994; Hasterok et al., 2011) and the values calculated in this thesis. Heat flow values estimated in the accretionary wedge and forearc close to the CTJ are one-third of the expected values, which can be explained by the influence of local hydrothermal circulation in the crest ridge and forearc. Thus, faults and fractures are indeed the pathway for fluids from two sources: one deeper source, where warm fluids flow through the seafloor, and an oceanic source, where cold seawater penetrates into the accretionary wedge and forearc, cooling the whole system.

Besides, when we observe geological parameters that favor gas hydrate formation in Chile such as the thickness of trench infill, heat flow values, accretionary prism

tectonics, and sedimentation rate, it is noticeable that almost all of them are quite similar in the studied area, with the exception of heat flow, which is the parameter strongly variable along the overriding plate. According to the estimates calculated in this thesis, relationships between heat flow and gas hydrate concentration is inversely correlated. Accordingly, when heat flow values decrease (e.g. over the Central and Patagonia regions), the methane hydrate concentration increase. On the contrary, close to the Chile Triple Junction, the higher is the heat flow; the lower is the concentration of the gas hydrate. This pattern can be explained because the stability of hydrate is more susceptible to changes in temperature than pressure (Ruppel, 2000) and, thus, a region of highly anomalous heat flow the dissociation of the hydrate is promoted.

Finally, according to the above, it is suggested that the organic carbon-bearing sediment accreted and deformation processes (e.g. faulting and fracturing) contribute to the formation of hydrates in the Chilean margin. However, the concentration of methane hydrate is strongly controlled by the heat flow through the overriding plate.

5.1 REFERENCES FROM SYNTHESIS

Bangs, N.L.; Sawyer, D.S.; Golovchenko, X. 1993. Free gas at the base of the gas hydrate zone in the vicinity of the Chile triple Junction. Geology. 21: 905–908.

Bangs, N.L.; Brown, K.M. Regional heat flow in the vicinity of the Chile Triple Junction constrained by the depth of the bottom simulating reflector. 1995. In Proceedings of the Ocean Drilling Program, Scientific Results; Lewis, S.D.,

Behrmann, J.H., Musgrave, R.J., Cande, S.C., Eds.; Ocean Drilling Program: College Station, TX, USA.141: 253–258.

Behrmann, J.H.; Lewis, S.D., Cande, S.; Leg ODP 141 Scientific Party. 1994. Tectonics and geology of spreading ridge subduction at the Chile Triple Junction; a synthesis of results from Leg 141 of the Ocean Drilling Program. Geol. Rundsch. 83: 832–852.

Behrmann, J.H.; Kopf, A. 2001. Balance of tectonically accreted and subducted sediment at the Chile Triple Junction. Int. J. Earth Sciences (Geol. Rundsch). 90: 753-768. doi: 10.1007/s005310000172.

Cande, S.C.; Leslie, R.B.; Parra, J.C.; Hodbart, M. 1987. Interaction between the Chile ridge and Chile trench: Geophysical and geothermal evidences. J. Geophys. Res. 92, 495–520.

Cohen, J.K.; Stockwell Jr.; J.W. 2008. CWP/SU: Seismic Un*x Release No. 41: An Open Source Software Package for Seismic Research and Processing. Center for Wave Phenomena, Colorado School of Mines.

Domenico, S.N. 1977. Elastic properties unconsolidated porous sand reservoirs. Geophysics 42, 1339-1368.

Fisher, A.T.; Becker, K.; Narasimhan, T.N.; Langseth, M.G.; Mottl, M.J. 1990. Passive, off-axis convection through the southern flank of the Costa Rica Rift. J. Geophys. Res. 95: 9343-9370.

Flueh, E.; Grevemeyer, I. FS SONNE Cruise Report SO 181 TIPTEQ-from the Incoming Plate to Megathrust Earthquakes. Rep. 06.12.2004–26.02.2005; Leibniz-Institut für Meereswissenschaften an der University Kiel: Kiel, Germany, 2005; 533p.

German, C.R.; Shank, T.M.; Lilley, M.D.; Lupton, J.E.; Blackman, D.K.; Brown, K.M.; Baumberger, T.; FrühGreen, G.; Greene, R.; Saito, M.A.; Sylva, S.; Nakamura, K.; Stanway, J.; Yoerger, D.R.; Levin, L.A.; Thurber, A.R.; Sellanes, J.; Mella, M.; Muñoz, J.; Diaz-Naveas, J.L. Inspire Science Team, 2010. Hydrothermal Exploration at the Chile Triple Junction – ABE's Last Adventure? American Geophysical Union, Fall Meeting 2010. Abstract #OS11D-06.

Grevemeyer, I.; Villinger, H. 2001. Gas hydrate stability and the assessment of heat flow through continental margins. Geophys. J. Int. 145: 647–660.

Grevemeyer, I.; Diaz–Naveaz, J.L.; Ranero, C.R.; Villenger, H.W. Ocean Drilling Program Scientific Party. 2003. Heat Flow over the descending Nazca plate in Central Chile, 32 S to 41 S: Observations from ODP Leg 202 and the occurrence of natural gas hydrates. Earth Planet. Sci. Lett. 213: 285–298.

Grevemeyer, I.; Kaul, N.; Diaz-Naveas, J.L.; Villinger, H.W.; Ranero, C.R.; Reichert, C. 2005. Heat flow and bending-related faulting at subduction trenches: case studies offshore of Nicaragua and Central Chile. Earth Planet. Sci. Lett. 236: 238–248. doi:10.1016/j.epsl.2005.04.048

Hasterok, D.; Chapman, D.; Davis, E. 2011. Oceanic heat flow: Implications for global heat loss. Earth. Planet. Sci. Lett. 311: 386–395.

Kim, Y.C.; Samuelsen, C.M.; Hauge, T. A. 1996. Efficient velocity model building for prestack depth migration. The Leading Edge. 15: 751–753.

Loreto, M.F.; Tinivella, U.; Accaino, F.; Giustiniani, M. 2011. Gas hydrate reservoir characterization by geophysical data analysis (offshore Antarctic Peninsula). Energies. 4: 39–56.

Ruppel, C. 2000. Thermal State of the Gas Hydrate Reservoir. In: Max M.D. (eds) Natural Gas Hydrate. Coastal Systems and Continental Margins, vol 5. Springer, Dordrecht.

Stein, C.A.; Stein, S. 1992. A model for the global variation in oceanic depth and heat flow with lithospheric age. Nature. 359: 123–129.

Stein, C.; Stein, S. 1994. Constraints on hydrothermal heat flux through the oceanic lithosphere from global heat flow. J. Geophys. Res.: Solid Earth (1978–2012) 99, 3081–3095.

Stein, C.A. 2003. Heat flow and flexure at subduction zones. Geophys. Res. Lett., 30. doi: 10.1029/2003GL018478.

Tinivella, U. 1999. A method for estimating gas hydrate and free gas concentrations in marine sediments. Boll. Geofis. Teor. Appl. 40: 19–30.

Tinivella, U.; Carcione, J.M. 2001. Estimation of gas-hydrate concentration and free-gas saturation from log and seismic data. Lead Edge. 20: 200-203.

Tinivella, U.; Accaino, F.; Camerlenghi, A. 2002. Marine Geophysical Researches. 23: 109. doi: 10.1023/A:1022407914072.

Tinivella, U.; Loreto, M.F.; Accaino, F. 2009. Regional versus detailed velocity analysis to quantify hydrate and free gas in marine sediments: The south Shetland margin target study. Geol. Soc. Spec. Publ. 319: 103-119.

Vargas-Cordero, I.; Tinivella, U.; Accaino, F.; Loreto, M.; Fanucci, F. 2010. Thermal state and concentration of gas hydrate and free gas of Coyhaique, Chilean Margin (44°30′ S). Marine and Petroleum Geology. 27: 1148-1156. doi: 10.1016/j.marpetgeo.2010.02.011.

Vargas-Cordero, I.; Tinivella, U.; Villar-Muñoz, L.; Giustiniani, M. 2016. Gas hydrate and free gas estimation from seismic analysis offshore Chiloé island (Chile). Andean Geol. 43: 263–274.

Vargas-Cordero, I.; Tinivella, U.; Villar-Muñoz, L; Bento, J.P. 2018. High Gas Hydrate and Free Gas Concentrations: An Explanation for Seeps Offshore South Mocha Island. Energies. 11(11), 3062, doi: 10.3390/en11113062

Villinger, H.; Tréhu, A.M.; Grevemeyer, I. 2010. Seafloor marine heat flux measurements and estimation of heat flux from seismic observations of bottom simulating reflectors. In: Riedel, M., Willoughby, E.C., Chopra, S. (Eds.), Geophysical Characterization of Gas Hydrates. Society of Exploration Geophysicists, Tulsa, 279–300.

Völker, D.; Geersen, J.; Contreras-Reyes, E.; Sellanes, J.; Pantoja, S.; Rabbel, W.; Thorwart, M.; Reichert, C.; Block, M.; Weinrebe, W.R. 2014. Morphology and geology of the continental shelf and upper slope of southern Central Chile (33S–43S). Int J Earth Sci (Geol Rundsch). 103, 1765. doi:10.1007/s00531-012-0795-y.

Yamano, M.; Uyeda, R.M.; Aoki, Y.; Shipley, T.H. 1982. Estimates of heat flow derived from gas hydrates. Geology 10: 339–343.

Yamano, M.; Uyeda, S. 1990. Heat flow studies in the Peru trench subduction zone Proc. Ocean Drill. Prog. Sci. Results. 112: 653-661.

6. CONCLUSIONS

The results of this research thesis regarding gas hydrates and heat flow in sediments on the Southern Chile continental slope allows concluding that:

i. The BSR along the Chilean margin (33° - 57° S) is identified in the marine sediments in the accretionary prism, at around 2000 m water depth, and between 90-600 meters below seafloor. Besides, in the region close to the Chile Triple Junction (~46° S), a shallower, strong and continuous BSR exists that deepens, weakens and becomes less continuous northwards. This change is directly related to the age of the downgoing oceanic plate.

ii. The heat flow density, estimated in the Central and Patagonia regions of the Chile Pacific margin, is one-third to two-thirds of the expected global mean for an oceanic crust of that age. These lower values may be related to increased hydrothermal circulation resulting from bend-faulting of the oceanic plate prior to subduction, in addition to faulting and fracturing in the overriding plate that facilitates the entry of cold seawater, thus cooling the forearc.

iii. Close to the CTJ, the heat flow estimated is up to 280 mW m^{-2}, indicating that the overriding South American Plate is effectively heated by subjacent zero-age oceanic plate material. However, heat flow density is overall only one-third of the expected values. This can be explained by the influence of local hydrothermal circulation in the subducted crest of the Chile spreading ridge and the overlying forearc.

Thus, faults and fractures are indeed the pathway for fluids from two sources: one deeper source, where warm fluids flow through the seafloor, and an oceanic source, where cold seawater penetrates into the accretionary wedge and forearc, cooling the whole system.

iv.   Hydrate concentration values close to the CTJ are on average 4% of the total rock volume. This relatively low value is due to the stability of hydrate being more susceptible to changes in temperature than pressure. Thus, highly anomalous heat flow promotes dissociation of the hydrate.

v.   In the Patagonia section of the Chilean Pacific margin region, there is an extensive methane hydrate concentration zone. The average thickness of the gas hydrate layer modelled is almost 300 m, with average concentrations up to 10%. These high concentrations and thicker layers likely exist because the accreted sediment sequences are affected by deformation, promoting the methane formation, accumulation and preservation as hydrates.

vi.   Generally, the masses of organic carbon-bearing sediment accreted and deformation processes (i.e. faulting and fracturing) contribute to the formation of hydrates in the Chilean margin. However, the concentration of methane hydrate is strongly controlled by the heat flow through the overriding plate.

93

LUCÍA ALEJANDRA VILLAR MUÑOZ

Home Addresse: Lesonia 463 depto. 106
                Viña del Mar, Chile
Phone: +56952264461
Date of Birth: 24.03.1979
Place of Birth: Puente Alto
e-mail: lucia.villar@gmail.com
Nationality: Chilean
Marital Status: Married

ACADEMIC EDUCATION

PHD STUDENT

Since 2010

Doctorate student at the GEOMAR Helmholtz Centre for Ocean Research Kiel, Germany

OCEANOGRAPHY

03.03.1997-13.06.2003

Bachelor of Science at the Pontificia Universidad Católica de Valparaíso, Chile

HIGH SCHOOL

1993-1996

Colegio Particular Los Pensamientos

Santiago, Chile